Leveraging Diversity and Spatial Connectivity in Multi-hop Vehicular Networks

Rui Meireles

CMU-CS-15-127

August 2015

School of Computer Science
Carnegie Mellon University
Pittsburgh, PA 15213, USA

&

Consortium of:
Universities of Minho, Aveiro and Porto
Portugal

Thesis Committee:

Peter Steenkiste, Co-Chair, Carnegie Mellon University
João Barros, Co-Chair, University of Porto
Srinivasan Seshan, Carnegie Mellon University
Ragunathan (Raj) Rajkumar, Carnegie Mellon University
Mario Gerla, University of California, Los Angeles
Paulo Ferreira, University of Aveiro

Submitted in partial fulfillment of the requirements for the degree of Doctor of Philosophy.

Support for this research was provided by the Portuguese Foundation for Science and Technology (FCT) through the Carnegie Mellon-Portugal Program under grant SFRH/BD/37698/2007 and projects Cloud Anchor (QREN Project 23151), PEst-OE/EEI/LA0008/2013 and DRIVE-IN — Distributed Routing and Infotainment through Vehicular Inter-Networking (CMU-PT/NGN/0052/2008).

The views and conclusions contained in this document are those of the author and should not be interpreted as representing the official policies, either expressed or implied, of any sponsoring institution, the U.S. government or any other entity.

Keywords: vehicular networks, multi-hop, routing, forwarding, diversity, spatial connectivity

Abstract

Vehicular Ad-Hoc Networks (VANETs) were created with the goal of increasing traffic safety and efficiency through wireless communication. Due to the vehicles' limited radio range, multi-hop communication is useful to extend coverage. However, it is not an easy proposition. The dynamic topology and spatial heterogeneity that characterize VANETs require a fundamental change from traditional topology-based routing protocols and make it challenging to design a scheme that performs well under all conditions.

In this thesis we focus on the development of specialized vehicular geographic multi-hop communication protocols that address these challenges. First we tackle topology instability with the Density-Aware Zone-based Limited (DAZL) forwarding protocol. Instead of choosing one relay per hop as is traditional, DAZL specifies a geographic forwarding zone and has multiple vehicles inside it cooperate in forwarding. We show experimentally that because different vehicles experience different loss patterns, forwarders can cover each other's losses, increasing reliability through *node diversity*. Moreover, zone nodes coordinate to prioritize the best forwarders and avoid replication.

Second, we propose the Look-Ahead Spatial Protocol (LASP). LASP addresses the issue of spatial heterogeneity by using *spatial connectivity* information describing the probability of delivery between different geographic areas. Collected vehicular connectivity data exhibited a strong correlation between location and packet delivery ratio, demonstrating that spatial connectivity makes for a good multi-hop heuristic. LASP combines global historical spatial connectivity information with real-time local neighborhood connectivity information to estimate end-to-end delivery probabilities and select, at each hop, the next hop node that maximizes this probability.

Finally we join both ideas in the LASP-MF (Multi-Forwarder) protocol, which combines LASP's spatial-connectivity routing heuristic with DAZL's zone-based forwarding approach in a single protocol. Instead of picking a specific next-hop node, LASP-MF uses spatial connectivity to select a forwarding zone where nodes cooperate in forwarding in a manner similar to DAZL.

To enable a realistic evaluation, we leverage two vehicular testbeds currently deployed in the city of Porto, Portugal, both as sources of data for analysis and a platform for experimentation.

Acknowledgments

I thank my advisors for all the guidance, constructive criticism and always believing in me even when I doubted. Dr. João Barros, Dr. Peter Steenkiste, I will cherish the lessons you taught me.

I thank my thesis committee for overseeing my work and ensuring its quality.

I thank all my fellow students for the camaraderie and discussions about both research and the ups and downs of graduate student life and everyone else at CMU's Computer Science Department and Instituto de Telecomunicações for the wonderful working environment.

I especially thank the colleagues who collaborated directly with me. Dr. Paulo Oliveira, Eng. João Rodrigues, Eng. Susana Cruz, Eng. Pedro Santos, Dr. Daniel Moura, Eng. Mark Macedo and Dr. Mate Boban, I am very grateful for your help.

I thank all the kind people at Veniam Works for giving me access to the vehicular testbed without which this thesis would not have been possible. Dr. Susana Sargento, Eng. Carlos Ameixieira, Eng. Filipe Neves and Dr. Tiago Condeixa, thank you.

I thank Dr. Jorge Cham, whose famous PhD Comics series, through some unlikely reverse psychology, actually inspired me to pursue a PhD degree.

Last but not least, I thank my friends and family for the unconditional love that gave me strength to overcome all the obstacles in my way.

Contents

1 Introduction **1**

1.1 Vehicular Ad-Hoc Networks 1

1.2 The Multi-hop Communication Challenge 3

1.3 Technological Context 3

1.4 Thesis Outline 5

1.5 Contributions and Thesis Statement 7

2 Challenges in Vehicular Multi-hop Communication **9**

2.1 Dynamic Topology 9

2.2 Link Instability 12

2.3 Spatial Heterogeneity 13

2.4 Protocol Evaluation 15

3 DAZL: Density-Aware Zone-based Forwarding **19**

3.1 Premise: Node Diversity 19

3.2 Protocol Design 22

3.2.1 Zone-based Forwarding 22

3.2.2 Forwarder Coordination and Prioritization 25

3.3 Experimental Evaluation 27

3.3.1 Setup 27

3.3.2 Results 29

3.4 Simulation Evaluation 31

3.4.1 Setup . . . 31
3.4.2 Results . . . 32
3.5 Related Work . . . 35
3.6 Summary . . . 37

4 LASP: Look-Ahead Spatial Protocol 39
4.1 Premise: Spatial Connectivity . . . 39
4.2 Spatial Connectivity Analysis . . . 41
4.2.1 Data Collection . . . 41
4.2.2 Lost Opportunities in Road-based Routing . . . 42
4.2.3 Use of Distance as a Routing Metric . . . 44
4.2.4 Spatial Location as a Predictor for PDR . . . 44
4.2.5 Temporal Stability of Historical Spatial Connectivity . . . 46
4.3 Protocol Design . . . 47
4.3.1 Overview . . . 47
4.3.2 Historical Spatial Connectivity Graph — Look-ahead . . . 50
4.3.3 Real-time Look-ahead Graph . . . 52
4.3.4 Choosing Relays . . . 53
4.3.5 Recovering From Dead Ends . . . 56
4.4 Trace-based Evaluation . . . 57
4.4.1 Setup . . . 57
4.4.2 Results . . . 62
4.5 Related Work . . . 67
4.6 Summary . . . 68

5 LASP-MF: LASP Multi-Forwarder 69
5.1 Premise: Complementarity of Node Diversity and Spatial Connectivity . . . 69
5.2 Protocol Design . . . 71
5.2.1 Overview . . . 71
5.2.2 Forwarding Zone Definition and Selection . . . 73

5.2.3 Forwarder Ranking Inside the Forwarding Zone 75
5.3 Trace-based Evaluation 78
5.3.1 Setup 78
5.3.2 Results 87
5.4 Experimental Evaluation 94
5.4.1 Setup 94
5.4.2 Results 100
5.5 Summary 107

6 Conclusions **109**
6.1 Contributions 109
6.2 Future Work 110

Glossary **115**

List of Figures

1.1 Classification of VANET applications from a communications perspective. 2

1.2 WAVE protocol stack for vehicular communication. 4

1.3 Thesis contents decomposition. 6

2.1 Link duration in a vehicular network. 10

2.2 Wireless Ad-Hoc Networks routing protocol taxonomy 11

2.3 Gray-zone of partial connectivity in a vehicular network. 12

2.4 Impact of line of sight conditions on packet delivery rates. 14

2.5 Leixões Harbor photographed from a container crane. 16

2.6 HarborNet deployment area and example topology. 18

3.1 Node diversity experimental scenario. 20

3.2 Effect of node diversity on packet delivery rates. 21

3.3 Diversity gain from additional receivers. 22

3.4 Contrast between neighbor-based and zone-based forwarding. 23

3.5 DAZL forwarding workflow diagram. 25

3.6 DAZL spreads forwarders in time according to their distance to the destination. . . . 26

3.7 DAZL experimental scenario. 27

3.8 DAZL and neighbor-based geographic header formats. 28

3.9 DAZL experimental evaluation performance results. 30

3.10 DAZL simulation evaluation performance results. 33

3.11 DAZL forwarder selection behavior. 35

4.1 Traditional versus spatial connectivity-based routing. 40
4.2 Logging data kept by each testbed node. 42
4.3 Porto road network and spatial connectivity. 43
4.4 Spatial connectivity analysis results. 45
4.5 Inter-link distance metric definition. 46
4.6 LASP spatial-connectivity abstraction. 47
4.7 LASP logical and physical architecture. 48
4.8 LASP merging of real-time and historical-connectivity. 49
4.9 Spatial connectivity graph visualization example. 52
4.10 LASP connectivity graph example. 55
4.11 LASP backtracking example. 56
4.12 Network conditions during LASP's trace-based evaluation. 61
4.13 LASP trace-based PDR results. 62
4.14 LASP trace-based network load results. 63
4.15 LASP cell size sensitivity PDR results. 65
4.16 LASP cell size sensitivity network load results. 66

5.1 Example combination of spatial connectivity and node diversity. 70
5.2 LASP-MF topology abstraction. 72
5.3 LASP-MF forwarder slotting. 73
5.4 LASP-MF sequence diagram for the scenario in Figure 5.1. 77
5.5 Multiple forwarder paths example. 81
5.6 General dependency relationship between two forwarding paths. 82
5.7 LASP-MF trace-based PDR results. 88
5.8 LASP-MF trace-based transmission count results. 90
5.9 LASP-MF trace-based replication results. 92
5.10 LASP-MF trace-based hop count results. 93
5.11 Router prototype architecture. 95
5.12 LASP-MF, LASP and GPSR geographic header formats. 97

5.13 Network conditions during LASP-MF's experimental evaluation. 99
5.14 LASP-MF experimental packet delivery ratio results. 101
5.15 LASP-MF experimental recovery mechanism usage results. 102
5.16 LASP-MF experimental transmission and hop count results. 103
5.17 LASP-MF experimental replication and latency results. 104

List of Tables

3.1 Linkbird configuration parameters for the node diversity experiments. 20
3.2 Linkbird configuration parameters for the DAZL experiments. 28
3.3 DAZL ns-3 simulation configuration parameters. 31

4.1 Configuration parameters for connectivity data collection. 42
4.2 Classification of vehicular communication relative to Porto's road network. 43
4.3 End-to-end delivery probability estimation for the connectivity graph of Figure 4.10. 56
4.4 Configuration parameters used in LASP's trace-based evaluation. 60

5.1 Configuration parameters used in LASP-MF's trace-based evaluation. 80
5.2 Configuration parameters used in LASP-MF's experimental evaluation. 96

Chapter 1

Introduction

1.1 Vehicular Ad-Hoc Networks

In modern society, land travel is a fundamental means of transportation for both goods and people. Unfortunately, it is not without its failings. According to the U.S. Department of Transportation, in 2012 alone there were a total of 5.6 million registered crashes resulting in 33.782 deaths in the United States [oT15]. Moreover, the U.S. Census Bureau reports that, in the year 2009, traffic congestion cost the country a total of around 1 billion dollars in delays and wasted fuel [Bur12]. Data from the European Union reveals a similar story, with a total of 29.000 fatalities in 2010 [B$^+$12].

One of the main causes behind these problems is that vehicles and their drivers coordinate through indirect and error-prone means such as traffic signs and signals, indicator lights, and horns. Using a wireless Vehicular Ad-hoc NETwork (VANET), information can be exchanged more reliably, in greater quantities, at much higher speeds, and without human intervention. This technology can be used to promote [BKS$^+$06, LCG08]: road safety (e.g. through a collision avoidance system); traffic efficiency (e.g. by disseminating traffic congestion information); and infotainment (e.g. public service announcements, advertisement, internet access).

From a communication requirements perspective, vehicular network applications can be classified as: i) single-hop broadcast, ii) unicast/multicast and, iii) geocast. The three types of applications are exemplified in Figure 1.1.

Applications that only require single-hop broadcasting of packets within their immediate neighborhood are classified under the single-hop broadcast category. A prime example of this type of application is collision avoidance [EGH$^+$06]. In such an application, vehicles periodically broadcast their position, and velocity and acceleration vectors, which are then used by other vehicles to either warn the driver of dangerous situations, or autonomously brake or steer away from an impending

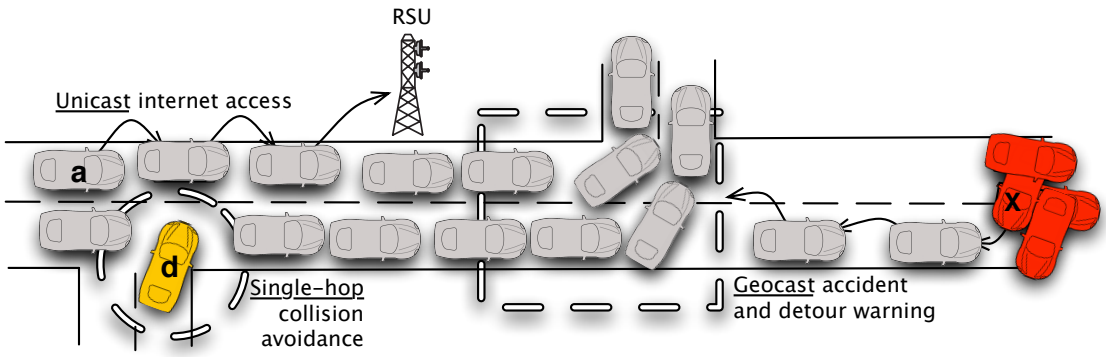

Figure 1.1: Classification of vehicular network applications from a communications perspective.

accident.

Unicast applications are a direct port of typical computer network applications where packets are addressed to a specific node uniquely identified by its IP address. Examples include media streaming and internet access through Road-Side Units (RSUs) [BRAHH04], which are used as gateways to the cloud. Multicast applications are conceptually similar, the difference being that packets are addressed and delivered not to a single node but to a group of nodes. An example would be multi-player online games [TB10].

The third application type, geocast, is more specialized. Geocast is a form of multicast where packets are addressed to a geographic Zone of Relevance (ZOR), rather than a set of node identifiers. Geocast is very important in the context of vehicular networks because many messages will only be relevant within a specific geographic region. Traffic congestion information, local business advertisement and parking spot discovery are all examples [Mai04].

From these three application types, only single-hop broadcast does not need multi-hop communication. Unicast and multicast need it to reach destinations outside the sender's immediate neighborhood. Likewise, in geocast, the potentially remote ZOR must be reached before the message can be disseminated inside it. Furthermore, studies have shown that VANET communication ranges can be as small as 100 m in city environments [NCMS11], due to line of sight obstructions and multipath. With such short communication ranges, multi-hop communication becomes key in increasing wireless coverage.

As an example, in Figure 1.1 a detour warning is sent to an intersection to warn drivers that they should take a detour because the road on the right is blocked, consequence of an accident. If communication is restricted to a single-hop, only the vehicles in the immediate vicinity of the accident will be informed. Consequently, a traffic jam will form in the stretch of road leading to the blockade. With multi-hop communication, however, the message can be propagated further

back. This will allow cars to exit the road before reaching the accident and altogether prevent the formation of a traffic jam and improve access for emergency response vehicles.

1.2 The Multi-hop Communication Challenge

As a consequence of the environment in which vehicular networks operate, multi-hop communication is difficult to implement reliably. One major challenge is the dynamic topology, which is caused by a combination of factors. The vehicles' high mobility combined with an environment rich in obstacles, such as buildings and hills, result in a harsh fading environment leading to an unstable network composed of unreliable links with partial and unpredictable connectivity [BSK10]. As a consequence, traditional topology-based routing schemes such as OLSR [CJ03], developed for other, less dynamic, ad-hoc networks, have been shown to perform poorly in vehicular environments [FGEG11].

Because of this, rather than relying on topology information, most dedicated VANET protocols are geographic in nature, using location to build paths hop-by-hop with the goal of getting the packet ever closer to the destination. For example, GPSR [KK00], one of the most popular geographic protocols, picks, at each hop, the neighbor closest to the destination as the next relay towards it.

But a simple geographic protocol such as this is not sufficient, because of a second big challenge that VANET multi-hop protocols have to contend with: spatial heterogeneity. GPSR's heuristic of choosing the closest node to the destination is based on the assumption that connectivity is uniform across space. Yet in reality, it varies according to the obstacles present in each location, making it very hard to accurately predict packet delivery beforehand. Furthermore, nodes are not uniformly distributed across space, so packets may not be able to reach the destination by following a straight path due to a lack of forwarder nodes.

Another challenge with vehicular network routing is proper evaluation. Because of cost and logistic constraints, multi-hop communication protocols are typically tested either using only synthetic simulations (e.g. A-STAR [SLL$^+$04]) or very small-scale experiments (e.g. DSR [JMB01]), which do not properly reflect actual operation conditions.

1.3 Technological Context

In order to support vehicular network applications, the IEEE created the 1609 family of standards, which detail the WAVE (Wireless Access in Vehicular Environments) protocol stack, depicted in Figure 1.2a.

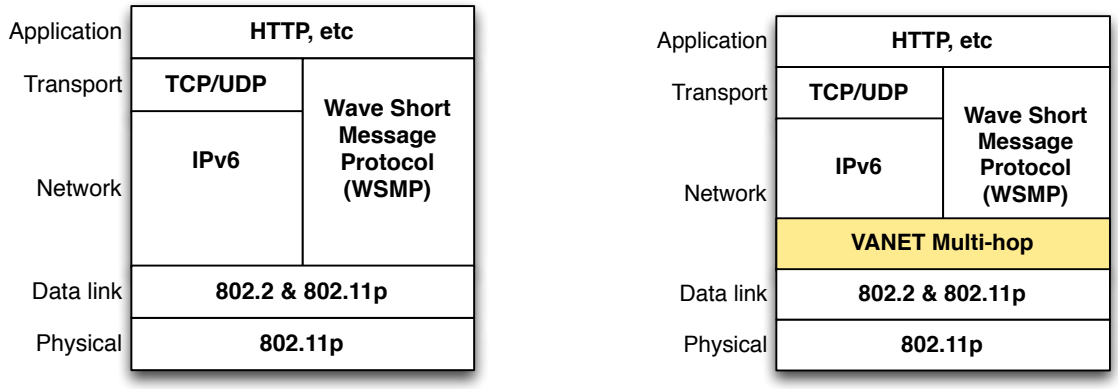

(a) Current form

(b) With additional multi-hop layer

Figure 1.2: WAVE protocol stack for vehicular communication.

At the base of the stack is the IEEE 802.11p standard [Soc10], which encompasses both medium access control and physical layers. This standard is based on the well-known IEEE 802.11a/g standard from infrastructure Wireless Local Area Networks (WLANs), with slight changes for increased robustness [CHC+08][1], and will operate in the Dedicated Short-Range Communications (DSRC) channels in the 5.9 GHz band [ETS05, Ken11]. The CSMA/CA (Carrier Sense Multiple Access/Collision Avoidance) medium access control scheme carries over from 802.11a without any relevant changes.

Of special interest for multi-hop are the network and transport layers, detailed in the IEEE 1609.3 standard [IEE10]. WAVE proposes a two-pronged approach of combining the traditional TCP/UDP/IP (Transmission Control Protocol/User Datagram Protocol/Internet Protocol) stack for internet applications with a specialized Wave Short Message Protocol (WSMP), specially designed for vehicular use. WSMP is a thin protocol for messages up to 1400 bytes in size that allows applications to control physical parameters such as transmit power and data rate.

WSMP does not directly support multi-hop communication, and as we have discussed in the previous section, traditional topology-based routing protocols are not suitable for vehicular environments. Furthermore, IP packets use IPv6 addresses and WSMP uses Medium Access Control (MAC) addresses, meaning that there is no built-in support for geocast applications, which require packets to be addressed to a geographical location.

As a consequence, designers of applications needing multi-hop communication must implement their own specialized protocol and embed it into the application itself. This is not a sustainable

[1]In order to mitigate the large delay and Doppler spread caused by vehicle movement, relative to 802.11a/g, IEEE 802.11p halves the bandwidth (10 vs 20 MHz) and doubles all of the Orthogonal Frequency-Division Multiplexing (OFDM) timing parameters (e.g. 8 vs 4 μs symbol interval).

proposition in the long term, as maintaining a large number of different protocols is both difficult and costly. Moreover, in such a scenario, only nodes having the same exact application installed would able to relay packets from that application.

1.4 Thesis Outline

In this thesis, our goal is to create a vehicular unicast multi-hop communication service to sit beneath both IP and WSMP as per Figure 1.2b, thus removing the burden of communication protocol design from application developers. This unicast service can then be used as a building block in the development of geocast and multicast protocols. Furthermore, we focus on multi-hop communication within a given connected component of the network. I.e., we do not consider a delay-tolerant networking approach.

The particular characteristics of vehicular networks lead us to explore a solution in the geographic realm, but introducing new ideas and mechanisms to better cope with the challenges posed by topology instability and spatial heterogeneity.

We divide the multi-hop communication problem into forwarding and routing. Forwarding is the process through which nodes choose the next hop relay for a given packet. Routing is the process through which the data structures used to abstract the network topology and inform forwarding decisions are created and maintained.

We start by looking at the forwarding problem, where the main issue is topology and link instability. Leveraging the fact that different nodes have channels with different loss patterns — *node diversity*, we propose having multiple nodes cooperate in forwarding each packet to increase communication reliability. We experimentally validate the potential benefits of cooperative relaying and then leverage it in the design of the DAZL (Density-Aware Zone-based Limited forwarding) protocol. In DAZL, packets are not sent to a particular relay, but rather broadcast to a geographic forwarding zone. Receivers inside the zone then coordinate to forward the packet. Compared with a single-relay strategy, this better tolerates unstable topologies because it does not rely on the quality of any specific link. Through the use of a novel implicit coordination scheme, DAZL prioritizes the most promising forwarders and spreads them in time, thus minimizing the potential delay and replication incurred by such a multiple-forwarder scheme.

In the second part of our work, we focus on the routing component and introduce LASP, for Look-Ahead Spatial Protocol. Due to the dynamic nature of vehicular networks, only local real-time connectivity information can reasonably be assumed available. This makes it difficult to guide the packet towards well connected areas in order to address the issue of spatial heterogeneity. In LASP we address this problem by introducing historical *spatial connectivity* as a *look-ahead* to comple-

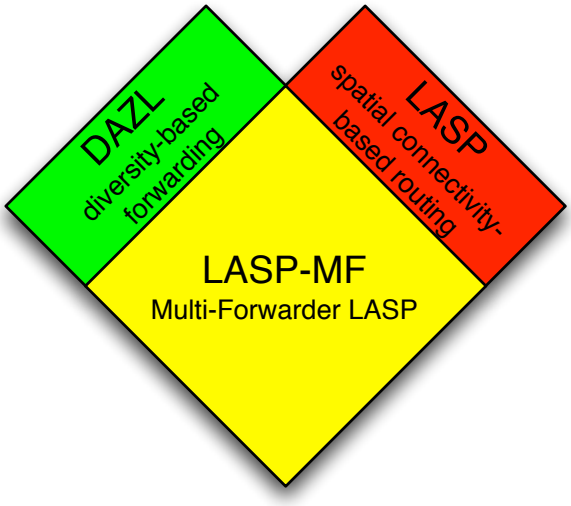

Figure 1.3: Thesis contents decomposition.

ment the local real-time information. Spatial connectivity describes the measured packet delivery probability between two physical geographic areas. By analyzing connectivity data collected from a vehicular testbed, we show that since communication in a given location is consistently affected by the same large physical factors, spatial connectivity is a good predictor of delivery probability.

By combining real-time with historical spatial connectivity the packet holder can, at each hop, compute the expected end-to-end delivery probability for each potential relay. LASP then performs an efficient best-first path search, choosing the most promising relay at each hop, and backtracking to recover from dead ends, if ever necessary.

LASP chooses only a single relay to forward a message at any give time. In our final protocol, LASP-MF, or Multi-Forwarder LASP, we combine LASP's spatial connectivity approach with DAZL's zone-based forwarding concept. In LASP-MF spatial connectivity is used not to select a specific next-hop relay but a geographical forwarding zone. The nodes inside the zone then use a DAZL-like forwarder coordination scheme to prioritize the better-connected nodes and minimize replication.

The thesis can then be decomposed into 3 interconnected parts, as depicted in Figure 1.3.

Our work is validated experimentally, taking as much advantage as possible of the two vehicular testbeds currently deployed in the city of Porto, Portugal: HarborNet [ACN+14], a network of around 30 trucks working in the Leixões Harbor; and PortoVANET, a network of roughly 400 buses and taxi cabs.

This thesis document is organized in the following manner. Chapter 2 details the challenges in

vehicular multi-hop communication and how previous efforts attempted to address them. Chapter 3 describes the DAZL forwarding protocol, while Chapter 4 introduces LASP. Chapter 5 combines the two strategies in the multi-forwarder LASP-MF protocol. Finally, Chapter 6 presents our conclusions and potential directions for future work.

1.5 Contributions and Thesis Statement

In this thesis we make the following technical contributions:

- We experimentally evaluate the potential gains of exploiting *node diversity* — the usage of independent channels from different vehicles — as a means to overcome topology instability in vehicular forwarding.
- We define, implement and evaluate DAZL, a forwarding protocol that leverages node diversity to improve forwarding reliability.
- We introduce and experimentally validate the concept of *spatial connectivity* as a means to deal with spatial heterogeneity in vehicular networks.
- We define, implement and evaluate LASP, a routing and forwarding protocol that leverages spatial connectivity to improve end-to-end communication reliability.
- We define, implement and evaluate LASP-MF, a routing and forwarding protocol that combines LASP routing with DAZL forwarding to further increase communication reliability.

The thesis can then be synthesized in the following statement:

Challenges in vehicular multi-hop communication can be turned into opportunities through the use of node diversity and spatial connectivity information.

Parts of the work developed in the context of this thesis were published in the following articles:

- Rui Meireles, Michel Ferreira, and João Barros. *Vehicular connectivity models: From Single-hop Links to Large-scale Behavior.* In Vehicular Technology Conference Fall (VTC 2009-Fall), 2009 IEEE 70th, pages 1-5. IEEE, Sep 2009.
- Rui Meireles, Mate Boban, Peter Steenkiste, Ozan Tonguz, and João Barros. *Experimental Study on the Impact of Vehicular Obstructions in VANETs.* In Vehicular Networking Conference (VNC), 2010 IEEE, pages 338–345. IEEE, Dec 2010.

- Mate Boban, Rui Meireles, João Barros, Ozan Tonguz, and Peter Steenkiste. *Exploiting the Height of Vehicles in Vehicular Communication.* In Vehicular Networking Conference (VNC), 2011 IEEE, pages 163-170. IEEE, Nov 2011.

- Rui Meireles, Peter Steenkiste, and João Barros. *DAZL: Density-Aware Zone-based Packet Forwarding in Vehicular Networks.* In Vehicular Networking Conference (VNC), 2012 IEEE, pages 234-241, Nov 2012.

- Mate Boban, Rui Meireles, João Barros, Peter Steenkiste, and Ozan K Tonguz. *TVR—Tall Vehicle Relaying in Vehicular Networks.* Mobile Computing, IEEE Transactions on, 13(5):1118–1131, May 2014.

- Carlos Ameixieira, André Cardote, Filipe Neves, Rui Meireles, Susana Sargento et al. *Harbornet: A Real-world Testbed for Vehicular Networks.* Communications Magazine, IEEE, 52(9):108–114, Sep 2014.

The DAZL protocol has also been awarded the following patent:

- João Barros, Rui Meireles and Peter Steenkiste. *Density-Aware Zone-based Packet Forwarding in Vehicular Networks.* WO Patent App. PCT/IB2013/059,012, May 2014.

Chapter 2

Challenges in Vehicular Multi-hop Communication

In this chapter we describe the major challenges in vehicular multi-hop communication, which stem from the network's dynamic nature and complex operating environment. Namely, we focus on the network's unstable topology and links, spatial heterogeneity and difficult evaluation.

2.1 Dynamic Topology

Vehicular networks must support node speeds that are at least an order of magnitude beyond what other types of mobile ad-hoc networks experience. Consider for example two vehicles in a freeway moving at 120 Km/h (75 mph) in opposite directions (i.e. 240 Km/h relative speed). Assuming an average communication range of 500 meters, which is agreement with experimental results [MBS+10], such a link will last less than 8 seconds. In urban environments, line of sight blockages created by buildings and terrain can conspire to reduce link durations even further.

To see how long vehicular links last in practice, we collected one week of connectivity data from the 30-node vehicular testbed HarborNet [ACN+14], which will be later described in detail in Section 2.4. Figure 2.1 shows the Empirical Cumulative Distribution Function (ECDF) of link duration for this data set. Nodes broadcast 10 messages per second and we considered a link to be broken once there was a period of 2 or more consecutive seconds without communication. As can be observed in the plot, over 50% of links lasted 5 seconds or less in this trial. 75% lasted 20 seconds or less. These results strongly corroborate the short-lived nature of most vehicular network links, which in turn results in a very dynamic network topology that routing protocols have to contend with.

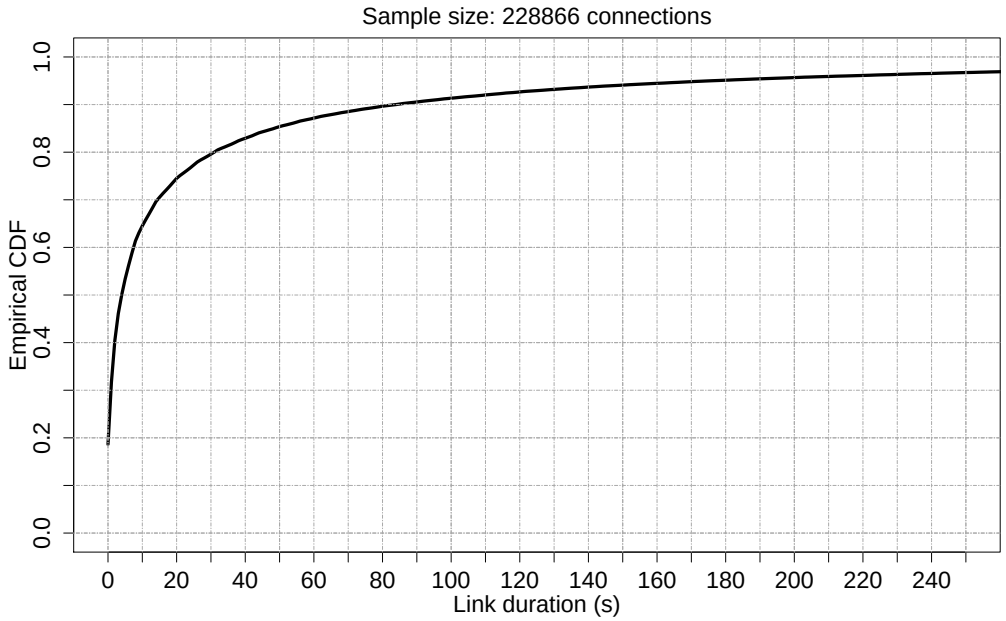

Figure 2.1: Link duration in a vehicular network.

Figure 2.2 shows a taxonomy of routing protocols proposed for wireless ad-hoc networks, divided according to the type of information they use. The protocols innitially developed for wireless networks were largely derivative of traditional wired network routing protocols, and as such, base their routing decisions on topology information that is periodically disseminated across the network. This class of *topology-based* protocols includes OLSR [CJ03], DSDV [PB94], Babel [Chr11] and Batman [JNA08]. While these protocols attempt to minimize control overhead (e.g., OLSR uses only a subset of neighbors for dissemination; DSDV shares only information between direct neighbors), these proactive protocols introduce control overhead even when the network is idle. And, most importantly, they have trouble reacting quickly to topology changes, which are very frequent in vehicular networks: by the time a route is done being disseminated through the network, it is likely that at least one of the links that compose it has already disappeared.

An alternative to proactive routing is reactive routing, e.g. DSR [JMB01] and AODV [Per99], where routes are only discovered on demand, reducing the overhead in situations where only a subset of nodes is communicating at any given time and therefore allowing for better scaling. Routes are discovered through a flooding discovery mechanism, and stored in routing tables by relay nodes (AODV) or in the packet header by the source (DSR). The latter meth-d is referred to as source-based routing. While reactive routing obviates the need for global topology knowledge and has been shown to provide a good improvement in throughput over periodic routing [FGEG11], it still requires routes to be stable.

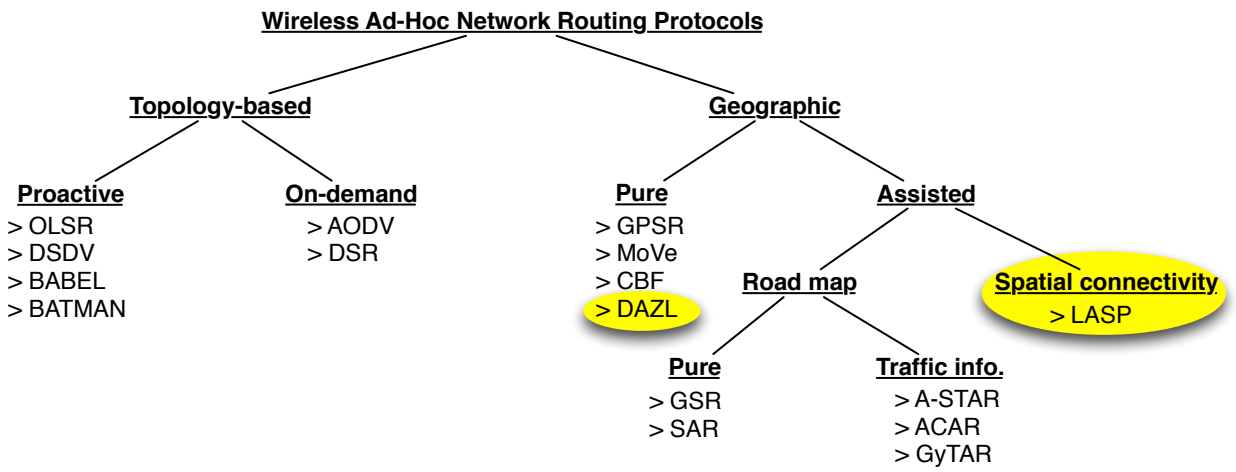

Figure 2.2: Wireless Ad-Hoc Networks routing protocol taxonomy

Abolhasan *et al.* [AHW09] evaluated OLSR, Batman, Babel and AODV using a small, static, 8-node indoor network. When a link was removed on purpose, the fastest protocol, Babel, took an average of 14.4 seconds to recover. This result shows how unsuitable topology-based protocols are in the high mobility context of vehicular networks, where links have short life spans—Figure 2.1.

For this reason, most of the research on routing for vehicular networks has focused on geographic protocols. In geographic routing, routes are not based on pre-determined routing tables, or placed in the packet header. Instead, the route is built on-the-fly as the packet travels towards the destination, one hop at a time, based on a geographic heuristic. Because the choice of next hop node is made very late (by the previous node), geographic protocols are able to more quickly adapt to changing conditions.

Geographic routing decouples routing from individual node identifiers. Instead, packets are routed to a given geographic location. This ties in perfectly with geocast applications. Regular unicast/multicast applications require an additional node location service [LJDC$^+$00, CBW02, GS06] or an equivalent type of side information to map node identifiers onto geographical coordinates.

When compared with traditional topology-based routing, geographic routing is inherently better suited to vehicular network use. However, geographic protocols still have to deal with two major challenges. First, link instability makes choosing a reliable next hop difficult. Second, the spatial heterogeneity of vehicular network connectivity makes it hard to choose a direction to forward the message in. We discuss these issues further in the following subsections.

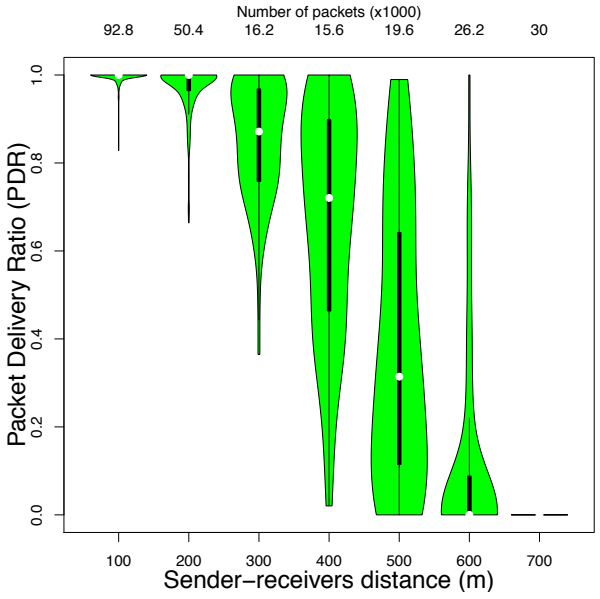

Figure 2.3: Gray-zone of partial connectivity in a vehicular network.

2.2 Link Instability

Geographic routing protocols differ mostly in the heuristic and associated metric used to select the next hop node. The simplest heuristics are greedy in nature [LS00], for example choosing the node that is closest to the straight line between the current node and the destination (i.e. compass routing), or simply the neighbor closest to the destination. The latter is a very popular heuristic used by a myriad of protocols, e.g. GPSR [KK00], GPCR [LMFH05], A-STAR [SLL+04] and Gytar [JSMGD07]. It is, however, problematic in that faraway nodes will generally experience poor channel quality. As a response to that, ACAR [YLL+10] takes link quality into account by using a modified Expected Transmission Count (ETX) metric [CABM05] to select well-connected relays. TVR [BMB+14], on the other hand, proposes the use of tall vehicles such as trucks where available, because they have a line of sight over the roof of shorter vehicles.

Since routing decisions are made hop-by-hop, geographic forwarding is less vulnerable to topology changes caused by node movement. However, there are other factors causing instability. Namely, obstacles such as buildings and terrain features like hills and mounds create strong slow fading, while the multipath from reflections on obstacles introduces significant fast fading. The result are unstable links with partial and intermittent connectivity.

To see this for ourselves we equipped 2 cars with NEC Linkbird-MX 802.11p communication devices [FBZ+08] and GPS receivers for location tracking and drove them around an urban loop in the city of Porto, Portugal. Figure 2.3 shows the Packet Delivery Rate (PDR) as a function of

sender-receiver for this experiment. While connectivity at short distances was good, the plot shows a large area of partial connectivity, with the median PDR crossing the 90% mark at 300 m and only dropping to zero at 600 m. This area is known as the *gray-zone* [BSK10].

In summary, there are very few good links in VANETs, and the ones that are good, tend to cover a short distance and thus be unattractive for multi-hop communication. Protocols that rely on a single relay per hop will end up experiencing reliability problems. To tackle this issue we introduce DAZL in Chapter 3, a protocol that removes the dependency on a specific link by allowing multiple potential relays to cooperate in forwarding each packet.

2.3 Spatial Heterogeneity

Pure geographic routing protocols, i.e. protocols that rely solely on the nodes' locations, like GPSR, try to guide packets ever closer to the destination. The reasoning behind this is that the closer the packet is to the destination, the more likely it will reach it in few hops, assuming connectivity is uniform across space. In practice however, this assumption does not hold. Connectivity is influenced by topography, including buildings, vegetation and elevation changes, all of which can differ between locations. These obstacles affect the line of sight between antennas, creating attenuation and multipath due to reflections [JS08, OBB09].

To quantify the effect of different line of sight blockages on channel quality we again equipped 2 vehicles with NEC Linkbird-MX 802.11p communication boxes [FBZ+08] and GPS receivers, and drove a series of urban, suburban and highway routes around Pittsburgh PA, USA, all the time collecting PDR information. Using video footage collected during the experiments, we were able to split the data into 3 categories: i) unobstructed line of sight; ii) line of sight obstructed by third-party vehicles; and iii) line of sight obstructed by static obstructions such as terrain and buildings.

Figure 2.4 summarizes that study's results [MBS+10], by showing PDR as a function of sender-receiver distance for the different categories. It is clear that static obstructions had a very significant impact on connectivity. If we consider a PDR threshold of 80%, static obstructions reduced the communication range by a factor of almost 4. Even blockages by third-party vehicles had a noticeable impact, which was not obvious before this study was performed. Mangel *et al.* [MMKH11] and Neves *et al.* [NCMS11] have since reported similar results for non-line of sight reception in intersections.

Another way in which spatial heterogeneity manifests itself is in terms of node density. Major roadways often experience traffic congestion, while back streets are often devoid of vehicles. Furthermore, a single road can experience significantly different node densities throughout the day.

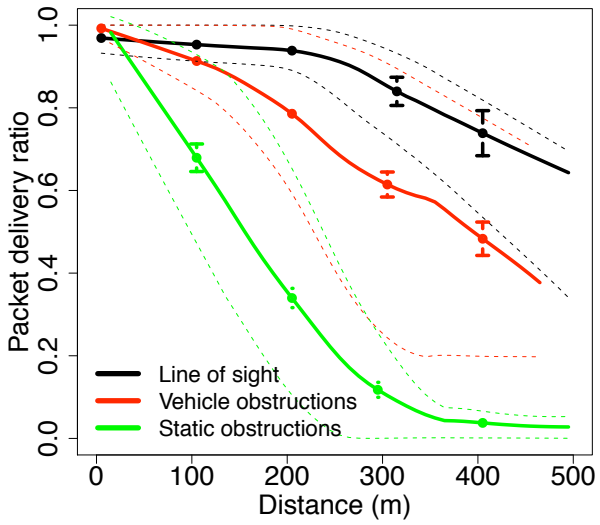

Figure 2.4: Impact of line of sight conditions on packet delivery rates.

Bai *et al.* [BK09] reported expected inter-vehicle spacings for a Toronto suburban freeway ranging between the extremes of 6 and 500 meters, depending on the time of the day.

Both extreme node densities, high and low, create difficulties for multi-hop protocols. When there are too many vehicles, it is important to control contention and avoid saturating the channel. When there is a dearth of vehicles, it becomes difficult to ensure end-to-end reliability.

Multiple strategies have been proposed to deal with reliability in low density scenarios. GPSR greedily attempts to send the packet ever closer to the destination, but when no neighbor closer than the current packet holder exists, it switches to perimeter mode, a recovery procedure where the protocol traverses the network graph using the right-hand rule[1] until greedy forwarding can resume. This strategy assumes, however, that network connectivity can be described by a unit graph in which all nodes within a fixed radio range are connected and nodes outside this range never are. Generally, this assumption does not hold in vehicular networks, where different nodes can experience different communication ranges.

Other geographic protocols attempt to circumvent areas without nodes by using additional information beyond neighbor locations. We classify them as assisted geographic protocols in Figure 2.2. Tipically, the extra information is a map of the road network, which is used to find a sequence of roads connecting source and destination locations. Messages are then forwarded along this specific sequence of roads to reach the destination. Roads are chosen as a backbone for routing for two main reasons. First, vehicles drive on roads, so by routing along roads, the probability of disconnec-

[1]The right-hand rule consists in picking as a relay the first node counter-clockwise relative to the line segment defined by the locations of the current node and destination.

tion is decreased. Second, roads go around buildings and mountains, serving as an approximation for signal propagation patterns. Examples of road map-based protocols include GSR [LHT+03], SAR [THR03]) and GyTAR [JSMGD07].

Road map-based geographic routing is a marked improvement over earlier proposals but does not completely address the spatial heterogeneity problem. This happens because there is a disconnect between the vehicles' and the packets' mobility. While vehicles can only switch from one road to another at intersections, data packets can hop across any two locations as long as the wireless signal can propagate between them. This is especially relevant in cities with a high density of roads. For example, packets may jump back and forth across parallel highways, parking lots, streets on opposing river banks, or streets with no buildings in between. By constraining packets to roads, all of these opportunities are left unexplored.

Furthermore, the selection of frequently-traveled roads on the assumption that more vehicles always leads to better performance can create problems, as having too many vehicles can lead to channel saturation. Studies have shown that in congested multi-lane roads, even a simple beaconing application can lead to network collapse if not designed carefully [vKKH09].

To tackle these limitations, instead of using a road map, we propose to use a spatial connectivity map in our LASP and LASP-MF protocols — Chapters 4 and 5. Noting that the topographic characteristics that influence signal propagation are highly correlated with location and do not change quickly with time, we propose to use a history of past communications to predict future connectivity, which can then be used as a backbone for geographic routing. Because it uses PDR measurements, this technique is able to indirectly incorporate all factors affecting connectivity, allowing the protocol to find better connected paths.

2.4 Protocol Evaluation

It is important for multi-hop communication protocols to be tested under conditions that are as close as possible to those found in production environments. This means testing VANET protocols using actual WAVE hardware mounted in actual vehicles driving on actual roads. Unfortunately, vehicular testbeds are very expensive and difficult to manage. For this reason, protocols in the literature have been evaluated either using simulation or small scale experiments.

Simulation tools try to approximate the vehicular wireless channel but are often devoid of crucial details [MFB09]. For example, many protocols, e.g. SAR [THR03] and ACAR [YLL+10], were evaluted using simulations where obstacles were not considered. And as we have seen in the previous section, obstacles can severely affect the wireless vehicular channel. When obstacles are considered, models are usually oversimplified, for example by having signal propagation between

Figure 2.5: Leixões Harbor's South Terminal as seen from the top of a gantry container crane. Image courtesy of Luís Cabrita [Cab].

streets completely blocked [HHH08].

Road topologies are also often made overly simple, with one popular choice being the Manhattan grid, e.g. as used by A-STAR [SLL+04]. Mobility is also often unrealistic, with synthetic trip and motion models being employed [HHH08]. Furthermore, protocols are not usually tested under high load scenarios: node densities are never as high as in real-world traffic jams and the number of flows is very limited.

When experimentation is used, it is usually very limited in scope. In a pioneering effort Johnson *et al.* [JMB01] tested the DSR protocol in 1999 using 802.11 hardware and 5 vehicles. In 2008 Jerbi and Senouci [JS08] performed tests with a platoon of 6 vehicles using 802.11b hardware and preconfigured, fixed routing paths. The following year Santa *et al.* [STE+09] evaluated OLSR with 4 vehicles. In 2011 Boban *et al.* [BMB+11] performed multi-hop experiments using 802.11p hardware but again only 4 vehicles.

These early experiments have shown large deviations from simulation results, thus highlighting the importance of experimental evaluation. With this in mind, in our work we used two vehicular testbeds currently deployed in the city of Porto, Portugal, totaling more than 400 nodes.

The testbed we used the most in our work was HarborNet [ACN+14]. HarborNet is a network of 30 nodes deployed on the Leixões Harbor, in Porto, Portugal[2]. Out of the 30 nodes, 5 are Road-Side Units (RSUs) and 25 are On-Board Units (OBUs). All units implement the IEEE 802.11p and WAVE standards for vehicular communication [AMM+11]. They are also equipped with a GPS receiver for location tracking and a cellular interface for remote management.

The OBUs are installed in the trucks that carry containers to and from the ships that dock at the harbor. They work around 10 hours a day, every business day. Figure 2.5 depicts the environment in which they operate. Containers are stacked and organized into rectangular areas akin to small city blocks. Between these areas, impromptu streets are formed, which are used by the trucks to move around the harbor. The end result is reminiscent of a miniature Manhattan-like street grid, with metal containers substituting buildings.

Figure 2.6 shows a satellite view of the 1 Km^2 harbor, complete with a network graph depicting an example network topology, recorded on June 2nd, 2014, circa 12 PM. Balloons represent nodes and lines represent active links between them. Red links have lower signal strength than yellow ones. As the figure demonstrates, HarborNet is deployed in a small area, resulting in a dense network. This, combined with the harbor's city-like structure which prevents the network from being fully connected, makes it suitable for multi-hop protocol evaluation.

The second testbed we used was PortoVANET. PortoVANET employs the same hardware and software as HarborNet but, instead of harbor trucks, the OBUs are installed in around 400 buses and taxi cabs that serve the city of Porto, Portugal. Because PortoVANET nodes are spread out across a very large area and only a portion of nodes are active simultaneously, connected subcomponents of diameter 2 hops or larger are not very frequent. For this reason we use PortoVANET for connectivity data collection but not for routing experiments.

The creation of both PortoVANET and HarborNet testbeds happened concurrently with the work presented in this document. In fact, the work developed by the authors contributed directly to their development. For this reason, only LASP and LASP-MF were able to make use of them. During the time in which DAZL was developed, our resources were limited to 5 OBUs that we deployed temporarily and specifically for each experiment we wanted to perform.

[2]More precisely, the harbor is located at coordinates 41 11' 25" N, 8 41' 24" W.

Figure 2.6: Leixões Harbor area and example HarborNet network graph. Imagery ©2014 Google, Cnes/Spot Image, DigitalGlobe and IGP/DGRF.

Chapter 3

DAZL: Density-Aware Zone-based Forwarding

This chapter introduces the DAZL forwarding protocol. DAZL forwards packets along a straight line towards the destination using zone-based forwarding to exploit node diversity and improve reliability. We start by evaluating the potential benefits of exploiting node diversity in vehicular forwarding. We then describe DAZL's design and finally evaluate the protocol using a combination of small-scale experiments and large-scale simulations.

3.1 Premise: Node Diversity

Traditionally, in geographic protocols, at each hop the node holding the packet selects one specific node from its immediate neighborhood to be the next hop and then proceeds to send the packet to that specific node, as per Figure 3.4a. As described in Chapter 2, this can be problematic: since vehicular links have a large gray-zone of partial connectivity, very few links (other than very short ones) consistently feature high packet delivery ratios. However, we note that, due to their spatial separation, different vehicles experience different multipath and shadowing effects from obstacles. We call this difference between the different nodes *node diversity*.

To evaluate whether it can be exploited to improve forwarding reliability, we performed an experimental study in the city of Porto, Portugal, using a set of 4 vehicles of average size[1]. Each vehicle was equipped with a GPS receiver for position tracking and a NEC Linkbird-MX 802.11p communication device [FBZ+08], configured according to Table 3.1.

[1]We used B and C-segment cars, the top selling segments in Europe. Vehicle dimensions varied between 1.3 and 1.5 m in height, and between 3.8 and 4.5 m in length.

Parameter	Value
Center frequency (MHz)	5900 (DSRC channel 180)
Bandwidth (MHz)	10
Data rate (Mbps)	3
Tx power (setting, dBm)	18
Antenna gain (dBi)	6
Beacon size (Byte)	36
Beaconing frequency (Hz)	10

Table 3.1: Linkbird configuration parameters for the node diversity experiments.

Figure 3.1: Node diversity experimental scenario. Imagery ©2014 Google, Cnes/Spot Image, DigitalGlobe and IGP/DGRF.

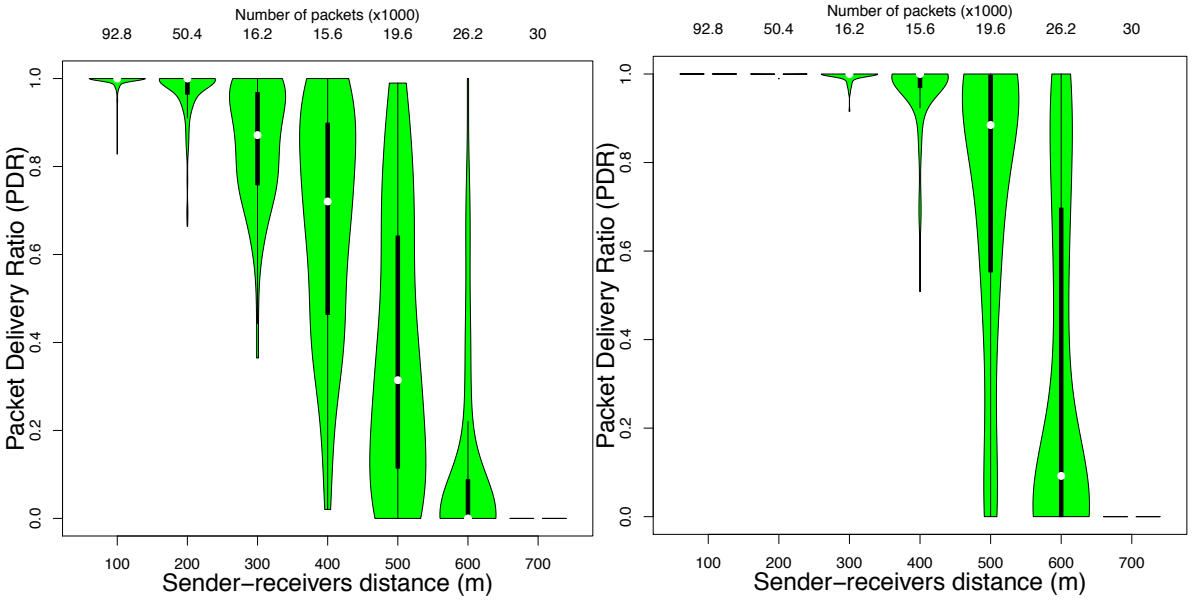

(a) PDR of a single receiver

(b) Combined PDR of 3 receivers

Figure 3.2: Effect of node diversity on packet delivery rates.

Figure 3.1 accurately depicts the scenario under which the experiments were performed. We parked a vehicle on Av. Brasil street in Porto (the red circle s in the figure), started broadcasting beacons and had 3 receivers drive a 4-Km long circuit (the yellow path in the figure) around it while collecting packet delivery data. To minimize the effect of spatial separation the 3 receivers drove in close formation, constantly trading positions as cyclists riding in a peloton. The surrounding environment was urban in nature, with 4-5 story buildings on one side of the street, and the Douro River on the other.

Figure 3.2a shows a violin plot of the PDR as a function of sender-receiver distance for a single receiver. Here we can observe that the channel began to degrade significantly at a distance of around 300 m, with a large gray-zone of partial connectivity from that point all the way to 600 m.

Figure 3.2b shows what happens when we consider the PDR aggregated over the three receivers, i.e. a message is said to be received as long as at least one receiver node was able to correctly decode it. This resulted in a very noticeable improvement: the median PDR now starts to drop only at 500 m.

Let us now analyze the gains attributable to each individual additional receiver. For this purpose we define the concept of *diversity gain* as the ratio of messages that can be decoded due to node diversity divided the number of messages that are lost by the first receiver. This tells us what percentage of the losses can be recovered using this strategy.

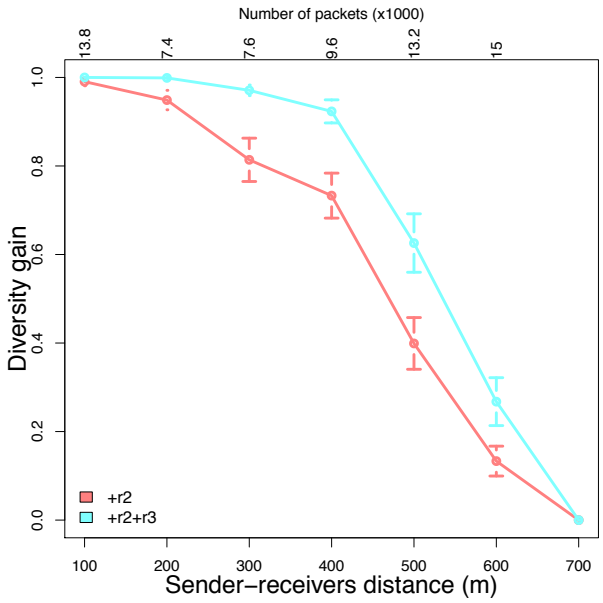

Figure 3.3: Diversity gain from additional receivers.

Figure 3.3 shows the diversity gain as a function of distance for two cases. The red line represents a situation where only one additional receiver, **r2**, is added to the baseline of the first receiver. This addition yielded a very significant gain of at least 75% of losses up to 400 m. Adding a third receiver, **r3**, which is represented by the cyan line, allowed us to recover 95% of all losses up to the same distance.

In summary these experimental results show that there are significant benefits to be gained by a protocol that is able to exploit node diversity. And that the returns diminish as the number of receivers increases.

3.2 Protocol Design

In this Section we describe the zone-based forwarding concept implemented by DAZL and how forwarders coordinate to prioritize the best-positioned among them and control congestion.

3.2.1 Zone-based Forwarding

Figure 3.4 shows the main distinction between DAZL and traditional geographic protocols. The latter forward messages to a specific neighbor, as per Figure 3.4a. DAZL, on the other hand, forwards packets to a geographic forwarding zone located between the sender and the destination. Any vehicle inside the zone can then forward the packet. As we have seen in the previous section,

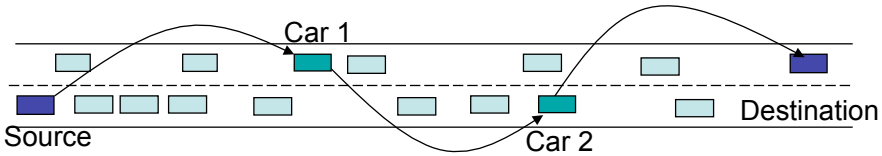

(a) Neighbor-based scheme

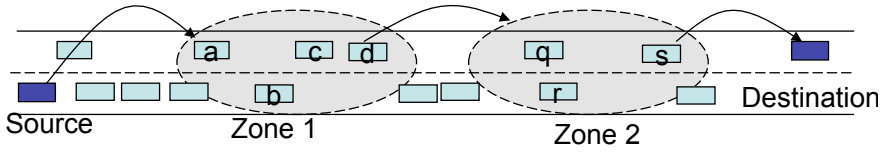

(b) Zone-based scheme

Figure 3.4: Contrast between neighbor-based and zone-based forwarding.

since different nodes experience different error patterns, this increases the likelihood that the packet is successfully forwarded.

DAZL's design is based on the following premises:

Addressing DAZL assumes that the destination's location is known, so that it can be used to guide the geographic forwarding process. This ties in directly with geocast applications, which inherently use geographic addressing. Traditional unicast/multicast applications should obtain the destination's location from a location service [LJDC+00, CBW02, GS06] or similar, which are outside the scope of this work.

Location awareness Nodes are assumed to be able to track their own location, be it through GPS, GLONASS or other means.

Beaconing Besides knowing their own location, DAZL assumes nodes are able to learn the location of their immediate (i.e. 1-hop) neighbors. For this we propose leveraging Cooperative Awareness Messages (CAMs), which were initially standardized by ETSI [ETS11] for use in safety applications. These messages are broadcast by every node 10 times per second and include the sender node's position. Therefore we can reuse them in DAZL, avoiding the introduction of additional control overhead.

We now describe the protocol operation. The source starts by encapsulating the packet with a geographic header, which includes: a message identifier; the destination's location; its own (the sender's) location and; its communication range in the destination's direction. The latter is defined as the distance between the sender and the destination minus the distance between the sender's neighbor which is closest to the destination and the destination. More formally, the communication

range *commRange* is defined as:

$$commRange(s, d) = dist(c, d) - \min\left[\forall\ n \in \mathcal{N}_s : dist(n, d)\right], \tag{3.1}$$

where s is the sender node, d is the destination, $\mathcal{N}_s$ is a set composed of the sender's neighbors and $dist(a, b)$ is the great-circle distance between a and b's locations.

Once the header is set, the packet is broadcast. Then, each node receiving the packet executes the workflow depicted by the activity diagram in Figure 3.5, which we now describe, step by step:

1. The receiver computes both its own distance to the destination and the sender's distance to the destination, based on the locations specified in the geographic header. If the receiver is farther from the destination than the sender, it drops the packet. Otherwise, it continues on to the next step.

2. The receiver compares its distance to the destination with the sender's distance to the destination minus the communication range specified in the packet header. If the receiver's distance is shorter than that, the packet is dropped. Otherwise, the protocol continues on to the next step. This is to avoid situations where the sender can not hear acknowledgments from the next hop because it is out of range.

3. The receiver now runs a ranking algorithm to compare its utility as a forwarder with the utility provided by other potential forwarders in its 1-hop neighborhood. The ranking algorithm is detailed in the next section.

4. If the receiver is thought to be one of the n best potential forwarders then it recognizes itself to be in the *forwarding zone*. Otherwise, it drops the packet.

5. Being in the zone, the receiver now waits a period of time inversely proportional to its rank before forwarding the packet (i.e. the lower the rank, the longer the wait). We call this *rank-based slotting*.

6. If, while in the waiting state, the receiver overhears the forwarding of the packet by another candidate forwarder, it knows that no further transmissions are needed and therefore cancels the forwarding operation. Otherwise, it forwards the packet after the required amount of time has elapsed.

This procedure is repeated in every hop until the destination can be found within the sender node's neighborhood. When that happens, the message is directly forwarded to it.

The *implicit acknowledgment* scheme described in the last step is used not only to cancel unnecessary forwardings but also to inform the previous hop node that the packet was successfully

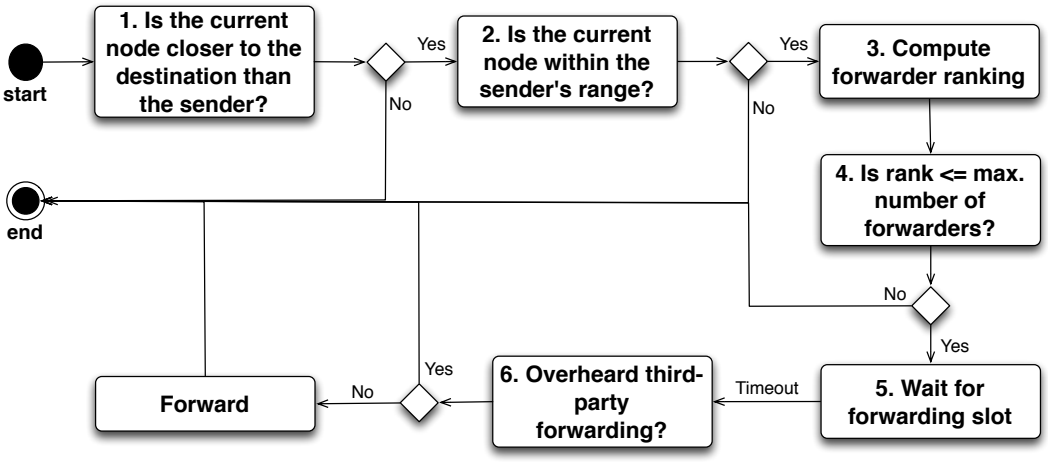

Figure 3.5: DAZL forwarding workflow diagram.

forwarded. When the previous hop does not overhear the forwarding of the packet by a relay or an explicit acknowledgement from the destination for a certain period of time, it assumes no one received the packet and retransmits it. In the event that an implicit acknowledgment does not reach the previous hop or any of the other potential forwarders due to changes in the channel conditions, it is possible for redundant forwardings to occur. To mitigate this problem DAZL implements a simple duplicate suppression scheme. Each node keeps a buffer of previously overheard packets and uses it to check whether an incoming message is a replica of a previously received one. If that is the case, it is immediately dropped.

As more receivers are added in high density scenarios, we get to a point of diminishing returns in terms of the benefits obtained from node diversity, as exemplified in Section 3.1. DAZL controls this tradeoff between diversity gain and contention by limiting the number of forwarders to a number n, a parameter. If we set n to say, 5, the performance in low density scenarios is maintained because in those conditions no one is excluded from forwarding. In high density scenarios, performance improves because we reduce both contention for medium access and the risk of redundant forwardings.

3.2.2 Forwarder Coordination and Prioritization

In DAZL, potential forwarders coordinate through a distributed algorithm. While the 802.11p MAC's Distributed Coordination Function (DCF) already implements some basic coordination, it has trouble accommodating very large numbers of nodes. Our solution is to introduce an additional level of slotting at the network layer. Time after packet reception is divided into a number of forwarding slots and candidate forwarders distribute themselves over them. The slot duration

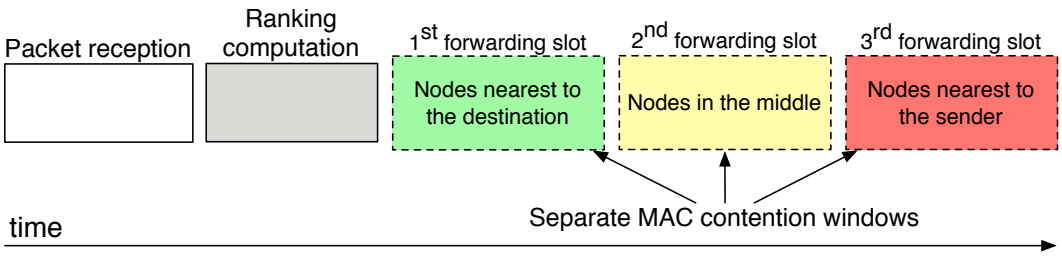

Figure 3.6: DAZL spreads forwarders in time according to their distance to the destination.

should be configured to be just slightly longer than the average MAC layer contention window so that nodes in different slots do not compete but also do not wait around needlessly.

The assignment of candidate forwarders to slots is done through the use of a ranking algorithm, which is also used to opportunistically maximize the distance traveled in each hop. DAZL achieves this prioritization through a smart assignment of nodes to forwarding slots: candidate forwarders close to the destination get earlier slots, while nodes closer to the sender get later ones, as per Figure 3.6. Using information about the neighbors' locations collected from the periodic CAMs and the communication range set by the sender in the packet header, each candidate forwarder node independently calculates the ranking as follows:

1. Compute a set of expected forwarders $\mathcal{E}_p$ for packet p, which is composed of the nodes that are closer to the destination than the previous hop and also within its radio range as specified in the packet header.

2. Build an array r from the nodes in the set $\mathcal{E}_p$. Now sort r according to each node's distance to the destination. The index i at which a node appears in r is now its rank.

3. For each node in $\mathcal{E}_p$, assign it a forwarding slot $s = \left\lceil \frac{rank}{nps} \right\rceil$, where $rank$ is the node's rank and nps is the number of nodes per slot, a protocol parameter. This ensures that the first forwarding slot is taken by the nodes providing the most progress towards the destination, in terms of distance traveled.

The nps parameter controls a tradeoff between replication and latency: if more nodes are allowed per slot, the expected latency decreases while replication is expected to increase. Also note that candidate nodes with ranks larger than the limit number of forwarders n, refrain from forwarding to avoid excessive replication.

Let us use the scenario of Figure 3.4b to go through an example of how this ranking works. For simplicity, assume that the forwarding zones are defined as pictured, that each node within a zone has all the other nodes in the same zone in their neighbor table, and that each node gets its own

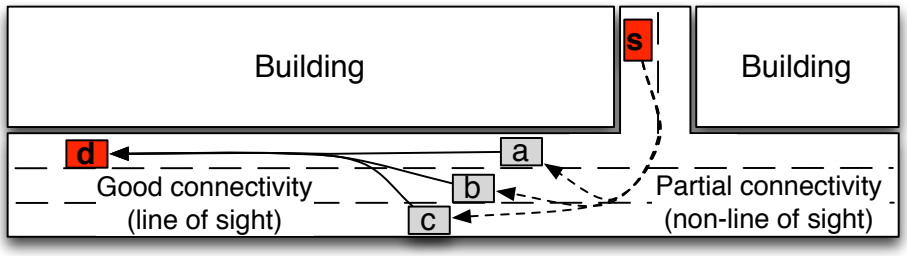

Figure 3.7: DAZL experimental scenario.

forwarding slot ($nps = 1$). Consider, as an example, that in the first hop the set of nodes that receive the packet is $\mathcal{A}_m = \{a, b, d\}$. However, these nodes do not know that c did not receive the packet, so they will consider all the nodes in the zone for their ranking, making the expected set $\mathcal{E}_m = \{a, b, c, d\}$. Ordering the nodes according to their distance to the destination, all candidate forwarder nodes will reach the same ranking $r = [d, c, b, a]$. Now, node d will the assigned the 1^{st} forwarding slot and c, b and a the 2^{nd}, 3^{rd} and 4^{th} slots, respectively. Realizing that it is in the 1^{st} slot, node d will immediately forward the packet. Nodes a and b will then overhear d's packet and cancel their own forwardings, avoiding any duplication.

Using this ranking algorithm nodes can reach a consensus on who should forward the packet first and maximize the forward progress towards the destination, while the closer nodes in the later slots act as failsafes to improve reliability.

3.3 Experimental Evaluation

In this section we present an experimental evaluation of DAZL using a small two hop-diameter network.

3.3.1 Setup

Buildings are known to have a significant negative impact on VANET communication [OBB09, MBS+10]. We experimentally evaluated DAZL under such conditions using the setup in Figure 3.7, which used all of the 5 nodes we had available at the time. The source and destination cars were parked on two adjacent sides of a building and were unable to communicate directly. However, there were three nodes near the corner of the building which could help by forwarding packets. Although it did not completely stymie communication, the building affected the quality of the channel between the source and the relays.

Parameter	Value
Center frequency (MHz)	5900 (DSRC channel 180)
Bandwidth (MHz)	10
Data rate (Mbps)	3
Tx power (setting, dBm)	5
Antenna gain (dBi)	6
Data packet size (Byte)	256
Beaconing frequency (Hz)	10

Table 3.2: Linkbird configuration parameters for the DAZL experiments.

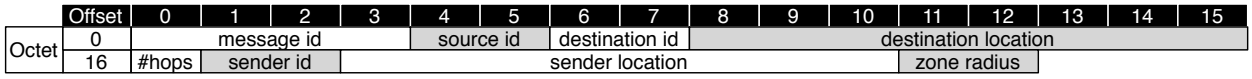

(a) DAZL header (29 bytes)

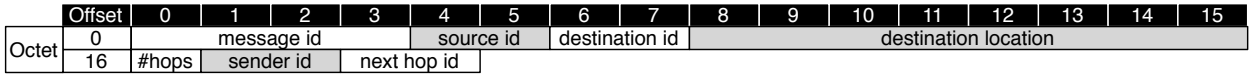

(b) Neighbor-based protocol header (21 bytes)

Figure 3.8: DAZL and neighbor-based geographic header formats.

Each vehicle was equipped with a NEC LinkBird-MX [FBZ+08] compatible with the IEEE 802.11p standard. The system configuration parameters are summarized in Table 3.2. CAM beaconing was used for neighborhood discovery and GPS receivers for location tracking.

Due to the LinkBirds's limitations, the protocols were implemented as an application running on a laptop connected to the LinkBird through ethernet. This means packets must travel across two protocol stacks and over the wire before being transmitted. This had two main implications for DAZL. First, overall latency suffered. Second, overheard packets took longer to process, increasing the likelihood of unnecessary replication. To mitigate this, we used longer 25 msec forwarding slots in our trials, giving the protocol more time to process overheard packets.

We tested DAZL against a traditional geographic protocol where the sender picks, at each hop, a specific neighbor to act as the next hop relay towards the destination. We shall refer to this protocol as the neighbor-based protocol. Picking a next hop involves a difficult tradeoff between delivery rate and distance travelled towards the destination. Because of this, the implemented protocol uses a conservative algorithm based on a metric that combines both distance and reliability. Specifically, this protocol chooses the node that is closest to providing 50% of the progress towards the destination given by the neighbor closest to the destination to be the next hop (i.e. the neighbor

closest to the middle of the radio range). For example, a node with three neighbors, a, b and c, respectively providing 200, 100 and 50 m of distance travelled towards the destination, will choose b as the relay. The value of 50% was taken from the results in Figure 3.2a, where the PDR of a single receiver remained under 80% in the second half of the communication range.

DAZL was configured to allow up to 3 forwarders ($n = 3$), one per forwarding slot ($nps = 1$). The conservative neighbor-based protocol picked the node closest to half of its radio range, which in this case was a. The format of the geographic headers used are specified in Figure 3.8.

Retransmissions were disabled for all schemes, in order to highlight the differences in robustness between the protocols. The experiment consisted of sending 100,000 250 bytes packets from source to destination using each of the protocols. Packets were generated at the source at a constant rate of 250 per second.

3.3.2 Results

Throughput

Figure 3.9a compares the mean throughput achieved by DAZL and neighbor-based forwarding in packets per second. The 95% confidence intervals are shown by means of ranges. Because the neighbor-based scheme uses a single relay, its performance was severely affected by losses on the source-relay link. In fact, it only managed to get 84 packets per second to the destination, 33% of the source rate. DAZL, on the other hand, does not rely on any single node. It is able to leverage multiple relays and separate them into different forwarding slots. This resulted in a throughput improvement of 63% relative to the neighbor-based protocol, or 137 packets per second.

Latency

Figure 3.9b shows the mean unidirectional end-to-end latency for the two protocols. Because of the platform limitations, the absolute values were larger than they would be in a production environment. In relative terms there was a delay increase of around 25 millisecond when moving from neighbor- to zone-based forwarding. This is due to the latency introduced by slotting. In a production version, the latencies would be lower: the protocol stack would be implemented by a single device, allowing for much shorter slots, i.e. a few hundred microseconds.

Number of Replicas

Figure 3.9c shows the mean number of replicas observed at the destination. Because retransmissions due to message losses were disabled, the neighbor-based protocol generated no replication. DAZL

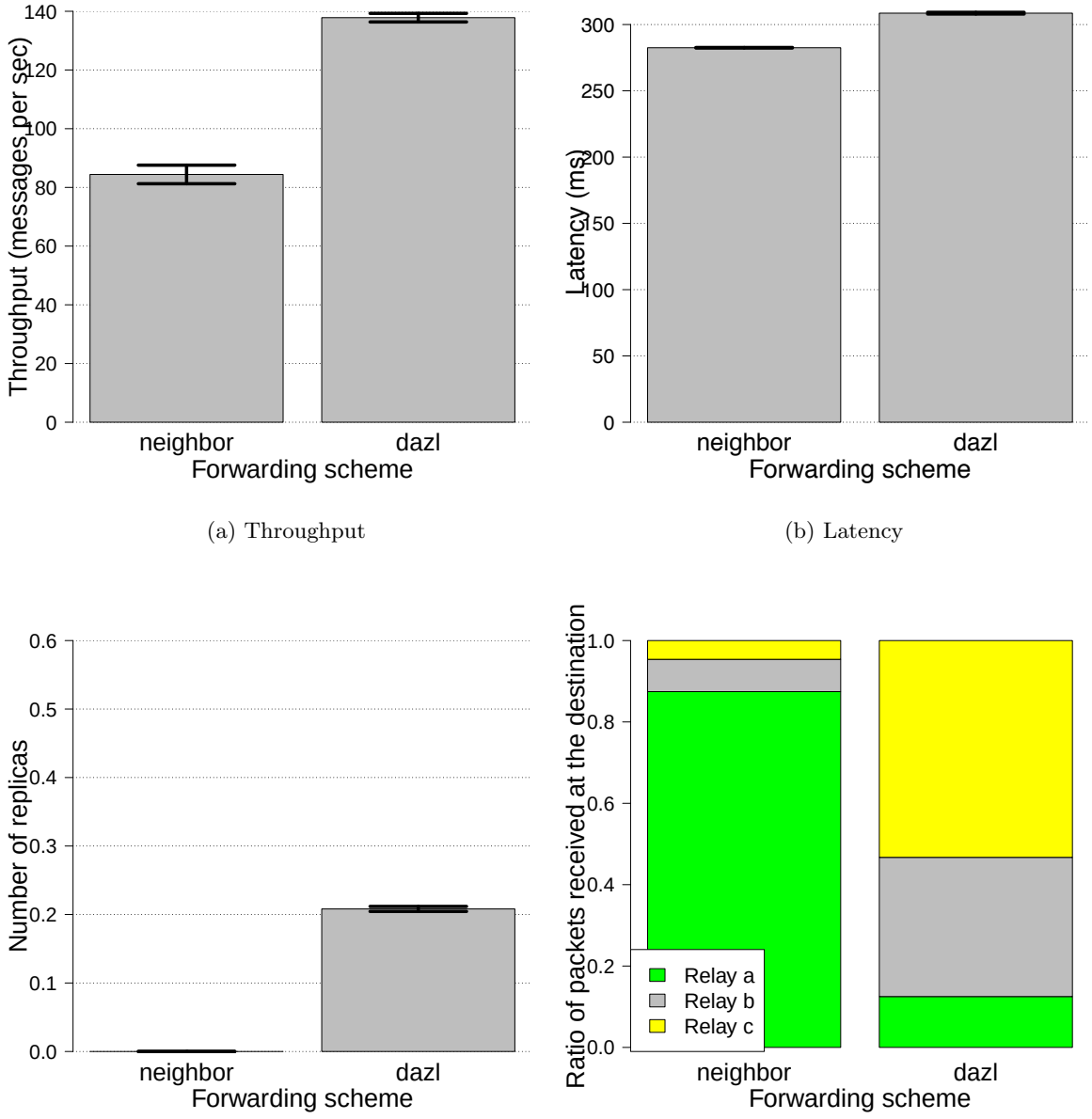

(a) Throughput

(b) Latency

(c) Number of replicas

(d) Relay diversity

Figure 3.9: DAZL experimental evaluation performance results.

generated, on average, 20% of replication. This number is artificially high because of the radio setup on the Linkbirds. When a node overhears a forwarded packet from another relay, it should refrain from forwarding. This is done by having the forwarding protocol tell the MAC to drop the now redundant message from its transmit queue. We were however unable to alter the MAC layer

on the Linkbirds to do this, which resulted in duplicate packets. Production systems would use a single stack implementation of DAZL, which would prevent this problem.

Relay Diversity

Finally we look at relay diversity: from all the packets reaching the destination, we computed the ratio that came from each of the different relays and plotted it in Figure 3.9d. The conservative neighbor-based scheme chose relay a roughly 90% of the time. The 10% attributed to relays b and c were likely caused by occasional losses of connectivity leading to node a temporarily being erased from the source's neighbor table.

DAZL assigns slots based on the distance to the destination so node c gets the 1^{st} slot, b the 2^{nd} and a the 3^{rd}. Node c has the highest priority and accounts for around 50% of the packets at the destination. Node b accounts for 40% and node a 10%, values that are consistent with their slot assignments.

These results highlight the benefits of the DAZL scheme, even when only a few forwarders are available.

3.4 Simulation Evaluation

In this section we present a simulation evaluation in DAZL using larger scenarios with up to 100 nodes.

3.4.1 Setup

We used the ns-3 simulator [ns3] with 802.11p support to perform our evaluation. The channel parameters used in the simulations are presented in Table 3.3.

Parameter	**Value**
Center frequency (MHz)	5900
Bandwidth (MHz)	10
Data rate (Mbps)	3
Tx power (dBm)	16
Fading model	Nakagami, m=1.5

Table 3.3: DAZL ns-3 simulation configuration parameters.

We compared DAZL with two benchmark protocols. The first was the conservative neighbor-based protocol previously used in the experimental evaluation. The second was an oracle zone-based protocol that allowed us to understand how close DAZL gets to an idealized protocol with access to perfect and global information. The oracle-based protocol works as follows:

1. The node currently holding the packet (initially the source) broadcasts the packet.
2. Every node in the network tells the oracle whether they have successfully received the packet or not.
3. Once the oracle has heard from all nodes it chooses the receiver closest to the destination to be the forwarder.

We also implemented neighbor-based forwarding using a greedy approach, which picks the neighbor closest to the destination (i.e. as in GPSR), and a random approach, (i.e. picking the next hop relay uniformly at random from the available neighbors), but, because their performance was consistently very poor, they are not discussed here.

Nodes were placed on a 1 Km-long road according to an exponential distribution representative of an actual highway [BK09]. In order to assess DAZL's behavior under different node densities we did multiple runs using average inter-vehicle distances ranging from 80 (sparse but connected) to 10 meters (traffic jam). Results for each distance were averaged over five 60 second runs with different random seeds.

The traffic pattern was as follows: a sender at one end of the road sent 322 byte data packets at a rate of 200 per second to a destination at the other end of the road. DAZL forwarding slots were set to 2 ms. The number of forwarders was limited to 7. The maximum number of retransmissions was set to two for all protocols.

3.4.2 Results

Throughput

We begin by looking at the throughput for the three schemes under scrutiny in Figure 3.10a. The vertical lines and hash marks represent the 95% confidence intervals, where available. The neighbor-based protocol hovered around 110 packets per second (55% of the source rate). This is the result of packets losses: 45% of the time the selected next-hop was unable to successfully receive the packet. The oracle scheme, however, does not rely on any specific node: it works as long as at least one node, any node, receives the packet. Due to this it got very close to the source rate of 200 packets per second. DAZL delivered up to 185 packets per second, which is within 10% of

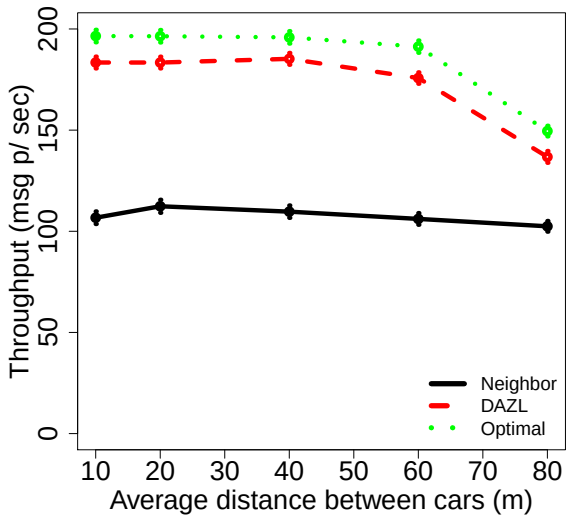

(a) Throughput

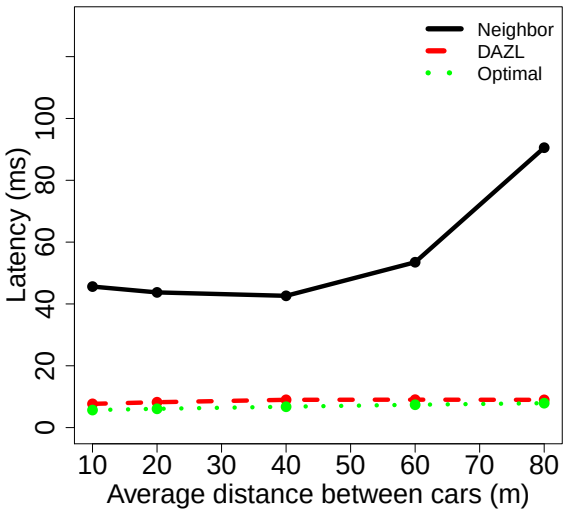

(b) Latency

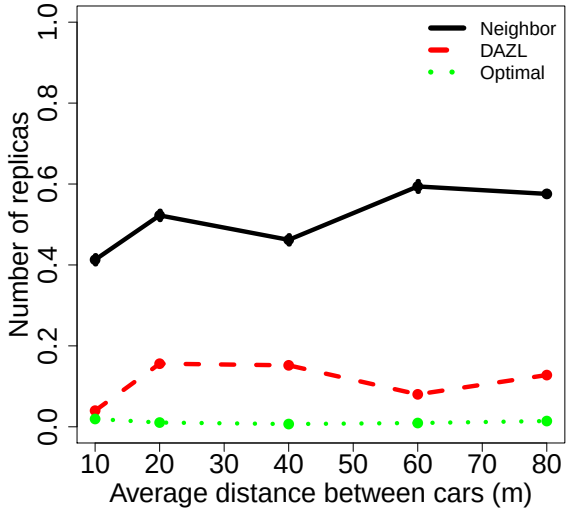

(c) Replication

Figure 3.10: DAZL simulation evaluation performance results.

the oracle protocol. The reason is that it can use up to 7 potential forwarders. Also, the fact that DAZL's throughput did not decrease at higher densities shows that slotting and the limit imposed on the number of forwarders were effective in preventing excessive contention and losses.

Latency

Figure 3.10b shows unidirectional end-to-end latency for all protocols. DAZL performed very similarly to the oracle protocol. Both obtained latencies below 10 milliseconds and the results were fairly consistent across densities. This indicates that the small delay introduced by DAZL through slotting did not impact overall latency significantly. When compared with the neighbor-based protocol, DAZL achieved significantly lower latencies. The reason is that neighbor-based forwarding resulted in more packets losses, and consequently required a lot of retransmissions to get packets across to the destination. These are very costly not only because of the additional transmission time, but also because the node has to wait before finally timing out and retransmitting.

Number of replicas

We now turn our attention to the number of replicas observed at the destination, depicted by Figure 3.10c. As expected, the oracle protocol did not generate any replicas. On the other hand, the neighbor-based scheme generated a significant amount of replication of up to 60% due to losses. Because the packet delivery ratio between previous hop and forwarder is not perfect, sometimes the former does not hear the forwarding done by the latter, leading to unnecessary retransmissions.

DAZL generates replication when the candidate forwarders fail to hear each other. Replication was well contained however, never going beyond 18%. This is due to the employed cancelation mechanism.

Forwarder Selection Statistics

In Figure 3.11a we look at the performance of this cancelation mechanism by comparing the number of candidate forwarders with the number of actual forwarders for the 10 m inter-vehicle spacing (i.e. highest density) scenario. Here we can observe that 97% of the time, there were two or more potential forwarders, a situation that could lead to replication. However, 99% of the time there was only one actual forwarder, a result that proves the effectiveness of our scheme in canceling unnecessary transmissions.

In Figure 3.11b we can observe the Empirical Cumulative Distribution Function (ECDF) for the distance traveled towards to the destination per hop in the various protocols. The optimal protocol,

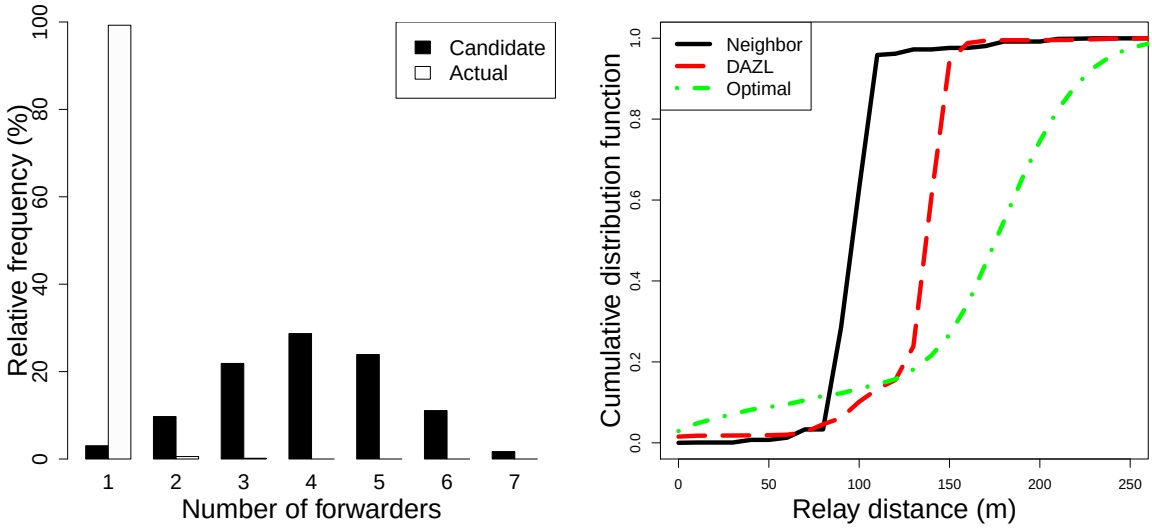

(a) Candidate vs actual forwarders in DAZL (10 m inter-vehicle spacing)

(b) Forwarder distance CDF

Figure 3.11: DAZL forwarder selection behavior.

by its nature, was able to selectively choose the longest hops. The neighbor-based protocol being conservative, achieved a median of 100 m per hop. DAZL, however, was able to use significantly longer hops, with a median close to 140 m. This shows that DAZL's prioritization mechanism was successful in optimizing hop length, when compared with the benchmark neghbor-based protocol.

In summary, the results here presented demonstrate the advantage of zone-based forwarding over node-based forwarding in vehicular wireless networks. DAZL was able to perform almost as well as the oracle protocol while using only local information and a distributed coordination algorithm.

3.5 Related Work

Prior work on routing and forwarding has generally been discussed in Chapter 2. Here we focus specifically on the use of diversity in wireless networks.

Diversity has been used in many ways and contexts to improve resilience to fading. Multiple-Input Multiple-Output (MIMO) [MW04] uses multiple antennas to obtain independent channels and hence increase both reliability and capacity. MIMO works at the physical layer level and focuses on a single vehicle, while DAZL's node diversity works at the network layer level over different vehicles. They are therefore not mutually exclusive but rather, complimentary.

Multi-Radio Diversity (MDR) [MBK05] is a low-level loss recovery scheme for WLANs where corrupt frames received at different access points are combined in a central node to try to extract a correct frame from the multiple corrupt copies. Unlike DAZL, this scheme requires a shared channel to a central node, rendering it unsuitable for vehicular use.

Opportunistic routing has been explored in the context of mesh networks, with the most prominent protocols being ExOR [BM05] and MORE [CJKK07]. Both these protocols leverage diversity by using multiple relays. The main difference between them is that ExOR coordinates the relays through scheduling to prevent duplication while MORE relies on random linear network coding for the same purpose. The same concepts have been applied to infrastructure WLANs by PRO [LSC09]. In PRO, nodes use beacons to exchange channel Received Signal Strength Indicator (RSSI) information. Then, when a transmission fails on a source-destination link, relays that overheard the packet and have good RSSI towards the destination opportunistically retransmit the packet on behalf of the source. Like DAZL, PRO offers reliability through redundancy and poor relays are filtered out to reduce contention. However, all of these protocols require network-wide knowledge of channel quality between every pair of neighbors, which is reasonable for WLANs and mesh networks but does not hold in VANETs.

The idea of reducing MAC layer contention by reducing the number of candidate transmitters first appeared in the context of broadcast communication as an answer to the broadcast storm problem [NTCS99]. Some protocols, such as SAPF [MLP08] and P-persistence [WTP+07] use a probabilistic rule to control the number of contending forwarders. This approach has the disadvantage of not prioritizing the best forwarders. Slotting for spreading forwarders in time was first introduced by Linda et al [Bri01] and later used in Slotted p-persistence [WTP+07]. These approaches use a fixed number of slots and are therefore unable to adapt to different node densities. Adaptive slotting based on workload and density has been previously proposed in some Time Division Multiple Access (TDMA)-based MAC protocols such as E-DTSAP [LWW07], DTST [KA10] and EP-TDMA [MJJ+08]. These protocols are not suitable for VANETs for two reasons. First, they rely on a different MAC than the 802.11p MAC specified for VANETs. Second, they incur large adaptation overheads when the topology changes, which is a frequent event in VANETs.

Contention-Based Forwarding (CBF) [FWK+03] is the closest forwarding protocol to DAZL. It uses node diversity as well, having receivers decide whether to forward or not using a probabilistic rule. Nodes closer to the destination are also prioritized. However, CBF nodes make their forwarding decisions without taking the neighborhood into account, which can create timing conflicts, unnecessary delays in low density areas and excessive contention and replication in high density ones.

3.6 Summary

Wireless vehicular links are lossy and unstable. Noting that the physical separation between nodes ensures channel independence, we ran an experiment that showed that nodes can cover for each other's losses: with 3 receivers the communication range with negligible losses doubled, relative to a single receiver arrangement.

This motived us to create DAZL, a forwarding protocol where multiple forwarders inside a geographic forwarding zone cooperate in packet relaying. To avoid replication caused by redundant transmissions, we introduced a distributed coordination scheme where nodes rank themselves against other potential forwarders based on a distance-to-destination metric. Forwarders then wait a period of time inversely proportional to their rank before forwarding and cancel the forwarding if they overhear any other forwarder's transmission. This allows better-positioned nodes to forward first and minimizes replication. Through a combination of experiments and simulations, we showed that DAZL can provide improvements in end-to-end PDR of upwards of 60% relative to a comparable single-forwarder protocol.

DAZL's applicability is, however, limited. Since it uses a simple distance-to-destination metric and features no recovery procedure, it can only forward along a straight path. This is why it was presented as a forwarding protocol, not a routing one. Knowing this, in the next chapter we present a complete routing and forwarding protocol featuring a sophisticated spatial connectivity-based metric and a recovery mechanism: LASP.

Chapter 4

LASP: Look-Ahead Spatial Protocol

This chapter presents LASP, a routing and forwarding protocol that uses spatial connectivity information to guide route selection. We start by introducing the concept of spatial connectivity and analyzing its potential use in vehicular multi-hop. We then describe LASP's design and finally evaluate its performance through an analytical analysis fed by connectivity traces collected from the HarborNet testbed.

4.1 Premise: Spatial Connectivity

The most effective wireless link metric is based on real-time PDR measurements [CABM05]. Unfortunately, in vehicular networks link quality changes rapidly [JBW05, MBS+10], so it is not realistic to have senders keep an up-to-date network topology with accurate information regarding all links that might be relevant to reaching a particular destination. This means that traditional routing solutions are not practical. Due to this dynamism, vehicular routing protocols are limited to local topology information, e.g., information concerning direct neighbors or at most nodes up to a few hops away. The routing protocol then needs to use heuristics to guide path selection beyond the local neighborhood.

One approach is to use distance, which has a major impact on communication quality. This leads to the popular heuristic of choosing the neighbor closest to the destination as a relay (e.g. [KK00, THR03, LCGZ05]), since this will, in theory, minimize the number of hops needed to reach the destination. This assumes that signal propagation is uniform across space, and hence, that connectivity is solely determined by distance. However, as we have seen in Chapter 2, this assumption does not hold in vehicular networks.

Figure 4.1a uses an example based on data collected from the HarborNet testbed [ACN+14] to

(a) Leixões Harbor example

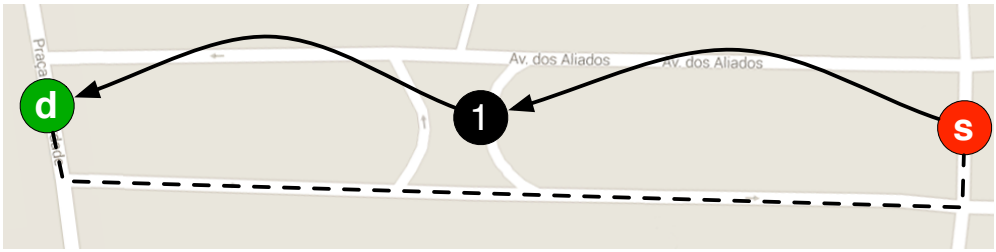

(b) Porto downtown example

Figure 4.1: Spatial connectivity allows protocols to find better connected paths (solid lines) when compared with traditional geographic protocols (dotted lines).

show how distance-based routing can fail to find a path to an otherwise reachable destination. The figure shows a map of the Leixões Harbor, in Portugal. Node s wants to reach d and can choose from one of two relays, 1 or 2, to do so. A traditional geographic protocol like GPSR would pick node 2, as it is closest to d. However, 2 has no connectivity to d. A protocol using measured connectivity, on the other hand, would learn that there is good connectivity between 1's and d's locations, which is due to a lack of obstacles in the blue area (water). Thus, such a spatially-aware protocol would route from s to d through node 1.

In order to try and overcome the shortcomings of distance-based routing, other protocols (e.g. [LHT+03, THR03, JSMGD07, YLL+10]) use road maps as an heuristic, forwarding packets along a sequence of roads towards the destination. As explained in Chapter 2 however, wireless signals are agnostic regarding road topology. Contrary to cars, packets can "jump" between roads, and features such as elevation changes and vegetation may in fact hinder communication along a road. Figure 4.1b shows an example of this jumping between roads, using data pulled from the PortoVANET testbed, in Liberdade Square, Porto, Portugal. A road-based protocol would choose a sequence of roads to connect s and d, e.g. following the dotted line in the figure. However, experiments show that, although they are not adjacent in the road map, messages can hop between the "vertical" streets in the figure, due to favorable line of sight conditions in the wide, open, city square. It is not possible to detect this path solely by looking at the road map.

Since dynamic link conditions make it impractical to track global connectivity at the node level,

we propose to use *spatial connectivity*. Spatial connectivity defines the connectivity between a pair of geographical areas we call cells and reflects the connectivity between *any* pair of cars inside those cells. The cells are small enough that vehicles inside a cell will share similar channels, e.g. regarding distance and line of sight blocking probabilities, to (vehicles in) other cells, making spatial connectivity useful for for identifying geographic paths to remote destinations.

Spatial connectivity can be gathered over a period of time to create a complete view of the network, forming a look-ahead used to identify statistically well-connected geographic paths to remote destinations. It does not help however, in selecting the actual sequence of vehicles that can forward the packet. For this purpose LASP collects real-time node-level connectivity information in its local neighborhood and then combines both information types to select the most promising next hop vehicle. Before we expand on this in Section 4.3, we first study the feasibility of using spatial connectivity as a routing heuristic.

4.2 Spatial Connectivity Analysis

For the use of spatial connectivity in routing to be justified, the following conditions must hold:

1. The number of routing opportunities missed by road-based routing techniques must be significant.
2. Distance alone must *not* be a good PDR predictor.
3. Spatial location must be a good PDR predictor.
4. Spatial connectivity must not change so quickly as to require constant updates.

We proceed to test these conditions by analyzing real-world vehicular connectivity data.

4.2.1 Data Collection

Our analysis uses data collected from both testbeds presented in Section 2.4: HarborNet, the 30-node harbor truck testbed, and PortoVANET, the 400-node public transportation testbed. In both testbeds nodes broadcast Cooperative Awareness Messages (CAMs) [ETS11] at a 10 Hz rate. All CAMs included the sender's location, speed and heading for a total of roughly 50 bytes in length and were sent using the configuration in Table 4.1.

In order to capture data for analysis, each unit kept two time-indexed (1 Hz resolution) logs, depicted in Figure 4.2:

Location log

timestamp	latitude	longitude	#sent
1	41.0	-8.0	10
2	41.0001	-8.0001	10

Reception log

timestamp	sender id	#received CAMs	mean RSSI
1	B	6	-90
1	C	9	-85

Figure 4.2: Logging data kept by each testbed node.

Parameter	**Value**
Center frequency (MHz)	5870 (DSRC channel 174)
Bandwidth (MHz)	10
Data rate (Mbps)	3
Tx power (setting, dBm)	23
Antenna gain (dBi)	5

Table 4.1: Configuration parameters for connectivity data collection.

1. A location log storing the unit's location and number of sent CAMs for each timestamp.

2. A communication log with the number of received CAMs from each sender for each timestamp.

The logs were then uploaded to a server. By combining the logs from all nodes we were able to recreate the evolution of the network's topology on a per-second basis, complete with nodes' locations and link PDRs.

4.2.2 Lost Opportunities in Road-based Routing

Road-based routing protocols route towards the destination along a sequence of roads. This assumes packets can only be exchanged between vehicles in the same road segment or in adjacent road segments. Here, we assess how many forwarding opportunities are ignored by road-based protocols due to this assumption.

For this we used connectivity data from the PortoVANET testbed[1], collected between December 16$^{\text{th}}$ and December 31$^{\text{st}}$, 2013. Figure 4.3 shows the recorded spatial connectivity in orange, overlaid

[1]The Leixões Harbor lacks a road map, rendering HarborNet unsuitable for this analysis. Another limitation of road-based protocols is thus exposed: their applicability hinges on the availability of a road map.

Figure 4.3: Porto road network (thin black lines) and spatial connectivity (thick orange lines).

with Porto's road network in black. Spatial connectivity is represented by having each pair of locations between which at least one CAM was successfully exchanged connected by a line segment.

For each successfully exchanged CAM, we took the communicating vehicles' positions and mapped them onto the closest road segments in the road network. We then classified the segment pairs into 3 classes: i) *same*, when both vehicles were mapped to the same road segment, ii) *adjacent*, when the vehicles were mapped to segments that share a vertex in the road network graph and, iii) *non-adjacent*, for all remaining cases.

	Frequency	
Type	**Absolute**	**Relative**
Within same road segment	6930	6%
Between adjacent road segments	15801	14%
Between non-adjacent road segments	90404	80%
Total	113135	100%

Table 4.2: Classification of vehicular communication relative to Porto's road network.

Table 4.2 summarizes the classification results. From all the links, only 6% occurred within the same segment, and 14% between adjacent segments. The large majority of CAM exchanges (80%) happened between non-adjacent road segments. This result clearly shows that the road network graph used by vehicles is fundamentally different from the vehicular network wireless connectivity graph. Assuming that communication can only occur within a single road segment or between adjacent segments, as many protocols do, would ignore a significant number of communication

opportunities.

4.2.3 Use of Distance as a Routing Metric

We now look at the relationship between PDR and sender-receiver distance or link length. Previous studies [MBS+10, MMKH11] have shown that sender-receiver distance alone can not fully explain PDR like existing protocols assume.

To see this for ourselves we took one month (November 2013) of connectivity data collected from the HarborNet testbed and plotted PDR as a function of link length. The box plot of Figure 4.4a shows the results. Because the Harbor is an environment rich in obstacles, links longer than 300 meters were rare, and are therefore not represented in the plot. As expected, the boxplot shows a large variance in PDR for most distance bins, especially the ones at distances of up to 250 meters. This variance makes it impossible to infer link performance from sender-receiver distance alone, making a strong case against the use of distance as a routing heuristic.

4.2.4 Spatial Location as a Predictor for PDR

To quantify how well spatial location predicts PDR we study the spatial autocorrelation in PDR data, i.e. whether co-located links exhibit similar connectivity. First we define an inter-link distance metric in order to quantify physical separation between links. In our analysis a link is defined by its endpoints: ab represents a link whose endpoints are a and b. We define inter-link distance as the minimum sum of distances between the endpoints of the two links, as per Equation 4.1:

$$d(ab, cd) = \min\Big\{\big[d(a,c) + d(b,d)\big], \big[d(a,d) + d(b,c)\big]\Big\}, \tag{4.1}$$

where $d(a, b)$ is the great-circle distance between a's and b's geographic coordinates. This inter-link distance satisfies all metric requirements: non-negativity, identity of indiscernibles, symmetry and subadditivity.

Figure 4.5 shows an example. Given the symmetric property, we need only consider two combinations between the endpoints of links ab and cd: $d(a,c) + d(b,d)$ and $d(a,d) + d(b,c)$. In this case, $d(a,c) + d(b,d)$ is minimal.

Again, we used connectivity data from the HarborNet testbed spanning the month of November, 2013. Due to the large amount of data available, a degree of discretization was needed to make the analysis computationally feasible. For this reason, space was discretized into a 10×10 m square grid and the PDR samples falling into the same cells were averaged. We then used standard spatial analysis tools on the resulting data set: variograms and correlograms [Cre93].

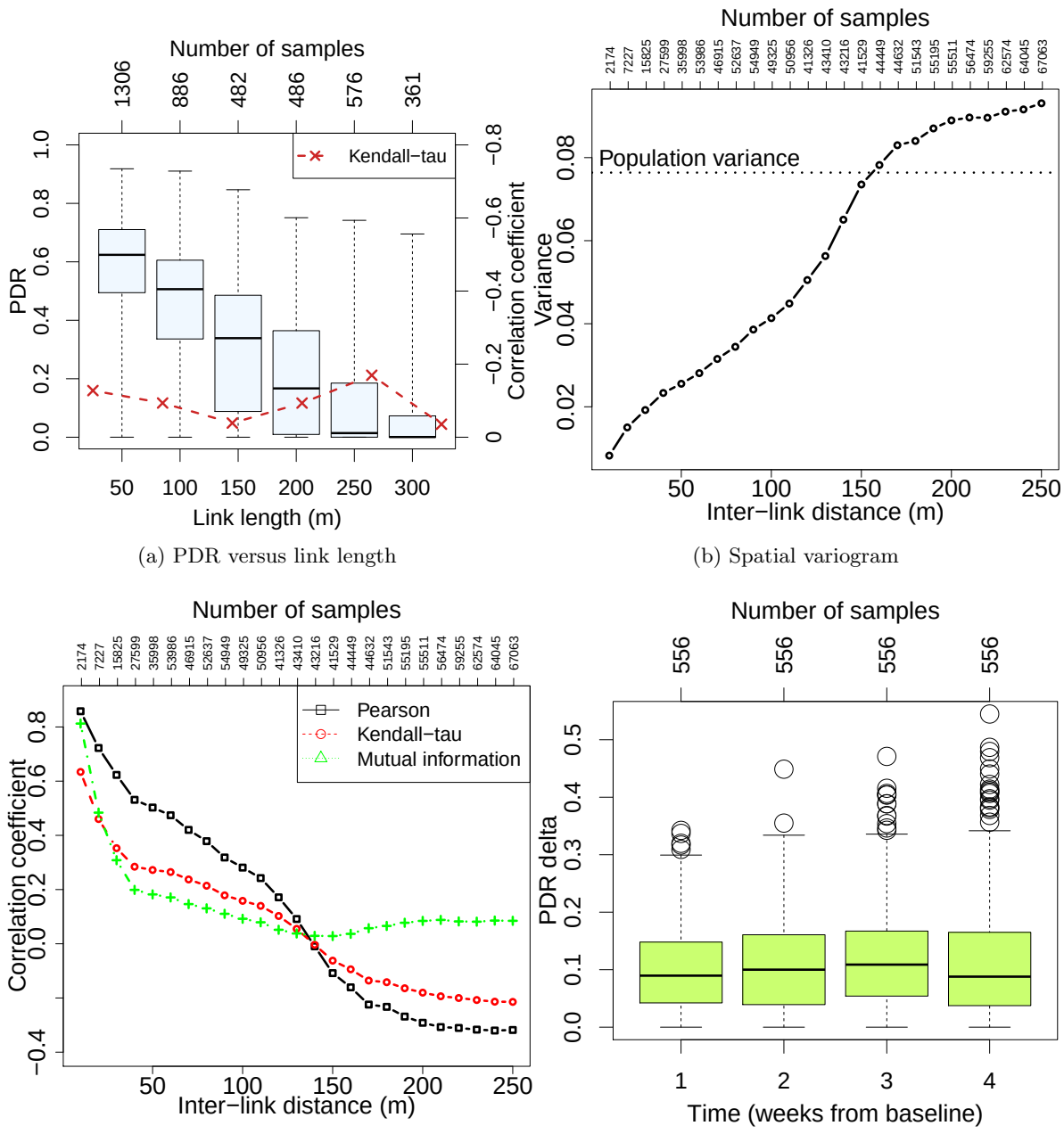

(a) PDR versus link length

(b) Spatial variogram

(c) Spatial correlogram

(d) PDR temporal variation

Figure 4.4: Spatial connectivity analysis results show that: i) distance alone can not predict PDR, ii) PDR exhibits spatial autocorrelation and iii) spatial connectivity is stable in time.

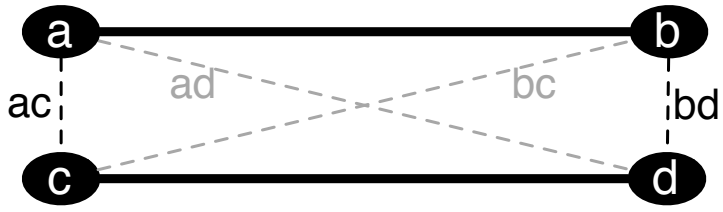

Figure 4.5: Inter-link distance is defined as the minimum sum of distances between the endpoints of the two links. Thus, in the figure, $d(ab, cd) = d(a, c) + d(b, d)$.

The variogram of Figure 4.4b shows how PDR variance as a function of inter-link distance for all link pairs. The low variance for short distances means that co-located links indeed experience similar PDRs. Variance then increases steadily as links grow apart. The fact that the plot crosses the population variance indicates that the chosen inter-link distance metric was able to explain the variance in the data well.

In Figure 4.4c we plot the correlation between PDRs as a function of inter-link distance. We use 3 distinct correlation metrics: Pearson, which captures linear relationships; Kendall-τ, which captures monotonic relationships; and mutual information, which captures any relationship. All metrics showed high levels of correlation for short inter-link distances, again confirming the relationship between spatial location and PDR. Correlation dropped gradually to zero around 150 m. At larger distances, mutual information stayed close to zero, while the other metrics exhibited negative correlation. This can be explained by the presence of links of disparate lengths at large inter-link distances: long, low PDR links correlate negatively with short, high PDR links. By comparing Figure 4.4c with Figure 4.4a we can see that spatial location correlateed with PDR better than link length alone.

4.2.5 Temporal Stability of Historical Spatial Connectivity

Finally we look at the temporal sensitivity of spatial connectivity data. For this we took the HarborNet data collected during the last week of October 2013 and computed the PDRs for each pair of discretized spatial cells. We then set that as a baseline and proceeded to compute the PDRs for the same cell pairs over the following weeks.

Figure 4.4d shows a box plot of the PDR delta between the baseline and the following weeks. The harbor can be considered a worst-case scenario for temporal variations because large metal containers are constantly being moved, as if in a city where buildings were constantly being erected and torn down. Despite this, the median PDR delta error hovered around 10%. There was a tendency for variance to increase with time, but not significantly. This allows us to conclude that infrequent (e.g. monthly) connectivity map updates would be sufficient to keep nodes up-to-date

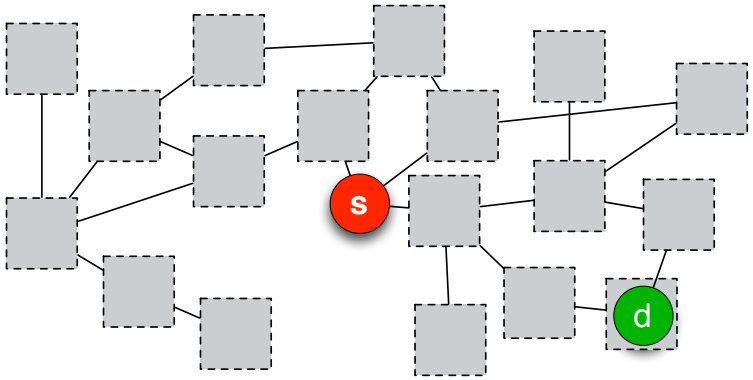

Figure 4.6: LASP abstracts the network topology as a spatial graph. Circles represent the source and destination nodes; squares represent spatial cells.

in this scenario.

4.3 Protocol Design

4.3.1 Overview

LASP is a geographic unicast multi-hop communication protocol whose goal is to maximize end-to-end delivery probability. The destination's location is assumed known (i.e. through the use of a location service [LJDC+00, CBW02, GS06]), enabling the use of geographical addressing, and nodes are assumed to be able to track their own location (e.g. through GPS). The protocol is divided into routing and forwarding components. Routing generates an abstraction of the network topology, which is then used by the forwarding algorithm to select, at each hop, the most promising next hop relay.

Traditionally, routing is based on a topology graph representing the connectivity between network nodes[2]. However, as previously discussed in Chapter 2, vehicular wireless links are unstable and short-lived, making network-wide dissemination of node-level connectivity information impractical. LASP's approach is to use spatial connectivity (Section 4.1) to model the network topology as a graph where vertices represent not network nodes but small geographical regions we name spatial cells, as depicted by Figure 4.6. Each edge (u, v) in this graph represents the statistical historical probability that, if a packet is sent by a node on cell u, it will be received by at least one node in cell v. By multiplying the edge probabilities over a spatial path, the multi-hop delivery probability between any two spatial cells can be estimated.

[2]Throughout the text the term *node* is used to mean a communication device that is part of the network, i.e. an OBU or RSU.

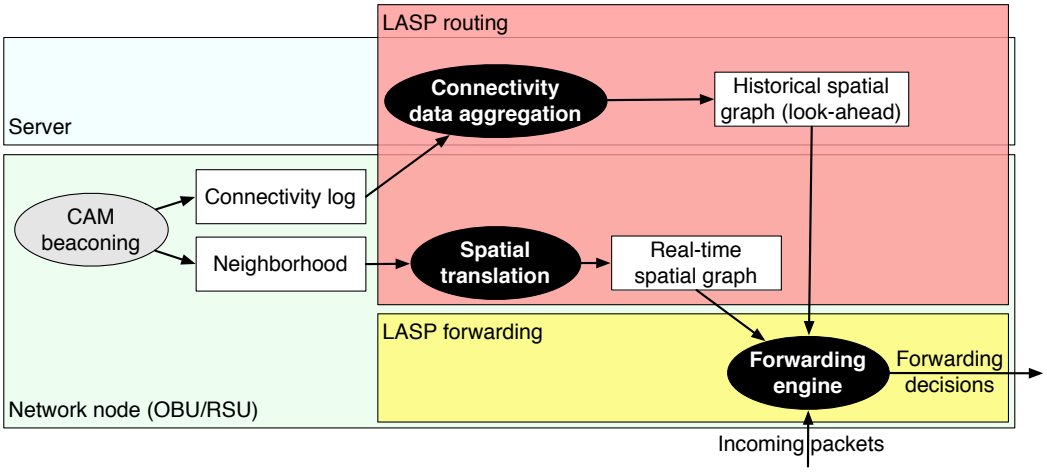

Figure 4.7: LASP's logical and physical architecture. Ovals represent processes, arrows represent interactions and the white rectangles represent data structures.

We refer to this historical spatial connectivity graph as a *look-ahead*, because it allows nodes to understand the network's connectivity patterns beyond their immediate vicinity. Compared with node-level connectivity, spatial connectivity provides a more abstract, stable and compact representation of the network's topology. In Section 4.2, we showed that vehicular connectivity exhibits a high degree of spatial autocorrelation and that historical spatial connectivity information does not become outdated quickly. This means using spatial connectivity as an heuristic for delivery probability is both feasible and attractive.

Note however, that the historical spatial look-ahead may not reflect current network conditions, which depend on additional variables such as present vehicle locations and transient obstacles. Therefore we want to use real-time connectivity information for the local neighborhood, where it is feasible. The local neighborhood is defined by the ids and locations of the nodes up to n-hops away from the current node, where n is a small natural number, and the PDRs of their links. LASP collects this information, which is then used to create a real-time connectivity graph of the node's vicinity.

We now explain how both the historical and real-time connectivity graphs are created and maintained by LASP's routing component and how they are used by the forwarding engine to select a next hop relay. Figure 4.7 depicts LASP's logical and physical architecture. At the basis of LASP is CAM (Cooperative Awareness Message) beaconing. CAMs were standardized by ETSI [ETS11] as part of a basic service set for vehicular networks. CAMs are broadcast by every node at a rate of 10 Hz. Each CAM includes the sender's id and location. This lets nodes keep track of their neighbors, which is useful for a multitude of applications, from collision avoidance to video streaming [LCG08].

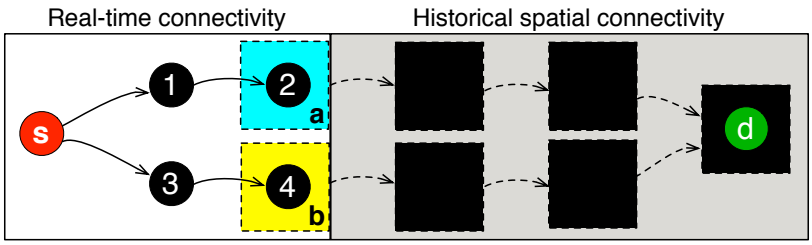

Figure 4.8: LASP merges the real-time and spatial graphs to estimate the end-to-end PDR for each possible next hop relay. In the figure circles represent nodes; squares represent spatial cells.

LASP routing leverages CAMs in two ways. First, nodes use CAM beaconing data to create a spatially-indexed connectivity log that says where and how many CAMs were sent and received, as in Section 4.2.1. Nodes can then opportunistically upload this log to a server, whenever connected to a RSU or WiFi hotspot [ETS09]. The server fuses all the data, creating the aforementioned historical spatial look-ahead graph describing connectivity between spatial cell pairs, which is then opportunistically downloaded by the nodes for use in forwarding.

Second, CAM reception data is used to learn the composition of the local neighborhood. From the sender's id and location included in each CAM, a 1-hop neighborhood can be inferred. If CAMs also include a list of the sender's neighbors, a 2-hop neighborhood can be inferred, and so on for larger neighborhoods. Although the available neighborhood will typically be small, LASP supports any size neighborhood. LASP's routing component uses the neighborhood to create a local real-time connectivity graph. LASP needs to evaluate each possible next hop relay individually, therefore this real-time graph must provide node-level granularity. On the other hand, LASP also needs to be able to combine the real-time graph with the historical look-ahead graph, which is defined at the spatial cell-level, to obtain an end-to-end view of the network.

LASP's solution is to define the real-time connectivity graph as a mixture of node-based and spatial cell-based vertices and edges. The direct neighbors of the node building the graph are included as vertices, and the links between the node and each neighbor as edges. But beyond that first hop, and regardless of the neighborhood size, graph vertices are spatial cells, namely the spatial cells at the outer edge of the neighborhood (i.e. cells that are reachable after n hops in an n-hop neighborhood), and the edges represent the spatial connectivity between each of the neighbors and each of the reachable cells. This makes the real-time graph compatible with the historical spatial look-ahead, while at the same time allowing for individual neighbor evaluation.

LASP's forwarding engine takes in both the real-time and the historical spatial connectivity graphs as inputs and uses them to find the next hop relay that maximizes the estimated end-to-end delivery probability to the packet's destination spatial cell. Figure 4.8 illustrates the concept. In the figure node s (left) wants to choose the best next hop relay for a packet addressed to node d

(right), using a 2-hop neighborhood of real-time connectivity and the historical spatial connectivity data for the remainder of the path. Node s can, for each possible next hop (nodes 1 and 3), use local neighborhood data to discover which spatial cells can be reached within the n-hops of the neighborhood, and with what probability. In the figure, relay 1 can reach cell a and relay 3 can reach cell b. The probability of delivering the packet to the destination through, for instance, relay 1, can then be estimated as the real-time probability of the packet reaching cell a multiplied by the historical statistical probability of reaching the destination's location from cell a. The candidate next hop relay that maximizes this probability is chosen to be the next hop[3].

In the following subsections we describe the construction of the historical and real-time connectivity graphs in more detail, and how they are merged to efficiently estimate the end-to-end delivery probability. Finally we explain how LASP recovers from dead ends when the spatial connectivity heuristic fails.

4.3.2 Historical Spatial Connectivity Graph — Look-ahead

The server receives spatially-indexed connectivity data from every node in the format previously described in Section 4.2.1, and is faced with the challenge of summarizing this vast amount of data into a compact and computationally-tractable representation to act as a look-ahead that allows nodes to assess the network's connectivity beyond their local neighborhood. For this we leverage a graph data structure. We build the historical spatial connectivity look-ahead graph $G_h = (V_h, E_h)$ as follows:

- Space is discretized into cells, with each cell becoming a vertex $v \in V_h$. For simplicity, the current implementation uses square cells. Communication inside each cell is assumed to be perfect. Hence, cell size represents a tradeoff between accuracy and complexity. In our prototype, cell dimensions are set to 50×50 m, a compromise in agreement with the spatial autocorrelation results of Section 4.2.

- For every pair of distinct spatial vertices (u, v) between which communication occurred (i.e. at least one message was successfully exchanged), a directed edge $e = (u, v)$ is added to E_h. In a general network, $|E| = \mathcal{O}(|V|^2)$, which would lead to a very large graph. However, because each $v \in V_h$ represents a distinct spatial cell and the radio range is limited, each vertex has but a handful of edges. Thus, the edge set grows linearly with the number of vertices, i.e. $|E_h| = \mathcal{O}(|V_h|)$, improving scalability.

[3]Note that the same data structures could be used to support a DAZL-like zone-based forwarding scheme. We focus on such a variant of LASP's design in Chapter 5.

Each directed edge $(u, v) \in E_h$ is weighted with an historical spatial delivery probability P_{hspdel}, representing the conditional probability that, if a packet is being held by a node (any node) at cell u, it can be successfully delivered to a node (any node) in cell v. P_{hspdel} is defined as the product of two probabilities:

1. The probability that, if there exists at least one node at vertex cell u (which we know to be true since the packet sender is there), the same is true for v. This can be obtained from the connectivity logs by dividing the recorded amount of time with nodes at both locations by the recorded amount of time with at least one node at cell u. I.e.:

$$P(nodesAt(v) \mid nodesAt(u)) = \frac{time(nodesAt(u, v))}{time(nodesAt(u))} \tag{4.2}$$

2. The conditional probability that, given the presence of nodes at u and v, a packet can be delivered from u to v using at most t transmission attempts (i.e. $t - 1$ retransmissions). This conditional P_{hdel} can be computed as the complement of the probability of having t unsuccessful transmissions given the historical edge PDR. I.e.:

$$P_{hspdel}(u, v, t \mid nodesAt(u, v)) = 1 - (1 - PDR_{u \to v})^t. \tag{4.3}$$

   Historical statistical edge PDRs are computed from the connectivity logs as the ratio between the total number of CAMS sent by a node at u that were received by at least one node at v, divided by the total number of CAMs sent from cell u, aggregated over all time periods when there were nodes at both u and v. We can then write:

$$PDR_{u \to v} = \frac{\#receivedCamsAtFrom(v, u)}{\#sentCamsAt(u))} \tag{4.4}$$

Bringing the two factors together we can write the historical delivery probability P_{hspdel} as:

$$P_{hspdel}(u, v, t \mid nodesAt(u)) = P(nodesAt(v) \mid nodesAt(u)) \times P_{hspdel}(u, v, t \mid nodesAt(u, v)). \tag{4.5}$$

Note that, by conditioning P_{hspdel} on the presence of nodes at u, we can compute the delivery probability of multi-hop spatial paths by simply multiplying the P_{hspdel} probabilities of the edges that compose the path.

To help illustrate the concept, Figure 4.9 provides a visual representation of the outgoing edges of the vertex represented by the green circle, located in the center of Porto, Portugal. Red and yellow represent edges with high P_{hspdel} values, while blue and black represent low values. The area to the right of the circle is surrounded by a wall, while the one to the left is open. This reflects itself in the graph, with the lefthand side having more and better connected edges. This shows how our graph representation is able to summarize the effects of obstructions affecting vehicular communication.

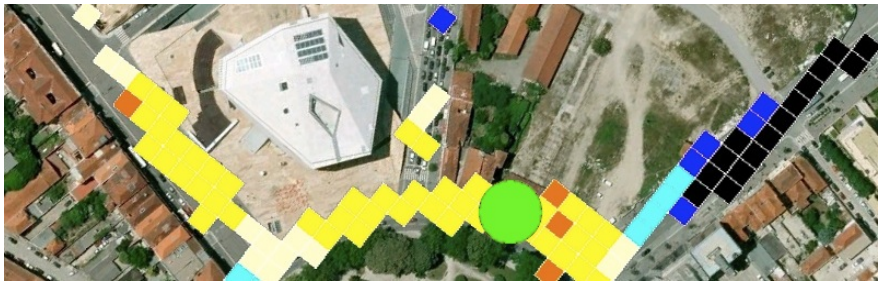

Figure 4.9: Spatial connectivity observed from the green circle: the warmer the color, the better the connectivity between the circle and that spatial cell (more precisely, red means 100% delivery probability, black means 10%).

4.3.3 Real-time Look-ahead Graph

Real-time connectivity information is inherently more accurate than historical statistical connectivity. Therefore, since it is available, we use local real-time information in lieu of historical information to model connectivity in the node's vicinity. The data included in CAMs is used to create and maintain a neighborhood that includes nodes up to n-hops away from the current node. From the perspective of a network node s, a neighbor is a node from which s received at least 1 CAM within the last x ms, where x is a parameter. A 2-hop-away node is defined recursively as a neighbor of one of s's neighbors, and so on for further away nodes.

An n-hop neighborhood can be represented by a node s as a graph, $G_n = \{V_n, E_n\}$, defined as follows:

- Every node up to n-hops away from s becomes a vertex $v \in V_n$. Node s, the one building the look-ahead, can be considered an implicit neighbor of itself, therefore it is included in V_n as well.
- For each pair of neighbors (i.e. directly-communicating nodes) u and v in the vertex set V_n, let (u, v) be an edge $e \in E_n$. Each edge $e = (u, v)$ is weighted with the probability of successfully delivering a packet from u to v using up to t transmission attempts. We call this probability P_{rdel} and compute it similarly to Equation 4.5, but with two subtle differences. First, we are computing the communication probability between a pair of nodes, not a pair of spatial cells. Second, instead of the PDR being an historical average, it is a real-time measurement obtained from CAM reception data. Formally we have:

$$P_{rdel}(u, v, t) = 1 - (1 - PDR_{u \to v})^t. \tag{4.6}$$

Note that there is a fundamental discrepancy between the neighborhood graph G_n, where vertices and edges are defined at the node-level, and the historical graph G_h, where vertices and edges

are defined at the spatial cell-level. In order to combine the two structures we must reduce the granularity of the finer-granularity data structure. I.e., we must express the neighborhood in a spatial form. With this in mind we define a real-time connectivity graph $G_r = \{V_r, E_r\}$ that has both node and spatial cell vertices, bridging the gap between the two representations. A node s can build G_r from an n-hop neighborhood graph G_n as follows:

1. Let s, the node building the graph, and all of its neighbors be vertices in V_r.

2. Let there be an edge $e = (s, n) \in E_r$ between node s and each of its neighbors n. Each of these edges represents the probability of a packet reaching a specific next hop relay from the current node. Therefore, each edge is annotated with a delivery probability P_{rdel}, taken directly from the equivalent edge (i.e. the edge connecting the same nodes) in the node-based G_n neighborhood graph.

3. Take the set of neighborhood nodes that are n-hops away from s (i.e. on the outer edge of the neighborhood). Call this set $\mathcal{Q}$. For each node $u \in \mathcal{Q}$, discretize u's position to find the corresponding spatial cell c and let c be a vertex in V_r.

4. For each unique combination of neighbor n and spatial cell vertex $c \in V_r$, let (n, c) be an edge $e \in E_r$. Each of these edges is annotated with the real-time spatial probability P_{rspdel} of delivering a packet to the spatial cell c from neighbor n. We define the probability of delivering a packet to a cell as the probability of delivering the packet to any node inside the cell. Because there can be potentially many paths to reach a node inside c, we define P_{rspdel} as the delivery probability of the best-connected path from all the possible ones. In turn, the probability of delivery for a path is the product of the delivery probabilities of its individual edges. The probability of delivery-maximizing paths can be obtained efficiently from G_r using the Floyd-Warshall algorithm. Formally we can write P_{rspdel} as:

$$P_{rspdel}(n, c, t) = \max_{Path_{n \to c}} \left[\prod_{(u,v) \in Path_{n \to c}} P_{rdel}(u, v, t) \right]. \tag{4.7}$$

Now, if we combine G_r with G_h we have a graph with node-level information for the first hop away from the current node and spatial cell-level information for the remainder. In the next subsection we describe how this structure can be used to select a next hop relay.

4.3.4 Choosing Relays

At each hop, LASP must evaluate its neighbors to find the one most suited to relay the packet. The goal is to select the neighbor n that, when used as next hop, maximizes the estimated end-to-end

delivery probability, which we call P_{edel}, between the current node s and the destination's spatial cell c_d. I.e.:

$$\text{chosen relay} = \arg\max_{n \in \mathcal{N}} \big[P_{edel}(s, n, c_d, t)\big]. \tag{4.8}$$

For each candidate next hop relay n, the end-to-end delivery probability P_{edel} can be thought of as the probability that 3 simpler events happen in succession. First, the packet must reach n from the current node s. Then the packet must reach a spatial cell c at the outer edge of the local neighborhood from node n. Finally the packet must reach the destination cell c_d from cell c.

The end-to-end delivery probability P_{edel} can then be defined as the product of these three probabilities. The first two factors correspond to the previously defined real-time delivery probabilities P_{rdel} and P_{rspdel}, respectively. The third factor is the product of the previously defined historical spatial delivery probabilities P_{hspdel} over all edges in the spatial path from cell c to cell c_d. Moreover note that, because each neighbor n can potentially reach multiple different cells c and there can be multiple different spatial paths between each c and c_d, we need to pick the probability-maximizing paths from within the ones available to each neighbor n.

Formally we write P_{edel} for a given current node s, destination cell c_d and neighbor n as:

$$P_{edel}(s, n, c_d, t) = \max_{c \in \mathcal{C}_n} \left\{ P_{rdel}(s, n, t) \times P_{rspdel}(n, c, t) \times \max_{Path_{c \to c_d}} \left[\prod_{(u,v) \in Path_{c \to c_d}} P_{hspdel}(u, v, t \mid nodesAt(u)) \right] \right\}, \tag{4.9}$$

where t is, as before, the maximum number of transmission attempts per hop and $\mathcal{C}_n$ is the set of look-ahead spatial cells at the outer edge of the look-ahead that are reachable from n.

As a failsafe, in the case when no historical data is available, the protocol assumes that connectivity conditions between cells c and c_d are the same as those between s and c. This means replacing the 3rd factor in Equation 4.9 with:

$$P_{hspdel}(c, c_d, t) = \big[P_{rdel}(s, n, t) \times P_{rspdel}(n, c, t)\big]^{\left\lceil \frac{dist(c, c_d)}{dist(s, c)} \right\rceil}. \tag{4.10}$$

Here the communication probability between the current node s and the intermediate spatial cell c is taken to the power of the expected number of hops under the aforementioned uniformity assumption.

If we merge the historical look-ahead graph G_h with the realtime graph G_r to obtain a global connectivity graph G, the solution to Equation 4.8 (i.e. the next hop that maximizes P_{edel}) can be found efficiently by running the Dijkstra algorithm on G with the current node s as the start vertex and the destination's cell c_d as the destination vertex. The best next hop relay will then correspond to the second vertex in the resulting optimal path.

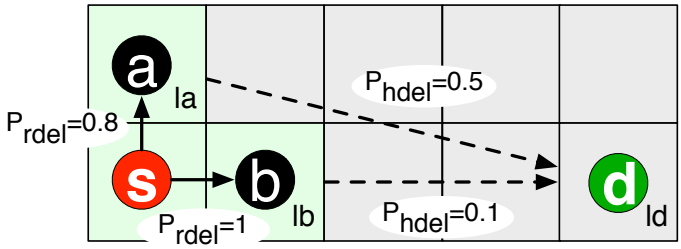

Figure 4.10: LASP connectivity graph for the example from Figure 4.1a. The circles represent nodes and the squares represent spatial cells. The solid arrows represent real-time edges between nodes while the dashed arrows represent historical edges between spatial cells.

This computation could be performed preemptively for all possible destination cells, in order to generate a forwarding table. However, given the dynamic nature of the real-time neighborhood information and the large number of possible destinations, we have chosen to compute the best next hop relay on the fly for each incoming packet. We do however cache the delivery probabilities for the historical part of the paths, since the historical look-ahead graph $\mathcal{G}_h$ does not change often.

We now present an instantiation of the protocol's operation by expanding on the example first introduced in Figure 4.1a. We consider the perspective of node s, who wants to choose a relay to deliver a message to d and has to choose between two candidate relays, a and b.

Assume the protocol is using a local neighborhood of just 1 hop and that the connectivity graph construction process results in the graph depicted by Figure 4.10. In order to pick a relay, node s computes the end-to-end delivery probability P_{edel} for both candidate relays and see which is highest. For this, it needs the three factors in Equation 4.9: the delivery probability between it and the candidate relay; the delivery probability from the relay to a spatial cell in the outer edge of the neighborhood and; the delivery probability between this last cell and the destination cell.

The real-time delivery probabilities between s and a and s and b are 0.8 and 1, respectively. In this example, c_a and c_b are the outermost cells that are reachable within the provided 1-hop neighborhood. Given that a and b can not communicate, a can only reach cell c_a and b can only reach cell c_b, so there is only one option per relay. Because these are the cells where the candidate relays are actually located themselves, the probability of delivering a packet to the cell, P_{rspdel}, is 1 in both cases. The probabilities of reaching the destination cell are given by historical data and are, in this instance, 0.5 for c_a and 0.1 for c_b.

Now the three factors can be multiplied to find P_{edel} for each candidate relay. The calculation is summarized in Table 4.3. Because it compensates a lower first hop probability with a higher spatial delivery probability, relay a ends up being chosen in this instance, with a P_{edel} of 0.4 against b's 0.1.

Relay (r)	$P_{rdel}(s,r)$	Cell (l)	$P_{rspdel}(r,c)$	$P_{hdel}(c,c_d)$	$P_{edel}(r,c_d)$
a	0.8	c_a	1	0.5	$P_{rdel}(s,a)*P_{rdel}(a,c_a)*P_{hdel}(c_a,c_d) = 0.8 \times 1 \times 0.5 = 0.4$
b	1	c_b	1	0.1	$P_{rdel}(s,b)*P_{rdel}(b,c_b)*P_{hdel}(c_b,c_d) = 1 \times 1 \times 0.1 = 0.1$

Table 4.3: End-to-end delivery probability estimation for the connectivity graph of Figure 4.10.

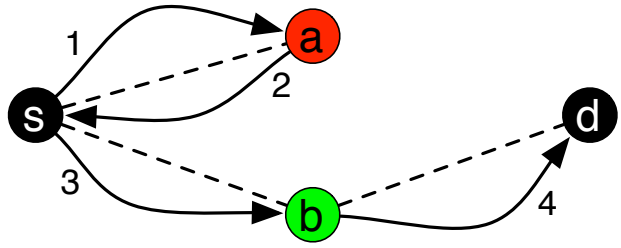

Figure 4.11: LASP backtracking example.

4.3.5 Recovering From Dead Ends

LASP picks, at each hop, the neighbor that maximizes the estimated probability of delivery to the destination. However, this computation is based on an heuristic (spatial connectivity), making it therefore susceptible to failure. The protocol must therefore be able to cope with such failures.

In LASP, if after sending a packet, no acknowledgment is heard from the chosen next hop, the node detects this as a failure and triggers a recovery procedure. Recovery starts by sending the packet to the neighbor with the second-highest estimated delivery probability. If this also fails, the packet is sent to the third-best neighbor, and so on. If none of the node's neighbors is successful in forwarding the packet, the node sends the packet backtracking to the node it first received it from. This node will then repeat the recovery procedure, trying neighbors neighbors with progressively lower estimated delivery probabilities and, if necessary, eventually backtracking the packet to the previous hop sender.

In summary, if we look at the network as a spanning tree starting at the source, LASP operates as a depth-first search algorithm where the order in which children are visited is dictated by the presented spatial connectivity-based delivery estimation procedure. In order to prevent nodes from being visited more than once, which could lead to a routing loop, LASP packets include in the header an ordered backtrace of previously visited nodes, which is used to filter the possible next hop neighbors.

We now illustrate the concept through a simple example, once again using the scenario in

Figure 4.1a as a backdrop. Again assume node s wants to send a packet to d and that, as per the previous subsection, candidate relay a is the one chosen to relay the packet because it has a higher estimated P_{edel} than the other candidate, b. Assume however, that upon receiving the packet, a realizes it has no new node to forward to. Figure 4.11 depicts the sequence of events that occur in this situation. Upon realizing that the packet is at a dead end node a backtracks the packet to s. Node s now looks at the remaining non-visited nodes and chooses the only remaining one, b, which is then able to deliver the packet to the destination. Even though the heuristic failed, the packet was successfully delivered, only using 4 hops instead of the optimal 2.

If the network topology does not change during the forwarding process, source and destination are in the same connected component and the number of retransmissions is sufficient, then this strategy ensures delivery, as, in the worst case, it will eventually visit every node in the source's connected component. However, since vehicular networks are very dynamic, these conditions do not hold in practice. Therefore, end-to-end reliability must be provided by a higher level protocol in the general case.

Furthermore, this strategy is loop-free in terms of nodes because no edge is traversed more than once in each direction. However we note that, if the heuristic fails and there is a high enough number of nodes in the network, it is possible for the packet to loop around a geographical path, using different nodes every time. This is expected to be a rare occurrence and is currently dealt with through the enforcement of a limit on the number of hops traversed by the packet.

4.4 Trace-based Evaluation

In this section we present an analytical evaluation of LASP's performance using connectivity traces. Later, in Section 5.4, we complement this with an experimental evaluation using a prototype implementation of LASP.

4.4.1 Setup

We leveraged extensive connectivity logs collected from the 30-node HarborNet testbed first introduced in Section 2.4 to perform a trace-based evaluation of LASP. By using real connectivity data we are able to more faithfully recreate actual network conditions, relative to previous works that relied on synthetic channel and mobility models.

For this analysis we used two weeks of data. The 4^{th} week of November 2013 was utilized to create the historical spatial look-ahead graph G_h employed by LASP. The 5^{th} week was used to recreate the network conditions under which the evaluation was to be performed. As described in

Section 4.2.1 the data was composed of time-indexed location and communication logs. In order to prepare the data for analysis, we split it by timestamp (1 Hz resolution), and for each of these slices of data, which we name snapshots, we defined the following:

Network topology Any two nodes that successfully exchanged at least one message between them during this timestamp were defined as adjacent in the network graph (i.e. neighbors). The graph edges were modeled as erasure channels with the delivery probabilities defined below.

Actual link PDRs The *actual* PDR for each edge was set as the ratio of received to sent CAMs in the current timestamp for the two nodes that make up the link (each node broadcasts 10 messages per timestamp).

Estimated link PDRs Allowing LASP to use the actual link PDRs would be unrealistic and constitute an unfair advantage. Therefore, the PDRs used by LASP were computed as the ratio of received to sent CAMs in the recent past, which is used as a predictor for the actual current PDR. By analyzing the connectivity logs we found that a window of 5 seconds minimizes the mean square error of the prediction. For that reason, that was the chosen window size.

With this model in place, the analysis was then performed as follows:

1. For each different 1-second snapshot in the source data set, take the network graph associated with it and execute the remaining steps independently.
2. For each distinct source-destination pair in this network graph, execute the remaining steps independently.
3. Find the path between source and destination using LASP and 3 other protocols chosen as benchmarks.
4. Compute performance metrics for the resulting paths. In this study we focused on three end-to-end metrics: hop count, packet delivery rate and transmission count. Details on the computation of these metrics are provided below.

We acknowledge the following limitations of our analytical setup:

- Our erasure channels used PDRs averaged over periods of one second and therefore were unable to capture variations occurring on a faster time-scale. To avoid this, finer-grained data would be necessary, which was not available with the technology currently used in the HarborNet testbed (e.g. 1 Hz GPS).

- For simplicity, our analysis did not include a timing model. We considered only an ordering of the events composing the execution of a given protocol. Namely, we assumed that all transmission events occurring after n hops occur after all $n-1$ hop transmissions, $\forall n \geq 1$. I.e., transmissions occur in ascending hop count order.

- Our analysis did not model capacity constraints or MAC-level interference. However, we imposed a limit on the maximum number of transmissions per hop (set to 5), as a simpler proxy.

Our goal with this analysis was to evaluate how LASP compares in terms of reliability and network load against both existing practical protocols and the theoretical optimum, which can not be achieved in practice. Furthermore, we wanted to evaluate the impact of local neighborhood size on LASP's performance. We now describe all the different routing protocols used in the analysis to accomplish these objectives.

In order to assess the impact of look-ahead size on performance we tested LASP with real-time neighborhoods of 1, 2 and 3 hops. LASP was implemented according to the protocol definition in Section 4.3. The only difference is that failure detection due to lack of acknowledgment from the chosen next hop relay was not implemented. If the forwarding fails, a different neighbor is not chosen (i.e. the packet is dropped). There is backtracking, but only in the case when a packet is received and all available neighbors have previously been visited.

We compared LASP against a well-known existing geographic routing protocol: GPSR. GPSR tries to minimize the end-to-end hop count by, at each hop, greedily choosing the neighbor closest to the destination to be the next relay. When no closer neighbor exists (i.e. a network hole), a recovery procedure called *perimeter mode* traverses the network graph using the right-hand rule until greedy forwarding can be resumed. While there are protocols that use more complex heuristics, we chose GPSR because it is representative of a large class of geographic protocols, has a reference implementation provided by the protocol authors and, unlike others, does not require external information such as road maps (which do not exist for the harbor).

Furthermore, to enable a more thorough comparison, we added support for arbitrarily large neighborhood information to the basic GPSR protocol. Regular GPSR picks the 1-hop neighbor closest to the destination as the next-hop relay: i.e. it uses only a 1-hop neighborhood to make its decisions. The implemented multi-hop neighborhood version of GPSR starts by looking at the nodes at the periphery of its possibly multi-hop neighborhood (i.e. the nodes n hops away in an n-hop neighborhood), and choosing the closest to the destination from those: call it c. Then, it selects as the next-hop relay the 1-hop neighbor that maximizes the PDR to reach node c.

In order to put both LASP's and GPSR's performances into context we compared them both

against the performance achievable by an optimal protocol that uses global topology knowledge to find minimum cost paths between any pair of nodes. While such a protocol is unfeasible in practice, it allows us to understand how close to optimal the protocols under investigation are. We implemented 3 optimal protocols variants, each optimizing one of the end-to-end metrics under scrutiny: PDR, transmission count and hop count.

The parameters used by the different protocols are summarized in Table 4.4.

Parameter	**Applicability**	**Value**
Max. transmissions per hop	All protocols	5
Look-ahead size (hops)	GPSR, LASP	1, 2, 3
Spatial cell size (m)	LASP	50×50

Table 4.4: Configuration parameters used in LASP's trace-based evaluation.

We now describe how the performance metrics were computed for each path found by the different protocols. The hop count follows immediately from the path by simple counting of the number of nodes that compose it. It can be seen as a proxy for latency, given that the smaller the number of hops, the sooner the packet should arrive. For the end-to-end PDR, we used the expected value which can be computed as the product of the edge delivery probabilities P_{rdel} (Equation 4.6) over the path p, given by:

$$PDR(p,t) = \prod_{(u,v)\in p} P_{rdel}(u,v,t), \tag{4.11}$$

where t is the maximum number of transmissions per hop. The P_{rdel} computation for each hop uses the actual PDR values previously defined for each individual link. PDR measures reliability. For the transmission count we also used the expected value. The Expected Transmission Count (ETX) for a link is defined as the inverse of probability of successfully delivering a packet and receiving an acknowledgment over a lossy link [CABM05]. To compute the end-to-end ETX, we summed the per-link ETX over all links in the path, yielding:

$$ETX(p) = \sum_{(u,v)\in p} \frac{1}{PDR_{u\to v} \times PDR_{v\to u}}. \tag{4.12}$$

ETX is a measure of both network load and path quality.

In order to evaluate LASP's sensitivity concerning spatial cell size we also executed the protocol using spatial cell sizes of 100×100, 200×200 and 500×500 m and compared the results with the baseline 50×50 m variant. Furthermore, to emulate the effect of an infinitely large spatial cell, we also ran LASP with a historical spatial connectivity map where the delivery probabilities between cells were chosen uniformly at random.

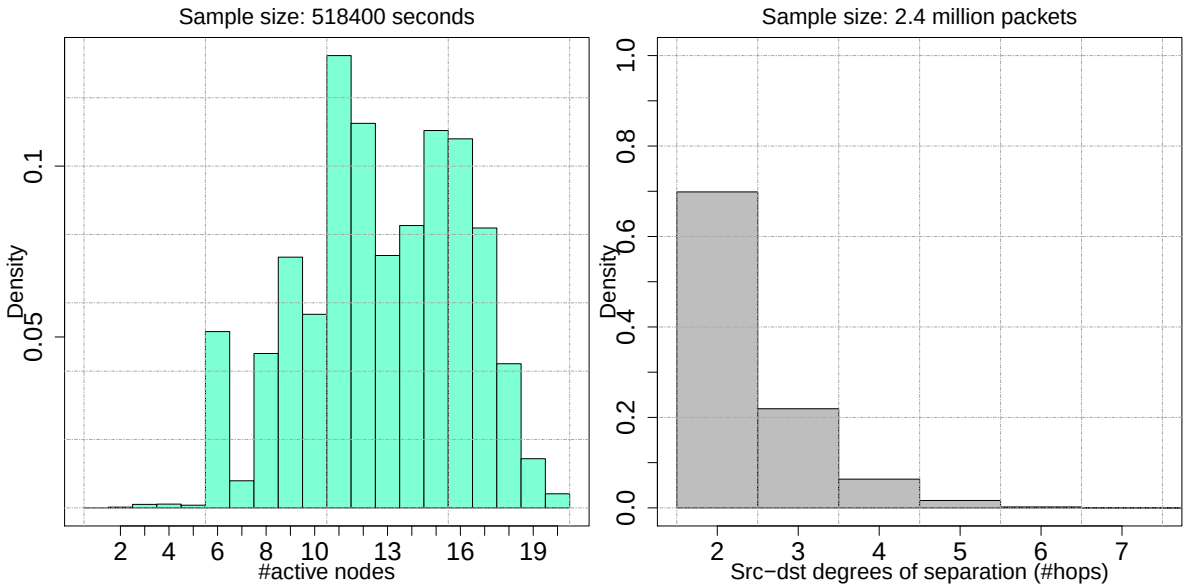

(a) Number of active nodes

(b) Hops of separation between source and destination

Figure 4.12: Network conditions during the period of LASP's trace-based evaluation.

We now look at the network conditions during the period covered by the collected connectivity traces: November 25$^{\text{th}}$ to November 30$^{\text{th}}$, 2013. Figure 4.12a shows a histogram of the number of simultaneously active nodes during this period. While HarborNet features a total of 30 nodes, not all are active at the same time. There are multiple reasons for this. One is that the number of trucks being used depends on the level activity within the Harbor, which fluctuates. Another is that trucks occasionally leave the harbor for maintenance and external work. Also, in order to be included in the traces, nodes need to have a working GPS receiver (for location tracking) and cellular connection (for connectivity log uploading). Due to all of these reasons, in practice the mean number of nodes in the traces was 12.8, with a standard deviation of 3.33. The mode was 11 and the maximum, 20.

Furthermore, because each ship is tended to by multiple vehicles, HarborNet nodes tend to cluster, resulting in a small diameter network. Figure 4.12b presents a histogram of the number of hops separating source and destination for the packets sent during the analysis. Less than 10% of source-destination pairs were separated by more than 3 hops. Roughly 70% of them were actually separated by only 2 hops.

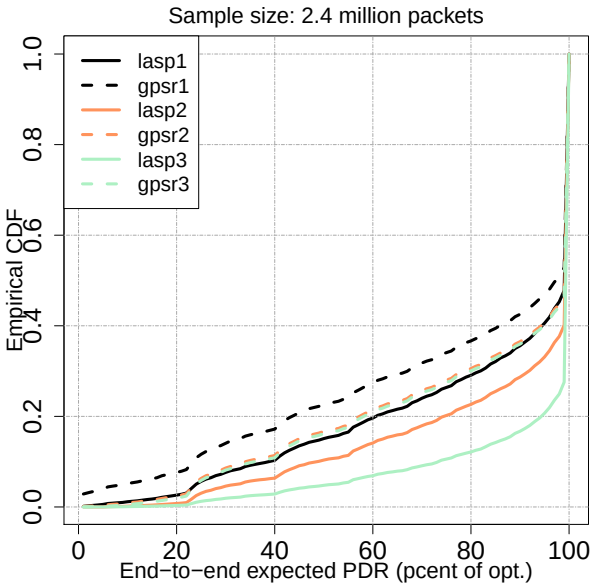

Figure 4.13: LASP trace-based evaluation results: expected end-to-end packet delivery ratio.

4.4.2 Results

We present PDR, ETX and hop count results relative to the optimal protocol that optimizes that specific metric. Empirical Cumulative Distribution Functions (ECDFs) are used to give a complete picture of the differences between protocols. For easy identification, each protocol variant is named by suffixing the neighborhood size to the main protocol name (e.g. lasp2 identifies LASP's variant using a real-time 2 hop neighborhood).

Packet Delivery ratio

Figure 4.13 shows the ECDF of the end-to-end PDR that the LASP and GPSR protocols were able to achieve, relative to an optimal protocol that maximizes end-to-end PDR. The plot shows PDR on the x-axis and ECDF on the y-axis, so the lower the curve, the better.

Let us first compare LASP and GPSR, both with 1-hop of real-time neighborhood information (lasp1 vs gpsr1). Both GPSR and LASP matched the optimal protocol for roughly 50% of the packets. The differences start appearing when we look at the lower half of the distributions. If we observe the first quartile (i.e. ECDF = 0.25), GPSR achieved 50% of the optimal PDR, while LASP obtained around 70% of the optimal, a 20% increase. This improvement is consistent throughout the entire lower half of the distributions and is explained by the fact that GPSR greedily chooses long hops regardless of the PDR, while LASP actively tries to maximize PDR by choosing well connected nodes.

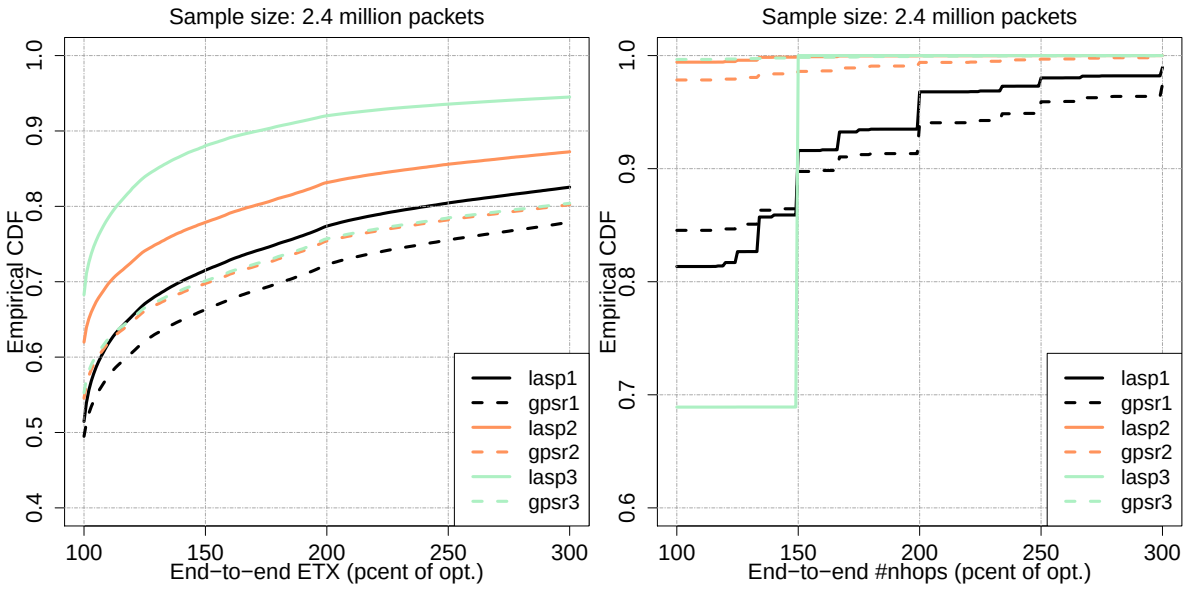

(a) Expected transmission count

(b) Expected hop count

Figure 4.14: LASP trace-based analysis results: expected transmission count and hop count.

Now we look at the effect of increasing the real-time neighborhood size. As expected, this boosted performance significantly. With 2 hops of neighborhood, both GPSR and LASP improved by around 20% at the first quartile. 3 hops of neighborhood, however, improved LASP performance greatly but left GPSR almost unaffected. The reason for this behavior can be be found by looking at the histogram of the number of hops of separation between source and destination in Figure 4.12b. Roughly 70% of source-destination pairs are separated by only two hops, so a greedy protocol like GPSR will not be able to make use of more than 2 hops of neighborhood very often. LASP on the other hand, is able to take advantage of this additional information because it tries to maximize end-to-end PDR, not hop count.

Transmission Count

Figure 4.14a shows the end-to-end ETX results. In this case, the faster the ECDF converges to 1, the better (i.e. fewer transmissions), so higher curves are preferable. All protocols were able to match the optimal value for at least 50% of the packets, so all the differences are concentrated on the upper half of the distributions.

When we compare the 1-hop neighborhood versions of LASP and GPSR (lasp1 vs gpsr1) at the upper quartile (i.e. ECDF = 0.75), we observe GPSR was within 200% of the optimal for 75% of the packets, while LASP fell within 160% of the optimal, a 40% improvement. While LASP does

not explicitly attempt to minimize packet transmissions, choosing well connected nodes indirectly contributes to this, as fewer retransmissions are required.

When furnished with larger real-time neighborhood sizes of 2 and 3 hops, LASP was able to leverage this additional information to find better connected paths and consequently, achieve significantly lower ETXs. GPSR, on the other hand, due to its focus on short paths, was unable to take as much advantage of this information. Going from 1 to 2 hops resulted in a good 40% improvement at the upper quartile but moving from 2 to 3 hops provided no meaningful benefit. This mimics the saturation tendency observed in GPSR's PDR results and can also be explained by the small number of hops separating source and destination.

Hop Count

Finally, we look at the end-to-end hop count results, depicted in Figure 4.14b. All presented values are relative to the optimal hop count, represented by shortest path possible between source and destination. Hence, higher curves are better. All protocols were able to match the optimal number of hops for at least 70% of the packets. The differences between protocols occur within the upper 30% of the distributions.

GPSR actively tries to minimize the number of hops, while LASP does not. In practice, for the 1-hop neighborhood case, LASP was very competitive with GPSR, with the ECDFs for the two protocols crossing each other at the 90% percentile mark. Behind this is the fact that when GPSR's greedy strategy fails, it goes into perimeter mode, potentially traversing many hops, which results in a long-tailed distribution. The backtracking mechanism used by LASP introduces additional hops as well, but, when compared with GPSR, it resulted in a shorter tail.

GPSR performed better in the 2 and 3-hop cases, basically matching the theoretical optimal protocol in the 3-hop variant. LASP with a 3-hop neighborhood however, used 50% more hops than optimal for roughly 30% of packets. This is a consequence of the fact that there is a large percentage of source-destination pairs separated by only 2 hops, as Figure 4.12b shows. With the destination only 2 hops away and 3 hops of real-time neighborhood information available, LASP, rather than going for the shortest path, will be able to detect any 3-hop paths that provide better end-to-end PDR than the shorter 2-hop path and use them whenever they exist.

Spatial Cell Size Sensitivity Analysis

We now turn our attention to LASP's spatial cell size sensitivity analysis, where we evaluate how the protocol's performance is affected by the granularity of the available spatial information. For this purpose we compare the baseline 50×50 m LASP with variants using larger 100×100, 200×200 and

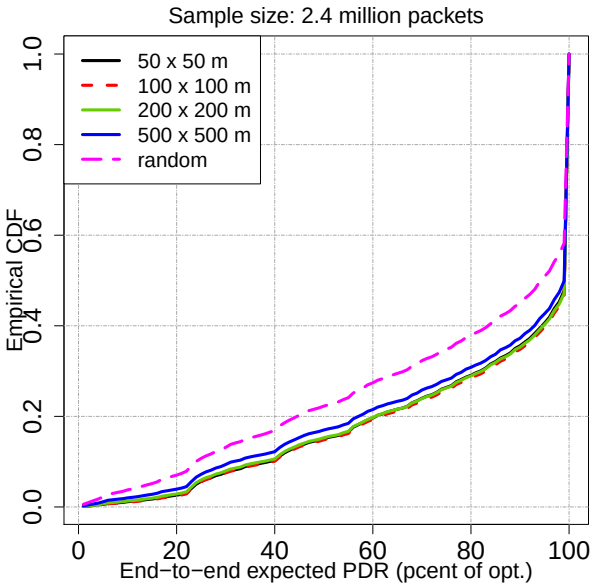

Figure 4.15: LASP cell size sensitivity analysis results: expected end-to-end packet delivery ratio.

500×500 m cells. Furthermore, the effect of an infinitely large cell where all spatial autocorrelation is lost is emulated through an additional variant where the historical delivery probability between (50×50 m) spatial cells is chosen uniformly at random. The size of the real-time neighborhood was set to 1 hop for all variants.

Figure 4.15 shows the ECDF of the expected end-to-end PDR relative to the optimal for all of the aforementioned protocol variants (i.e. lower curves are better). The main result is that LASP did not exhibit a significant sensitivity to spatial cell size. The 50×50, 100×100 and 200×200 variants were basically indistinguishable from one another. It was when the cell size was increased to 500×500 m that the performance started to deteriorate. If we consider the PDR values at the ECDF first quartile (i.e. ECDF $= 0.25$), the 500×500 m variant obtained 68% of the optimal performance, while the baseline 50×50 m variant obtained 73% (i.e. 5 % more). The worst case scenario, represented by the random historical connectivity variant, resulted in a 17% performance loss at the ECDF's first quartile: i.e. 55 versus the baseline's 73% of the optimal.

Figure 4.16a shows the Expected Transmission Count (ETX) results for the sensitivity analysis, once more using the ECDF of the ratio between the achieved ETX and the the optimal ETX (i.e. higher curves are better). The results were similar to the PDR results. The 50×50, 100×100 and 200×200 m variants were practically indistinguishable from one another. The 500×500 m variant resulted in a small increase in the expected number of transmissions relative to the baseline. If we consider the distributions' upper quartile (i.e. ECDF $= 0.75$), the 500×500 variant transmitted 191% of the optimal number of packets, compared with baseline's 180% of the optimal,

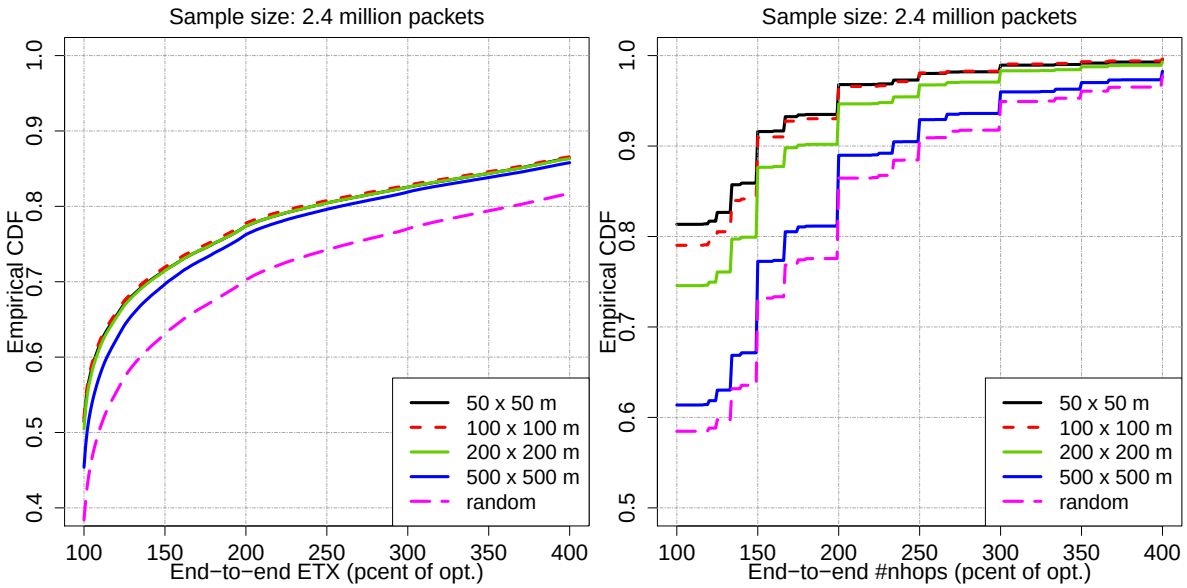

(a) Expected transmission count

(b) Expected hop count

Figure 4.16: LASP cell size sensitivity analysis results: expected transmission count and hop count.

an increase of 11%. The random historical connectivity variant resulted in a much higher expected number of transmissions, with the distribution only crossing the upper quartile at 263% of the optimal, an 83% increase compared with the baseline's 180%. This is an indication that random connectivity information leads to the selection of poorly connected links, which require a large number of retransmissions.

Finally we consider the expected hop count results, shown in Figure 4.16a as the ECDFs of the ratio between the obtained expected hop count and the optimal value (i.e. higher curves are better). Relative to the other metrics, here we can observe larger differences between the different protocol variants. For brevity we focus on the hop count at the ECDF's upper quartile (i.e. ECDF = 0.75). Both the 50×50 and the 100×100 variants cross this quartile at 100% of the optimal hop count, which is ideal. The 200×200 m variant crosses the same quartile at around 125% of the optimal, while the 500×500 variant does it at 150% of the optimal. This leads us to believe that having larger cells increases the number of relay selections leading to dead ends, which when resolved through backtracking, increase the overall number of hops traversed. The random variant performs worst of all, crossing the upper quartile at 167% of the optimal number of hops.

In summary, cell sizes larger than 100×100 m resulted in an increase in the number of hops, while a noticeable effect on expected end-to-end PDR and ETX was only observed once the cells grew in size to 500×500 m.

4.5 Related Work

To the best of our knowledge we are the first to study and propose spatial connectivity as an heuristic for a vehicular multi-hop communication protocol.

Vehicular connectivity has been studied in the past but not from a spatial connectivity perspective and not using real data from a vehicular testbed. Previous connectivity studies mostly used synthetic mobility and channel models. For example, Fiore *et al.* [FH08] used simplified mobility models and a fixed transmission range, as did Viriyasitavat *et al.* [VTB09]. Ferreira *et al.* [FCaFT09] and Loulloudes *et al.* [LPD10] used real vehicle positions but maintained the fixed transmission range.

Experimental connectivity studies have been small in scale and hence more focused on channel characterization (e.g. [OBB09, MBS+10, MMKH11]) than overall network behavior. In contrast, in our work we leveraged connectivity data collected two larger-scale vehicular networks and performed a complete spatial autocorrelation analysis and trace-based evaluation.

As first introduced in Chapter 2, earlier attempts to overcome spatial heterogeneity in vehicular multi-hop have focused on the use of road maps as a backbone for route selection. These protocols select a sequence of roads that connect source and destination and then forward the packets along them. The choice of roads can be dictated simply by shortest distance (e.g. GSR [LHT+03], SAR [THR03]), or by using statistical traffic information to assign weights to each road segment, with the goal of promoting the selection of frequently-traveled, and hence well-connected, roads (e.g. A-STAR [SLL+04], ACAR [YLL+10], GyTAR [JSMGD07]). As we have previously discussed, this bounding of packets to roads limits connectivity. Furthermore, it precludes the utilization of these protocols in areas where there are no maps, such as the harbor we used in our evaluation.

For forwarding along roads, most road-based protocols greedily choose the neighbor closest to the beginning of the next road segment as the next hop relay (e.g. SAR, GSR, GyTar). ACAR is the closest to LASP in this regard, in that it chooses next hops based on a metric that estimates the expected end-to-end probability of delivery, in this case using a modified ETX link quality metric. However the way ACAR does this calculation assumes connectivity is uniform across space, which we know not to be the case.

It is possible for forwarding to fail due to lack of vehicles, necessitating the use of a recovery procedure. Some protocols simply have the current packet holder carry it until a suitable relay can be found (e.g. SAR, GyTAR), which can lead to very high latencies. Other protocols blacklist the current road and attempt to forward along a different road (e.g. A-STAR). By backtracking to a previous node, LASP is able to explore alternative routes more quickly.

The idea of using a multi-hop neighborhood in routing has appeared in many different contexts..

Manku *et al.* [MNW04] showed that a 2-hop neighborhood allows for an asymptotically optimal routing protocol for peer to peer networks, using the hop count metric. Terminodes [BGLB02] and GeO-LANMAR [DRGM06] are two protocols that use GPSR-like geographic forwarding combined with a 2-hop neighborhood. However, contrary to LASP, they use the distance to destination heuristic, ignoring spatial heterogeneity.

4.6 Summary

In this chapter we presented LASP, a spatial connectivity-based routing and forwarding protocol for vehicular networks. We started by questioning the assumptions behind the metrics used by prior protocols. Namely, that distance is a good predictor for connectivity and that wireless vehicular connectivity closely mimics the topology of the road network the vehicles move in. Using the HarborNet and PortoVANET vehicular testbeds, we showed that neither of these assumptions hold in practice. Analysis of collected data exhibited little correlation between sender-receiver distance and link PDR and 80% of the registered packet exchanges took place between vehicles in non-contiguous road segments.

The data showed, however, a high degree of correlation between the PDRs of co-located links, supporting the idea that spatial location can be used to predict connectivity between nodes. With this in mind, we presented a means to gather and process spatial connectivity information summarizing connectivity between different geographical areas. LASP then uses a combination of real-time and historical spatial connectivity information to estimate end-to-end delivery probabilities and pick, at each hop, the most promising next hop relay. Additionally, LASP features a backtracking mechanism that allows it to recover from local minima.

Further leveraging the HarborNet testbed, we performed a thorough evaluation using a mathematical analysis fed by real connectivity traces. LASP showed improvements in end-to-end PDR of upwards of 20% relative to the benchmark protocol GPSR. In the next chapter we shall see that these improvements are consistent with experimental results obtained from a prototype implementation deployed on the HarborNet testbed.

While LASP uses a sophisticated connectivity metric that allows it to deal with the spatial heterogeneity present in vehicular networks, unlike DAZL, it uses but a single forwarder per hop. This makes it susceptible to the unstable nature of wireless vehicular links. To address this, in the next chapter we introduce LASP-MF, a multi-forwarder version of LASP that combines LASP's spatial connectivity metric with DAZL's node diversity-based forwarding.

Chapter 5

LASP-MF: LASP Multi-Forwarder

In this chapter we introduce LASP-MF, a routing and forwarding protocol that combines both DAZL's node diversity-based approach and LASP's spatial connectivity concept to maximize routing reliability. We start by describing how node diversity and spatial connectivity can complement each other in vehicular multi-hop. We then describe how LASP-MF's design achieves this. Finally we evaluate LASP-MF using both an analytical trace-based setup and actual experiments performed on the HarborNet testbed.

5.1 Premise: Complementarity of Node Diversity and Spatial Connectivity

As discussed in Chapter 2, the main challenges for vehicular network routing derive from link and topology instability, as well as spatial heterogeneity, i.e. differences in connectivity across different spatial regions.

In Chapter 4 we presented LASP, a geographic multi-hop communication protocol that uses spatial connectivity information to pick, at each hop, the relay that maximizes the expected probability of successfully delivering the packet to the destination. By using spatial connectivity LASP is able to overcome spatial heterogeneity, directing packets through well-connected areas that maximize the likelihood of finding nodes to relay them towards the destination. Furthermore, by building paths hop-by-hop rather than all at once, LASP is able to cope with link and topology instability better than traditional topology-based protocols. However, since the next hop relay is chosen beforehand by the sender, it still relies on the quality of a specific wireless link, which can create problems.

In Chapter 3 we presented DAZL, a forwarding scheme that leverages node diversity to address

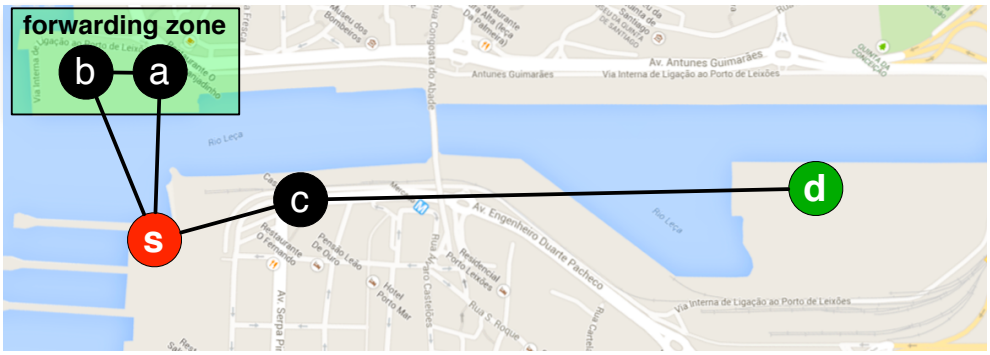

Figure 5.1: Example scenario where exploiting node diversity can increase LASP's performance by allowing any node inside the forwarding zone (green rectangle) to forward the packet.

this issue. In DAZL, instead of choosing a specific next hop node, the sender addresses the packet to a geographic forwarding zone and the candidate relays inside it run a distributed coordination algorithm to decide who should actually forward the packet. This frees the protocol from relying on the quality of any particular link. In Section 3.1 we showed experimentally how allowing multiple vehicles to cooperate in forwarding decreases the likelihood of packet loss, effectively creating a reliable *virtual* link out of multiple unreliable real ones by leveraging node diversity.

As we see here, the main concepts behind these protocols, spatial connectivity (LASP) and node diversity (DAZL), operate on different levels (routing and forwarding, respectively) and effectively complement each other. In this chapter we combine the two concepts to create LASP Multi-Forwarder, or LASP-MF.

Figure 5.1 shows an example of how LASP-MF can improve reliability relative to regular LASP. Similarly to the running example used throughout Chapter 4, the figure depicts the Leixões Harbor in Portugal, 5 network nodes and the links between them, represented by lines. Node s wants to communicate with d and can choose between three possible relays to convey the packet. Assume the available spatial connectivity information says that the path around the top of the figure is more reliable so, if running LASP, s would choose either node 1 or 2 to relay the packet. But, as we have explored in Chapter 2, links in vehicular networks often exhibit partial and unpredictable connectivity. Consequently, even with retransmissions, there will be a non-zero probability that the message can not be decoded by the chosen relay. If, on the other hand, we leverage the shared nature of the wireless medium to allow both nodes a and b to cooperate in relaying the packet, the likelihood that at least one of them will be able to decode the packet increases because, as a consequence of their physical separation, their links' loss patterns are independent. This is exactly the same node diversity concept previously leveraged by the DAZL forwarding protocol, and that we employ in LASP-MF as well.

5.2 Protocol Design

5.2.1 Overview

LASP-MF is a geographic multi-hop communication protocol that combines the best features of both LASP's and DAZL's designs. To avoid unnecessary repetition, we assume the reader is familiar with both LASP and DAZL, previously described in Sections 3.2 and 4.3.

LASP-MF makes the same assumptions as LASP and DAZL: i) the destination's location is known; ii) nodes know their own location and; iii) nodes periodically broadcast CAMs with their id and location and optionally, neighborhood information covering up to a given certain of hops.

Like LASP, LASP-MF divides the problem into forwarding, the process through which a next hop relay is chosen, and routing, the process through which a network topology abstraction used to guide forwarding decisions is created. LASP-MF shares its logical architecture (Figure 4.7) and routing component with LASP. CAM beaconing data is used to create a historical spatial connectivity graph, which we name look-ahead, and a real-time connectivity graph covering the local neighborhood (nodes up to n-hops away from the current node).

The key difference between LASP and LASP-MF is how the routing information is used by the forwarding engine to pick a next hop. In LASP, at each hop, the node sending the packet uses the connectivity graphs to pick the next hop relay that maximizes the estimated end-to-end packet delivery probability to the destination.

In contrast, LASP-MF uses the connectivity graphs in a DAZL-like two-step zone-based forwarding process. First, on the sender side, the graphs are used to pick not a node but a geographical forwarding zone that maximizes the estimated end-to-end delivery probability. The packet is then broadcast and the connectivity graphs are used a second time, now by each receiver node inside the forwarding zone, to rank their own probability of delivery to the destination relative to the other nodes inside the zone, and thus define a forwarding priority. This strategy contrasts with DAZL's implementation of zone-based forwarding, which uses a simple distance to destination metric to both define a forwarding zone and prioritize forwarders inside it.

Figure 5.2 illustrates LASP-MF's two-step forwarding process, which contrasts with LASP's single-stage process (Figure 4.8). Assume node s wants to send a packet to node d, and nodes 1 through 6 are its neighbors that can act as relays. Consider the real-time neighborhood is 2-hops large. Node s starts by defining the candidate forwarding zones. For this, it starts by considering the individual spatial cells in which each neighbor is located. Then it aggregates the cells between which neighbors can communicate to create larger candidate forwarding zones in order to maximize the potential node diversity gains. In Figure 5.2, nodes 1 and 2 can communicate, so their spatial

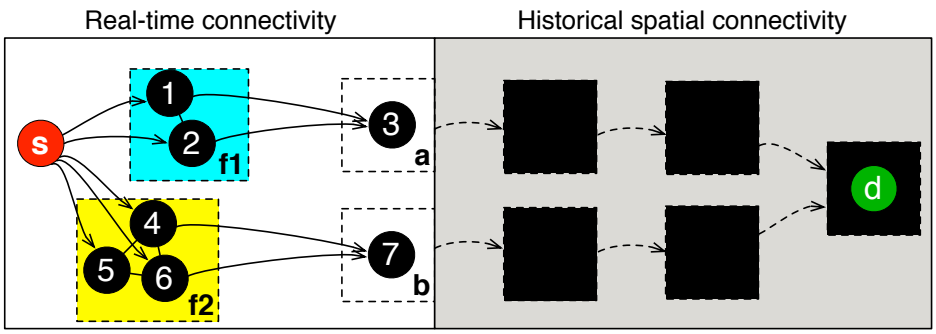

Figure 5.2: LASP-MF uses LASP's connectivty graph to choose geographical forwarding zones and prioritize nodes inside them.

cells are aggregated into a single candidate forwarding zone $f1$. Likewise for nodes 4, 5 and 6, whose cells define zone $f2$. Now, to find the best zone, node s must estimate the end-to-end delivery probability for each candidate forwarding zone. It does this by calculating the probability that at least one of the nodes inside the forwarding zone receives the packet and then delivers it to the destination, using a combination of real-time and historical spatial connectivity information.

Assume zone $f2$ maximizes the estimated end-to-end delivery probability. That zone's coordinates would be placed in the packet header and the packet would then be broadcast. Now, each node inside $f2$ that receives the packet, which we call a candidate forwarder, must make its own decision as to whether it should forward the packet or not. This is performed using a distributed coordination and prioritization scheme.

Figure 5.3 illustrates LASP-MF's forwarder coordination procedure, which is similar to the one employed by DAZL (Figure 3.6), but using spatial connectivity instead of distance as a prioritization heuristic. In LASP-MF, each candidate forwarder uses the historical and real-time connectivity graphs created by the routing component to estimate its own end-to-end probability of delivering the packet to the destination P_{edel} and also the same probability for each of the other candidate forwarders. Then it creates a ranking by ordering all candidates (including itself) in decreasing delivery probability order.

The candidate's rank within the raking (i.e. the position it appears in) defines its forwarding decision. If the rank is not one of the r best, where r is a protocol parameter, the candidate drops out of contention to avoid creating unnecessary congestion. Otherwise, the candidate assigns itself a forwarding slot with an associated waiting time that is inversely proportional to its rank (i.e. a high rank leads to an earlier slot). The candidate then enters a waiting state. If a forwarding from another candidate is heard while in this state, the forwarding is cancelled to avoid redundancy. Otherwise, the candidate forwards the packet after the waiting time has elapsed.

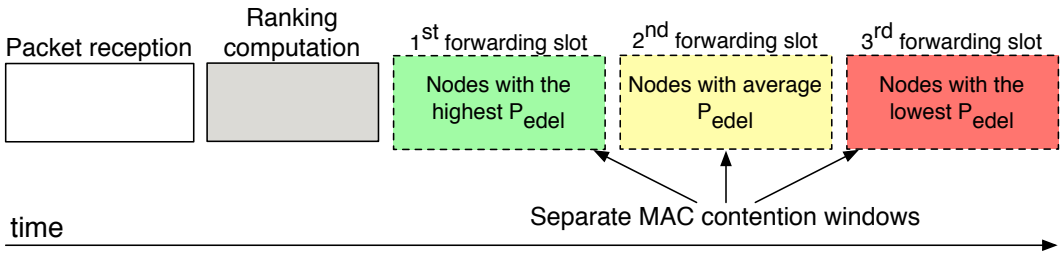

Figure 5.3: LASP-MF spreads forwarders in time according to their estimated end-to-end delivery probabilities.

Each candidate forwarder executes this procedure independently. The resulting effect is that the candidates with higher estimated delivery probabilities are prioritized (i.e. are assigned earlier forwarding slots) relative to candidates with lower probabilities, as depicted in Figure 5.3. The goal is for lower-ranked candidates to forward only when higher-ranked ones failed to receive the packet.

The following sections describe forwarding zone selection (Section 5.2.2) and forwarder coordination (Section 5.2.3) in further detail.

5.2.2 Forwarding Zone Definition and Selection

Having the packet sender choose a forwarding zone is the first step in LASP-MF's two-step forwarding process. The forwarding zone is the geographical area inside which nodes cooperate to forward a given packet. LASP-MF's goal is ultimately to maximize end-to-end delivery probability. This could be achieved by defining a very large forwarding zone that encompasses all of the possible next hop relays, as this would maximize node diversity and the probability that at least one of them would receive the packet. However, the larger the forwarding zone, the higher the likelihood of hidden terminals. If candidate forwarders are hidden from each other, LASP-MF's implicit acknowledgments will not be heard by all, increasing the likelihood of redundant transmissions and replication. LASP-MF must therefore strike a balance between the size of the zone and how well connected vehicles inside it are.

LASP-MF forwarding zone selection is made using spatial connectivity information, which is defined at the spatial cell level. It makes therefore sense for us to use spatial cells to define forwarding zones as well. However, each spatial cell only covers an area of 50×50 meters, which may be insufficient to exploit node diversity. Our solution is to define a forwarding zone as a set of one or more spatial cells, which allows the tailoring of the zone's size to each specific forwarding scenario.

To balance the conflicting requirements of size and connectedness, the strategy adopted by LASP-MF is to find the forwarding zone (i.e. set of spatial cells) that maximizes the expected end-to-end delivery probability while obeying the following constraint: any two cells in the forwarding zone must be able to communicate amongst themselves with PDR $\geq p_{min}$, where p_{min} is a protocol parameter. To do this, LASP-MF starts by enumerating all the possible forwarding zones that obey this constraint and then estimates the end-to-end delivery probability for each of them in order to find the best candidate.

The set of candidate forwarding zones $\mathcal{C}$ is built as follows:

1. For each neighbor n of the current node, let the spatial cell where n is located be a zone $z \in \mathcal{C}$. Note that since $\mathcal{C}$ is a set, duplicates will be automatically discarded.

2. Now, for each $z \in \mathcal{C}$, extend z with the set of spatial cells reachable from z in a single hop with PDR $\geq p_{min}$. This allows us to maximize the size of the candidate forwarding zone while at the same time ensuring that it remains well connected. If the protocol is being executed with a 2-hop or larger real-time neighborhood, this information can be extracted from the real-time connectivity graph $\mathcal{G}_r$. Otherwise (i.e. if the neighborhood covers only 1 hop), this will be obtained from the historical connectivity graph $\mathcal{G}_h$. Zones that, after extended, end up being composed of the same exact set of spatial cells as a pre-existing candidate are considered duplicates and thus discarded. Partial overlaps between zones, on the other hand, are permitted (i.e. the different candidate zones are not necessarily disjoint).

The goal is then to choose the candidate zone $z \in \mathcal{C}$ that maximizes the probability of delivery to the destination's cell c_d, P_{zondel}. I.e.:

$$\text{chosen forwarding zone} = \arg\max_{z \in \mathcal{C}} \big[P_{zondel}(s, \mathcal{N}, c_d, t)\big], \tag{5.1}$$

where s is the current node, $\mathcal{N}$ is the set of neighbors of the current node s that are inside candidate zone z and t is the maximum number of transmissions per hop.

We define the end-to-end zone probability of delivery P_{zondel} as the probability that at least one of the neighbors inside the zone successfully receives the packet and then delivers it to the destination's spatial cell. It is easier to compute this as the complement of the probability that all neighbors in $\mathcal{N}$ fail to either receive the message or receive the message but fail to deliver it to the destination. This failure probability can itself be written as the complement of the probability of success of the same compound event. This leads us to the following equation:

$$P_{zondel}(s, \mathcal{N}, c_d, t) = 1 - \prod_{i=1}^{|\mathcal{N}|} 1 - \big\{P_{rdel}(s, \mathcal{N}_i, t) \times \max_{n \in \{\mathcal{N}_i, \mathcal{N}_i.neigh\}} \big[P_{edel}(\mathcal{N}_i, n, c_d, t)\big]\big\}. \tag{5.2}$$

The product between brackets represents the end-to-end delivery probability for a specific neighbor $\mathcal{N}_i$, which is inside the forwarding zone z. The first factor in this product, P_{rdel}, represents the delivery probability between the current node s and its direct neighbor $\mathcal{N}_i$, as previously defined in Equation 4.6. This calculation uses real-time connectivity information. The second factor represents the end-to-end delivery probability between $\mathcal{N}_i$ and the destination's spatial cell c_d, and is defined as the maximum probability over the probabilities yielded by the different possible paths between $\mathcal{N}_i$ and c_d. P_{edel} represents the spatial delivery probability between each neighbor $\mathcal{N}_i$ and the destination location, when passing through node n, a direct neighbor of $\mathcal{N}_i$. P_{edel} was previously defined in Equation 4.9. As described in Section 4.3, it uses a variable combination of real-time and historical look-ahead information, depending on the size of the available real-time neighborhood. When the real-time local neighborhood is only 1-hop large, we have no information regarding $\mathcal{N}_i$'s neighbors. In that case $\mathcal{N}_i$ is defined to be a neighbor of itself (with PDR 100%) and the P_{edel} computation uses only historical information.

In the next subsection, we describe how nodes inside the forwarding zone cooperate in forwarding the packet.

5.2.3 Forwarder Ranking Inside the Forwarding Zone

After a forwarding zone is chosen and the packet is broadcast, receiver nodes inside the forwarding zone must coordinate to decide which node is to actually forward the packet. This is the second step in LASP-MF's two-step forwarding process. The coordination is achieved through the computation of a forwarder ranking, which defines priorities by specifying how long a node inside the forwarding zone will wait and listen for other forwarders' transmissions before itself forwards the packet.

In LASP-MF, each node that receives the packet computes the ranking independently. There are two parts to this computation. First, the receiver must decide which nodes are to be part of the ranking: we name this the expected candidate forwarder set, $\mathcal{F}$. Then, the receiver must rank the candidates in $\mathcal{F}$ relative to one another.

The expected forwarder set $\mathcal{F}$ should ideally include all nodes inside the forwarding zone that actually received the packet. But since that information is not directly available, an estimation is required. Clearly, the node computing the ranking must be part of $\mathcal{F}$, for it received the packet and is inside the zone. The composition of the rest of the set depends on the size of the local real-time neighborhood:

≥ 2 **hop real-time neighborhood** If the protocol is configured with a real-time neighborhood of at least 2 hops, the node computing the ranking knows what are the previous hop's 1-hop neighbors and their locations. All of those neighbors that do not appear in the packet's

backtrace and are inside the forwarding zone are considered candidate forwarders and are added to the set $\mathcal{F}$. The ones that do appear in the packet's backtrace are not included because they will not forward the packet: they will discard it as a duplicate to prevent the formation of a routing loop.

1 hop real-time neighborhood With a real-time neighborhood of size 1 hop, the node computing the ranking only knows its own neighbors, and therefore lacks information regarding the neighbors of the previous hop. In this case, the candidate forwarder defines the expected forwarder set $\mathcal{F}$ to be composed of itself and all of its neighbors that are simultaneously inside the forwarding zone and not a part of the packet's backtrace.

With the expected candidate forwarder set $\mathcal{F}$ defined, we now focus on the ranking of the nodes that compose it. This is done according to the following procedure:

1. For each node $u \in \mathcal{F}$, the probability of u successfully delivering the packet to the destination, P_{edel}, is estimated using Equation 4.9, the same equation used by LASP to choose a next hop relay.

2. Now the candidate forwarders in $\mathcal{F}$ are sorted in decreasing delivery probability order. The index i at which a candidate forwarder appears in the ordering is its rank. I.e. the candidate with the highest estimated probability of delivery has rank 0, the highest possible rank.

Now the node computing the rank must translate its own rank into a forwarding slot. If the node is one of the r best-ranked potential forwarders, where r is a protocol parameter, it is assigned a forwarding slot $s = \left\lceil \frac{rank}{nps} \right\rceil$, where $rank$ is the node's rank and nps the number of nodes per slot, also a protocol parameter. Then, the waiting time is simply the product of s times the chosen slot duration. This prioritizes the better-connected nodes by giving them an earlier forwarding opportunity. If the node's rank is outside of the r best, then it does not forward the packet to avoid unnecessary congestion.

We now go through an example of the protocol's operation, using the scenario in Figure 5.1, which, according to our empirical observations of the HarborNet testbed, represents a realistic situation. For this purpose, let us assume the following protocol parameters: 1 hop real-time neighborhood, 2 competing forwarders maximum ($r = 2$) and 1 node per forwarding slot ($nps = 1$). The sequence diagram depicted in Figure 5.4 shows the actions of the different nodes (horizontal axis) and the timing at which they occur (vertical axis). We describe the sequence as follows:

1. The source analyzes its forwarding zone options and calculates that a forwarding area encompassing both forwarder 1 and 2 maximizes the expected end-to-end probability of delivery.

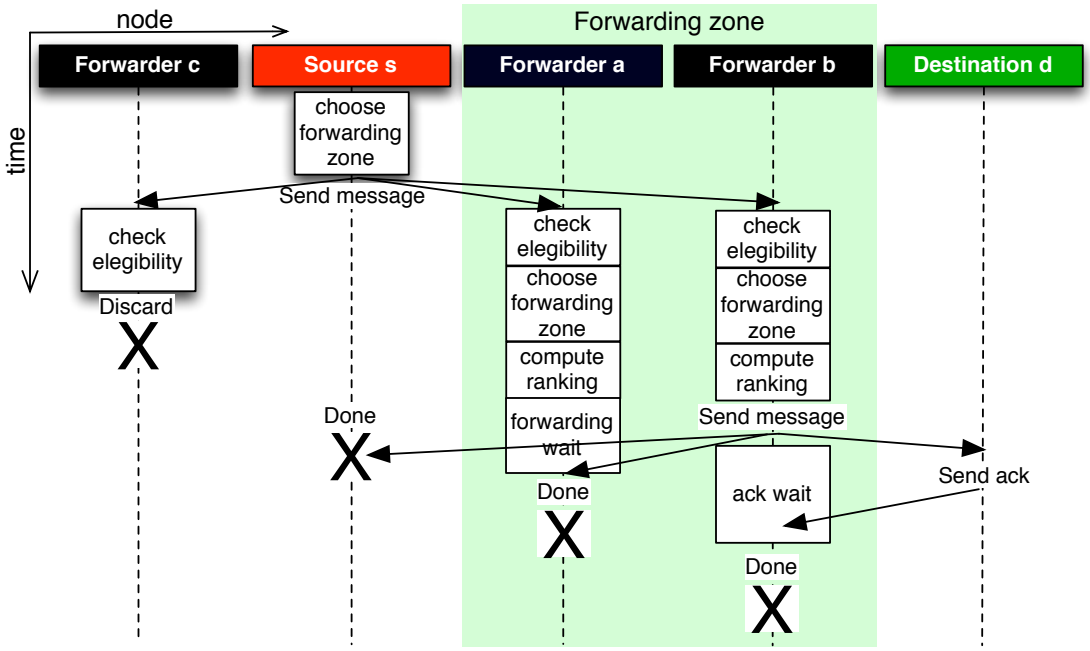

Figure 5.4: LASP-MF sequence diagram for the scenario in Figure 5.1.

The source then broadcasts the packet. Assume all candidate forwarders (1, 2 and 3) receive it.

2. Upon reception, candidate forwarder 3 realizes it lies outside of the forwarding zone and therefore discards the packet.

3. Candidate forwarder 1 ($f1$) starts by confirming that it is in fact inside the forwarding zone. Then it chooses the forwarding zone for the next hop, which in this example would coincide with the destination's spatial cell. Then $f1$ proceeds to compute the forwarding ranking. First it defines $\mathcal{F} = \{f1, f2\}$, for it expects forwarder 2 ($f2$) to attempt to forward the packet as well, given that it is inside the zone. Assume the expected probability of delivery to the destination by $f1$ is lower than for $f2$, so $f1$ ranks itself lower than $f2$. Hence $f1$ obtains the 2^{nd} forwarding slot and enters a waiting state before forwarding.

4. In a similar manner, candidate forwarder 2 ($f2$) also confirms it is inside the forwarding zone, chooses the next hop forwarding zone as the destination's spatial cell and proceeds to compute the forwarding ranking. Candidate forwarder 2 defines $\mathcal{F} = \{f1, f2\}$ and computes the ranking. Because we have established that $f2$'s end-to-end delivery probability is higher than $f1$'s, $f2$ ranks itself highest ($rank = 0$). Therefore it gets the 1^{st} forwarding slot, forwards the packet immediately and enters a waiting state where it waits to listen for an

acknowledgement from the next hop.

5. Both the source s and $f1$ overhear $f2$'s forwarding and mark their forwarding events as successfully completed.

6. The destination d receives $f2$'s forwarding and acknowledges the reception to $f2$, which then marks its forwarding event as done. The process is now complete.

5.3 Trace-based Evaluation

In this section we present a trace-based analytical evaluation of LASP-MF's performance against LASP, DAZL, and several theoretical optimal protocols, each maximizing a specific performance metric.

5.3.1 Setup

LASP-MF's trace-based evaluation benefits from the setup previously employed to evaluate LASP, which was described in detail in Section 4.4. The same two weeks of connectivity data collected from the HarborNet testbed were utilized: one for creating the spatial connectivity look-ahead graph G_h and one for running the analysis itself. Like before, the data was split into 1-second snapshots and the network topology, actual link PDRs and estimated link PDRs defined for each of them. Then, for each possible source-destination pair in each snapshot, LASP-MF was executed and compared to a series of benchmark protocols.

The goal of this analysis was to compare LASP-MF against its precursors, LASP and DAZL. Namely, we wanted to answer the following questions:

1. How large is the effect of multi-forwarder support in terms of packet delivery probability?

2. What is the tradeoff between increased reliability and additional load placed on the network?

3. How much does the maximum number of competing forwarders inside the forwarding zone (the r parameter from Section 5.2.2) impact LASP-MF's performance?

Furthermore, we wanted to understand how LASP-MF compares with optimal protocols designed to optimize specific performance metrics, something that could not be done experimentally since most of these protocols are unfeasible in practice. With these objectives in mind, the following protocols were considered:

LASP LASP served as a baseline to assess the improvements provided by LASP-MF's opportunistic multi-forwarder routing approach. We used a 1-hop real-time neighborhood variant of LASP for this.

1-forwarder-per-hop optimal This represents a series of "oracle" protocols with complete and perfect knowledge of the network's topology, that use a single forwarder per hop (i.e. do not exploit node diversity), and are optimal regarding a specific end-to-end path metric. We implemented 2 variants, one optimizing end-to-end PDR and one optimizing hop count. The hop count obtained by the latter protocol represents a performance upper bound that can not be surpassed by any other protocol, regardless of the number of forwarders employed. On the other hand, note that the PDR achieved by the PDR-optimal 1-forwarder-per-hop protocol can potentially be surpassed by protocols employing multiple forwarders per hop. These protocols optimize a single metric, disregarding any compromises that may entail for other metrics. E.g. the hop count-optimal protocol does not impose a minimum PDR requirement and the PDR-optimal protocol does not impose a hop count limit.

DAZL Implementing DAZL allowed us to quantify the improvements provided by LASP-MF's spatial connectivity-based approach relative to DAZL's greedy geographic approach. We varied the number of potential forwarders between 1 and 4, for a total of 4 DAZL variants.

LASP-MF We contemplated 3 distinct LASP-MF variants, differing in the number of potential forwarders: 2, 3 and 4. Each is executed independently. The real-time neighborhood was limited to 1-hop for all variants.

Broadcast Because our analysis models channels as erasure channels, which do not model the effects of interference and congestion, a broadcast protocol is optimal regarding end-to-end PDR (to see this notice how a broadcast protocol explores each and every possible link). Therefore, we used broadcast as a PDR upper bound against which other protocols could be judged. We also use the broadcast protocol as a comparison point for the expected number of replicas observed at the destination and the total number of transmissions. The broadcast protocol we implemented works as follows: i) the packet is initially broadcast by the source, ii) any node receiving the packet for the first time, rebroadcasts it, iii) any node receiving a duplicate packet, drops it (i.e. each node forwards at most once).

The parameters used by the different protocols are summarized in Table 5.1. The choice of having no (i.e. zero) minimum PDR between forwarding cells in the means that the forwarding zone is the entire range of the packet sender. This maximizes PDR at the cost of potential replication caused by hidden terminals.

Parameter	Applicability	Value
Max. transmissions per hop	All protocols	5
Max. number of hops	All protocols	$2 \times \|edges\|$
Spatial cell size (m)	LASP, LASP-MF	50×50
Real-time neighborhood size (hops)	LASP, LASP-MF	1
Nodes per forwarding slot	DAZL, LASP-MF	1
Minimum PDR between forwarding zone cells	LASP-MF	0

Table 5.1: Configuration parameters used in LASP-MF's trace-based evaluation.

This analysis has the same limitations as LASP's trace-based analysis, previously described in Section 4.4. Namely, the 1Hz-resolution erasure channels, the lack of capacity modeling and the lack of a timing model. Although transmissions are not timed, they are ordered according to the following rules:

1. Transmission events occurring after n hops occur after the transmission events occurring after $n-1$ hops, $\forall n \geq 1$.
2. Within the same hop, in the multi-forwarder protocols, higher priority forwarders transmit before lower priority ones.

The metrics used to evaluate the resulting LASP-MF paths were:

Expected end-to-end PDR PDR is a measure of the level of reliability achieved by the different protocols.

Expected total transmission count Transmission count represents the load placed on the network by the different protocols. In our analysis we modeled the total number of transmissions, including the redundant transmissions that can occur in multi-forwarder protocols such as the broadcast protocol and LASP-MF.

Expected hop count We computed the expected number of hops that the packet must traverse before reaching the destination. It is a measure of network load and also latency, since fewer hops will, in principle, translate to less processing and transmission overhead.

Expected number of replicas The number of replica (i.e. duplicate) packets observed at the destination is a measure of the additional load placed on the network by multi-forwarder protocols. The use of a distributed coordination mechanism in LASP-MF means that erasures and hidden terminals can potentially lead to the creation of duplicate copies of packets.

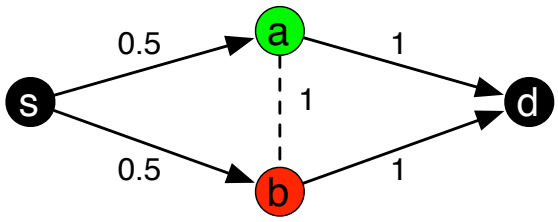

Figure 5.5: Example of how multi-forwarder protocols produce multiple possible paths to the destination.

Running a multi-forwarder protocol like LASP-MF or DAZL for a given source-destination pair will not produce a single path, but rather a set of possible paths $\mathcal{P} = \{p_1, p_2, p_3, \ldots, p_n\}$. This is caused by the fact that the paths in a multi-forwarder protocol are probabilistic: the existence of a given path depends on whether a certain set of nodes receives the packet or not, resulting in multiple possible outcomes. Each path is unique in that it is distinguishable from every other path in the set by either visiting a different set of nodes or visiting the same set of nodes in a different order. To illustrate why these multiple possible paths exist, we go through the scenario depicted in Figure 5.5, where the circles stand for network nodes, lines represent links and the numbers their PDRs. Start by assuming node s wants to send a message to node d using the LASP-MF protocol. Let us follow the protocol execution:

1. Node s broadcasts the packet. Both node a and node b receive it with probability 0.5 each.

2. If node node a received the packet, it computes the forwarder ranking. Assume a is the highest-ranked node. In this case, a immediately forwards it to the destination d. The probability that a receives and forwards is thereby equal to the reception probability, i.e. 0.5.

3. If node b received the packet, it computes the forwarder ranking and realizing that a is higher ranked than it, waits to hear a's transmission. If b does not hear from a, it forwards the packet to d. Since the (a, b) link is perfect (i.e. PDR = 1), the probability that b receives the packet and forwards it is equal to the probability that b receives it and a does not, i.e. $0.5 \times 0.5 = 0.25$.

4. Node d receives the packet from node a with probability 0.5.

5. Node d receives the packet from node b with probability 0.25.

So in this case, depending on the outcome of the erasure channels, d can receive the message through either path (s, a, d) or path (s, b, d), i.e. $\mathcal{P} = \{(s, a, d), (s, b, d)\}$. Note also that this happens even in the absence of replication: since the link between a and b is perfect, b only

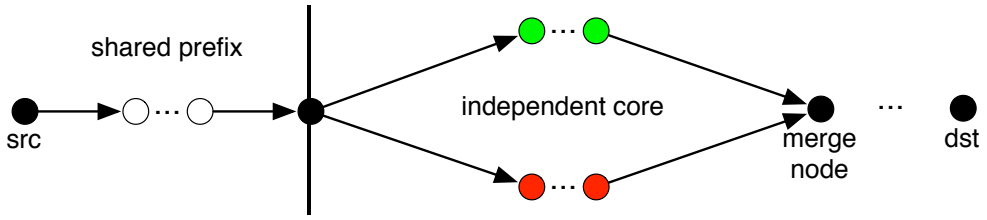

Figure 5.6: General dependency relationship between two forwarding paths.

transmits if a does not. Replication in this situation, which could be caused in this example by an imperfect (a, b) link, would alter the path probabilities but not the paths themselves.

The existence of a set of possible paths rather than a single path affects the way in which the different performance metrics are computed. Following, we describe how the different metrics are calculated, using the single-path metrics defined in Section 4.4 as buildings blocks, where appropriate.

Packet Delivery Ratio

As we have seen, the execution of a multi-forwarder protocol for a given source-destination pair yields a set $\mathcal{P}$ of possible paths. The overall expected end-to-end PDR for $\mathcal{P}$ can be defined as the sum of the individual PDR contributions of the different paths, PDR_{add}, for each path $p \in \mathcal{P}$. Formally we can write:

$$PDR(\mathcal{P}, t) = \sum_{i=1}^{|\mathcal{P}|} PDR_{add}(\mathcal{P}, i, t). \tag{5.3}$$

The computation of the contribution of each individual path is nontrivial because paths in $\mathcal{P}$ are not guaranteed to be independent from one another. In general, any two forwarding paths exhibit the dependency relationship depicted by Figure 5.6. All paths start at the same node, the source, and share a sequence of edges—shared prefix, until a point where the paths must diverge through the use of two different forwarders (the paths must diverge at some point, otherwise they would be one and the same). Once the paths split ways, they proceed independently of each other until they converge at a shared node we call the merge node. The paths can converge either at a node in the middle of the paths or at the destination, and are guaranteed to converge because they both must end at the destination.

Because, to prevent loops, each node can only forward a given message once, the merge node is a point of conflict between the two paths. Only if the first path to potentially reach the merge node fails to reach it can the second path's packet be forwarded by the merge node. Herein lies a dependency relationship: the second path's probability of success depends on the first path's

probability of failure. Furthermore, this failure must occur during the independent portion of the first path, because if it occurred during the shared prefix, the second path would have failed as well.

With this in mind, to compute the PDR contribution of each path $p \in \mathcal{P}$ we start by ordering $\mathcal{P}$ in such a way that any path p_v dependent on a path p_u appears in $\mathcal{P}$ after p_u. More precisely:

$$\forall p_u \in \mathcal{P}, p_v \in \mathcal{P} : p_v \text{ depends on } p_u \Rightarrow \mathcal{P} = \big\{ \ldots, p_u, \ldots, p_v, \ldots \big\}. \tag{5.4}$$

To create this ordering we must define the direction of the dependency relationship between each path pair. Consider paths p_a and p_b, merging at merge node m:

1. If p_a reaches m in fewer hops than p_b then p_b is said to depend on p_a. Likewise, if p_b reaches m in fewer hops than p_a, then p_a depends on p_b.

2. If both paths reach the merge node after the same number of hops, a lexicographical ordering of the sequences of node ids that make up the paths is used to decide the direction of the dependency relationship: the lexicographically larger path is said to depend on the lexicographically smaller path.

With this ordering in place we can now define the contribution of $\mathcal{P}_i$, the i^{th} path in $\mathcal{P}$, to the set's overall PDR as the probability that $\mathcal{P}_i$ succeeds in reaching the destination while the paths that it depends on fail before reaching the node where they merge with $\mathcal{P}_i$. More formally we have:

$$PDR_{add}(\mathcal{P}, i, t) = PDR(\mathcal{P}_i, t) \times \big[1 - PDR(\mathcal{I}, t)\big], \text{ where } \mathcal{I} = \big\{ \mathcal{P}_j^{\text{indep of } \mathcal{P}_i} : j < i \big\}. \tag{5.5}$$

This a multiplication of two factors. The first is $\mathcal{P}_i$'s PDR when the path is considered in isolation. The second represents the probability of all paths with lower indexes in the ordered set $\mathcal{P}$ failing to reach the node where they merge with $\mathcal{P}_i$. This set, which we name $\mathcal{I}$, only considers the portions of the paths that are independent of $\mathcal{P}_i$, because a failure in a shared prefix would mean $\mathcal{P}_i$ would fail as well. We write the probability of failure of $\mathcal{I}$ as the complement of the probability of its success. This allows us to apply Equation 5.3 to compute it, which will in turn use Equation 5.5 again, to sum over the contributions of the individual paths in $\mathcal{I}$. The definition of a set's PDR is therefore recursive. Note that in each step, the size of the path set for which the PDR is to be computed decreases, which ensures progress and eventual termination. The base case is the empty set, which has zero PDR. Also note that, just as in LASP's evaluation, all path PDRs depend on the number of transmissions per hop, t.

Lastly, we must specify how the PDR of an individual path p is calculated:

$$PDR(p, t) = \prod_{(u,v) \in p} P_{comm}(u, v, t) \times P_{(fwd|rcv)}((u, v).f, v.prio). \tag{5.6}$$

This is the product over all edges in the path p, of the communication probability of each edge (u, v), previously defined in Equation 4.6, times the probability that v, the node on the receiving end of the edge, actually forwards the packet upon reception. In the broadcast and single-forwarder protocols (LASP and 1-forwarder optimal) this latter term is 1. But, in DAZL and LASP-MF, forwarding can be cancelled by the overhearing of an implicit acknowledgment from a higher-priority forwarder, hence the need for this additional term. The probability of forwarding given that a reception has occurred depends on v's priority and the potential forwarders competing with v. This information is associated with the forwarding event linked to the edge, which we write as $(u, v).f$. For conciseness and readability, we defer the complete discussion regarding the calculation of this probability to the discussion on the estimation of the total number of packet transmissions, which follows (more precisely, Equation 5.11).

Transmission Count

Transmission count is a measure of network load. It can be thought of as a combination of hop count and number of retransmissions per hop. In order to estimate the total number of transmissions generated by the protocols under scrutiny we must consider not just the transmissions generated within the paths reaching the destination but rather the transmissions generated in all of the forwarding events in the network. A forwarding event occurs when a node transmits a packet one or more times until an acknowledgment is received or the maximum number of retransmissions is reached.

Given a set of forwarding events $\mathcal{F}$ generated by a protocol, we can define the total expected number of transmissions as the sum over all forwarding events of the probability of the forwarding event occurring times the expected number of transmissions for that particular forwarding event. Formally:

$$E_{trans}(\mathcal{F}, t, proto) = \sum_{\forall f \in \mathcal{F}} P(f) \times E_{fwdtrans}(f, t, proto). \tag{5.7}$$

The probability of a particular forwarding f occurring is determined during the execution of the protocol's logic. The expected number of transmissions for a particular forwarding event depends on the protocol and on the maximum number of transmissions, t. We must define it differently according to the nature of each protocol. Formally we have:

$$E_{fwdtrans}(f, t, proto) = \begin{cases} t & \text{if } proto = \text{Broadcast} \\ \min\left[t, ETX(f_u, f_v)\right] & \text{if } proto \in \{\text{LASP,OPT-1}\} \\ \sum_{i=1}^{i \leq t} i \times P_{stop}(f, i, t) & \text{if } proto \in \{\text{LASP-MF,DAZL}\} \end{cases}, \tag{5.8}$$

which can be described as follows:

Broadcast In order to maximize reachability, the broadcast protocol always transmits the maximum allowable number of times, t. This is what makes broadcast an upper bound for end-to-end PDR.

LASP and 1 forwarder-optimal Both LASP and the 1 forwarder-optimal protocols use only a single forwarder per hop. There the expected number of transmissions can be estimated as the minimum of the maximum transmission count t and the ETX between the current node u and the chosen next hop relay node v.

LASP-MF and DAZL The LASP-MF and DAZL protocols potentially use multiple forwarders per hop, relying on implicit acknowledgments to avoid redundant transmissions that create unwanted load and duplication. This makes for a more complex estimation because we must take into account the probability of receiving an acknowledgment after each transmission.

The expected number of transmissions of a single forwarding event can be calculated as the sum over all possible transmission counts i (from 1 to t) of i times the probability of stopping after i transmissions, $P_{stop}(f, i, t)$. These protocols stop once either one of the following conditions occurs: i) an implicit acknowledgment is heard or, ii) the limit number of transmissions is reached.

Therefore P_{stop} can be defined as follows:

$$P_{stop}(f,i,t) = \begin{cases} \left[1 - \sum_{j=1}^{i-1} P_{stop}(f,j,t)\right] \times P_{ack}(f) & \text{if } 1 \leq i < t \\ 1 - \sum_{j=1}^{i-1} P_{stop}(f,j,t) & \text{if } i = t \end{cases}. \tag{5.9}$$

While the protocol does not run out of transmissions, the stopping probability is the product of the probability of not having stopped previously by the probability of receiving an acknowledgment for the current transmission i. The probability of transmitting the maximum number of transmissions is the complement of the probability of having stopped before that point.

The probability of receiving at least one implicit acknowledgment for a given transmission can be described as the complement of the probability of receiving no acknowledgment at all. The latter can be defined as the product of the probability of not receiving an acknowledgment from each individual node in the potential forwarder set $f.fwders$. This probability is the complement of the probability of receiving an ack from the forwarder, which in turn translates to the product of the PDRs between the current node and the forwarder and the probability that the forwarder actually forwards the message upon receiving it. More formally, we have:

$$P_{ack}(f) = 1 - \prod_{k=1}^{|f.fwders|} 1 - PDR_{f.cur \rightarrow f.fwders_k} \times P_{(fwd|rcv)}(f,k) \times PDR_{f.fwders_k \rightarrow\ f.cur}. \tag{5.10}$$

The probability of a node forwarding a message upon reception is dictated by its rank k within the potential forwarder set. If the node is ranked 1st, then it forwards with probability 1. Otherwise it forwards only if it has not heard an implicit acknowledgment from a higher-ranked forwarder. This turns into a product over all higher ranked (i.e. rank $< k$) forwarders of the probability of not receiving an acknowledgment from that node. The latter depends on the PDRs between the two forwarders and the probability that the higher-ranked forwarder actually transmits a message. This leads us to the following recursive definition:

$$P_{(fwd|rcv)}(f,k) = \begin{cases} 1 & \text{if } k = 1 \\ \prod_{l=1}^{k-1} \Big[1 - PDR_{f.cur \to f.fwders_l} \times P_{(fwd|rcv)}(f,l) \\ \qquad \times PDR_{f.fwders_l \to\ f.fwders_k} \Big] & \text{if } k > 1 \end{cases}. \tag{5.11}$$

Hop Count

We now focus our attention on the expected hop count, which given the lack of a timing model in our analysis, can be seen as a measure of latency. The expected hop count for the possible path set $\mathcal{P}$, which we define to be the expected number of hops of the first path in the set to reach the destination. This is computed as the arithmetic mean of the hop counts of the individual paths that make up $\mathcal{P}$, weighted by each path's contribution to the set's overall PDR. Formally:

$$E_{nhops}(\mathcal{P},t) = \frac{\sum_{i=1}^{|\mathcal{P}|} PDR_{add}(\mathcal{P},i,t) \times nhops(\mathcal{P}_i)}{PDR(\mathcal{P},t)}. \tag{5.12}$$

The hop count of each individual path is simply its length. The path's contribution to the set's overall PDR is given by the previously defined PDR_{add}. The sum of product of these two factors over all paths in $\mathcal{P}$ is then divided by $\mathcal{P}$'s overall PDR to obtain the set's expected hop count.

Number of Replicas

Finally, we turn our attention to the expected number of replicas observed at the destination, which is a measure of network load and protocol efficiency. In the protocols considered in this analysis, each node forwards a given message at most once. Hence, the total number of message copies that the destination receives can be computed as the sum over all of the destination's direct neighbors, of the multiplication of three factors. These factors are, for each direct neighbor u:

1. The probability that neighbor u receives the message;

2. The probability that, upon reception, u forwards the message (i.e. that its forwarding is not cancelled by the overhearing of a transmission from a higher priority forwarder);

3. The communication probability of the edge linking neighbor u and destination.

If this expected number of copies is 1 or less, there will be no (i.e. zero) replication, for the first copy is not a replica. If the number of copies is larger than 1, then replication can be computed as the expected number of copies minus 1.

To formalize the concept, let us start by letting $\mathcal{G}$ be the network graph and N the set of 1-hop neighbors of the destination d, i.e.:

$$\mathcal{N} = \big\{u : (u, d) \in \mathcal{G}\big\}. \tag{5.13}$$

Also let $Q_u = \big\{q_1, \ldots, q_n\big\}$ be the set of paths between the source and the destination's neighbor u found by a given routing protocol. Finally let Q be the list of sets $\mathcal{Q}_u$ for all neighbors in $\mathcal{N}$:

$$\mathcal{Q} = \big\{Q_u : u \in \mathcal{N}\big\}. \tag{5.14}$$

Now we can define the expected number of packet copies received at the destination as:

$$E_{copies}(\mathcal{Q}, \mathcal{N}, t) = \sum_{i=1}^{|\mathcal{N}|} \sum_{j=1}^{|\mathcal{Q}_i|} PDR_{add}(\mathcal{Q}_{\mathcal{N}_i}, j, t) \times P_{(fwd|rcv)}(\mathcal{Q}_{\mathcal{N}_i}.f_{last}, \mathcal{N}_i.prio) \times P_{comm}(\mathcal{N}_i, d, t), \tag{5.15}$$

where $\mathcal{Q}_{\mathcal{N}_i}.f_{last}$ represents the last forwarding in the path $\mathcal{Q}_{\mathcal{N}_i}$ and t is the number of transmissions. The path's contribution for a node's overall PDR, PDR_{add}, follows the definition in Equation 5.5. The probability of forwarding upon reception $P_{(fwd|rcv)}$ is computed using Equation 5.11. Lastly, the edge communication probability P_{comm} obeys Equation 4.6.

Finally, the expected number of replicas is defined as:

$$E_{replicas}(E_{copies}) = \begin{cases} 0 & \text{if } E_{copies} \leq 1 \\ E_{copies} - 1 & \text{if } E_{copies} > 1 \end{cases}. \tag{5.16}$$

5.3.2 Results

We now describe the results of our trace-based evaluation of LASP-MF. For each metric we start by analyzing DAZL's performance, then LASP's and finally we compare LASP-MF with DAZL and LASP.

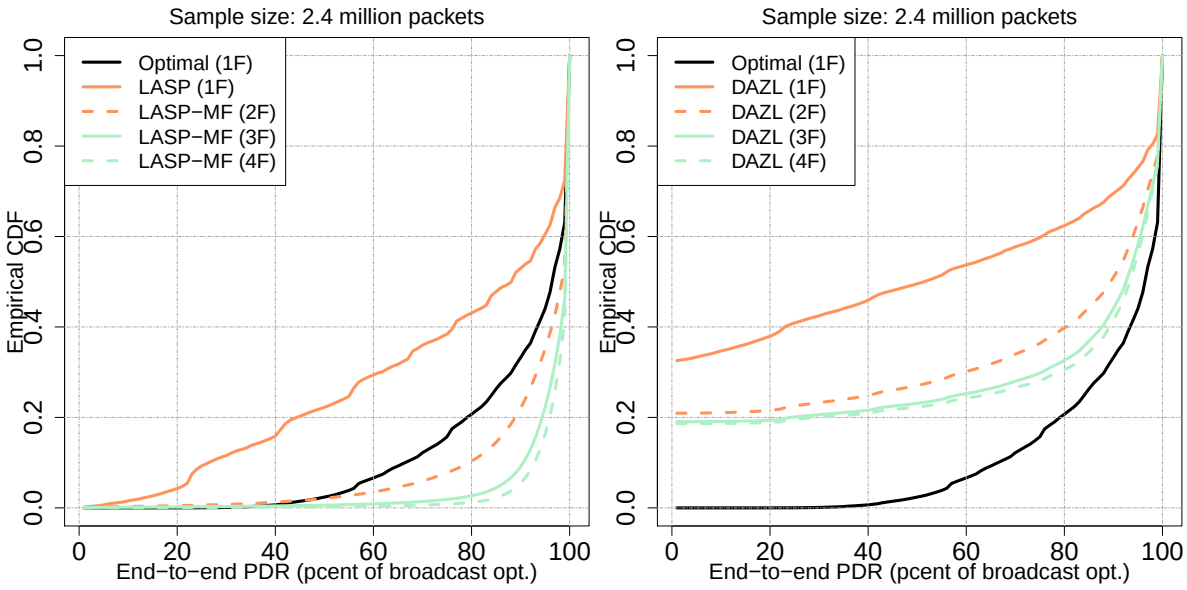

(a) LASP-MF

(b) DAZL

Figure 5.7: LASP-MF trace-based expected end-to-end PDR results.

Packet Delivery Ratio

We start by looking at the expected end-to-end PDR results, depicted in Figure 5.7. The plots show the Empirical Cumulative Distribution Function (ECDF) of the percentage of the optimal expected end-to-end PDR achieved by each protocol, with the optimal being defined by the broadcast protocol. This means that lower curves are better. In the plots, each protocol variant features a tag of the form (rF), where r is the maximum number of potential forwarders allowed by the variant in question.

DAZL, in the rightmost plot—Figure 5.7b, achieved the worst PDR performance. Without a recovery procedure and with a simple, greedy distance-based heuristic, 1-forwarder DAZL failed to find a path between source and destination for roughly 35% of the packets (i.e. at PDR zero, the ECDF is equal to 0.35). Performance improved significantly with the addition of a second potential forwarder per hop. The percentage of packets for which no path could be found dropped from 35 to 20% and performance became competitive with 1-forwarder LASP for a significant percentage of the remaining cases. Adding a 3$^{\text{rd}}$ and 4$^{\text{th}}$ forwarders yielded progressively smaller improvements. This makes sense since, as the channels are independent due to to physical separation, the probability of failure for each hop equates to the product of the individual forwarder failure probabilities, which quickly tends to zero with an increasing number of forwarders. It also matches the tendency observed in the experimental results previously presented in Chapter 3, Figure 3.3.

The leftmost plot—Figure 5.7a, shows the PDR achieved by LASP and the different LASP-MF variants. All protocols achieved PDRs above zero for all packets and all were able to match the optimal PDR for at least 25% of the packets. Most of the differences between protocols are found in the lower half of the ECDFs (i.e. ECDF ≤ 0.5), so that is what we focus on.

When we compare the first quartile (i.e. ECDF $= 0.25$) values, we find that LASP obtained at least 50% of the optimal PDR for 75% of the packets, while the 2-forwarder variant of LASP-MF achieved at least 90% of the optimal for the same percentage of packets. This represents a 40% improvement. Moreover, 2-forwarder LASP-MF surpassed even the 1-forwarder optimal protocol. This shows how important the additional reliability provided by node diversity is in the vehicular environment, where radio links are unstable.

Similarly to DAZL, allowing for a 3^{rd} and 4^{th} potential forwarders yielded progressively smaller benefits for LASP-MF. Both variants came very close to matching the optimal broadcast protocol, achieving at least 95% of the optimal PDR at the first quartile. The difference between the 3- and 4-forwarder LASP-MF protocols was almost negligible, indicating that a saturation point was reached. We note that, since the source data is the same, the separation degree between source and destination follows the same distribution presented in LASP's evaluation, Figure 4.12b. This means that 70% of source-destination pairs were separated by only two hops. In larger networks with longer paths, the saturation point for the number of forwarders is expected to be higher, as small per-hop gains will be compounded over longer forwarding chains.

Transmission Count

We now consider the expected end-to-end total transmission count, a measure of the load placed on the network by the different protocols. Figure 5.8 shows the ECDF of the ratio between the transmission count obtained by each protocol and the broadcast protocol, expressed as a percentage. Therefore higher curves are better. Note however that although the broadcast protocol is used as a benchmark, it does not represent a worst-case scenario. The reason is the following. In the broadcast protocol, each node attempts to forward a packet at most once. In the LASP and LASP-MF protocols, this may not be the case because in the event that a network hole is found, nodes have to forward again to backtrack the packet to a previous node so other alternative paths can be explored. It is therefore possible for LASP and LASP-MF to transmit more messages than the broadcast protocol. Since it features no recovery mechanism, DAZL, on the other hand, can never transmit more messages than the broadcast protocol.

To enable a fairer comparison, the packets for which at least one of the protocols was unable to find a path due to their lack of recovery mechanism had to be discarded, hence the smaller sample size when compared with the PDR analysis (1.6 vs 2.4 million packets).

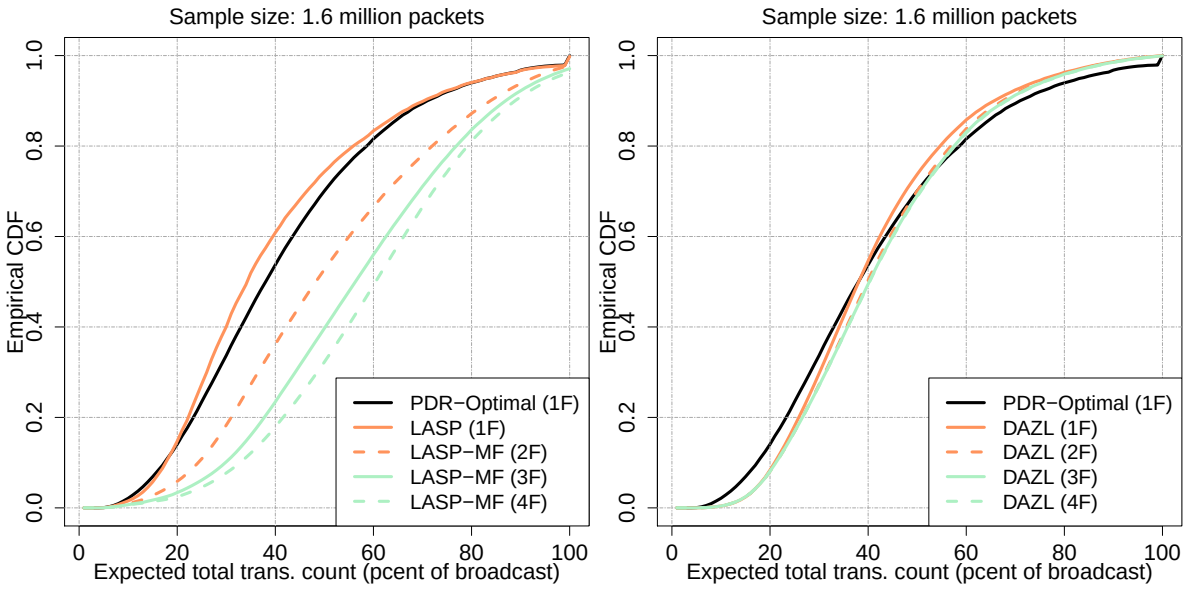

(a) LASP-MF

(b) DAZL

Figure 5.8: LASP-MF expected end-to-end transmission count analytical results.

Figure 5.8b shows the transmission count ECDFs for the different DAZL protocols. All DAZL variants transmitted few messages, being competitive with the 1-forwarder PDR optimal protocol. We can pinpoint two main reasons for these results. First, as previously discussed, DAZL did not achieve very good end-to-end PDR results. This means that many packets will be lost midway towards the destination, which has the side effect of reducing the overall number of transmissions. Furthermore, since DAZL uses a greedy metric that does not take PDR into account, increasing the number of potential forwarders also increases the likelihood that at least one of them has a good link to the previous hop, requiring fewer retransmissions on its part. This is why increasing the number of potential forwards in DAZL did not increase the expected number of transmissions, as can be seen in the plot.

In the leftmost plot—Figure 5.8a, we can observe LASP-MF's performance compared with LASP and the 1-forwarder PDR-optimal protocol. The first thing to note is that all LASP and LASP-MF variants used significantly fewer transmissions than the broadcast protocol for almost all packets. This is very important. The broadcast protocol achieves optimum end-to-end PDR at the cost of a high number of transmissions. This makes it impractical, especially in larger networks, due to capacity constraints. By almost matching the broadcast end-to-end PDR and at the same time significantly reducing the number of transmissions, LASP-MF becomes a much more practical proposition.

The LASP protocol behaved very similarly to DAZL, with the lowest number of expected transmissions. Taking into account the higher PDR achieved by LASP relative to DAZL, this means that LASP's spatial connectivity-based heuristic results in better connected paths requiring fewer retransmissions. Relative to LASP, the LASP-MF protocols, with their additional forwarders, transmitted more messages. For example, if we take the median of the distribution (i.e. ECDF = 0.5), the expected number of transmissions relative to broadcast increased from around 35% in LASP to 50% in 2-forwarder LASP-MF. The 3- and 4-forwarder variants transmitted more messages still, but as with the PDR, we can observe saturation starting to occur in the 4-forwarder protocol.

This correlation between potential forwarders and transmissions can be explained by two main factors. First, as seen before, the multi-forwarder protocols increase the probability of message delivery, which consequently leads to a higher expected transmission count because packets will not be lost before reaching the destination as often. Second, the duplicate suppression scheme employed by LASP-MF depends on the ability of forwarders to overhear each other. In this analysis LASP-MF was configured to maximize PDR through the use of a large forwarding zone, making it more susceptible to hidden terminals. Consequently, redundant forwarding cancellation will be imperfect and some duplicates will be generated.

Number of Replicas

We now discuss the expected number of replicas received at the destination, which is another measure of network load. Figure 5.9 shows the ECDF of the expected number of replicas for all the multi-forwarder protocols: DAZL, LASP-MF and broadcast. Since replication is undesirable, higher curves are better in these plots.

LASP and the 1-forwarder PDR-optimal protocol are not included in these plots. The 1-forwarder PDR-optimal protocols do not create replication. LASP can theoretically generate some small level of replication if a chosen next hop successfully forwards the packet but the sender fails to receive an acknowledgment and tries to recover by forwarding to a different neighbor. However in our implementation this was not modeled. I.e. the packet is dropped by the sender regardless of whether it receives an acknowledgment or not. There is backtracking, but it occurs only when, upon packet reception, all available neighbors have been previously visited.

The first thing to note is that all protocols produced no (i.e. zero) replication for at least 45% of the packets. Hence we shall focus on the second half of the distributions, which is where the differences lay.

Figure 5.9b shows the replication results for the DAZL family of protocols. All variants exhibited significantly less replication than the broadcast protocol. For instance, the broadcast protocol created 1 or more replicas for 25% of packets, while the worst-performing DAZL variant only did so

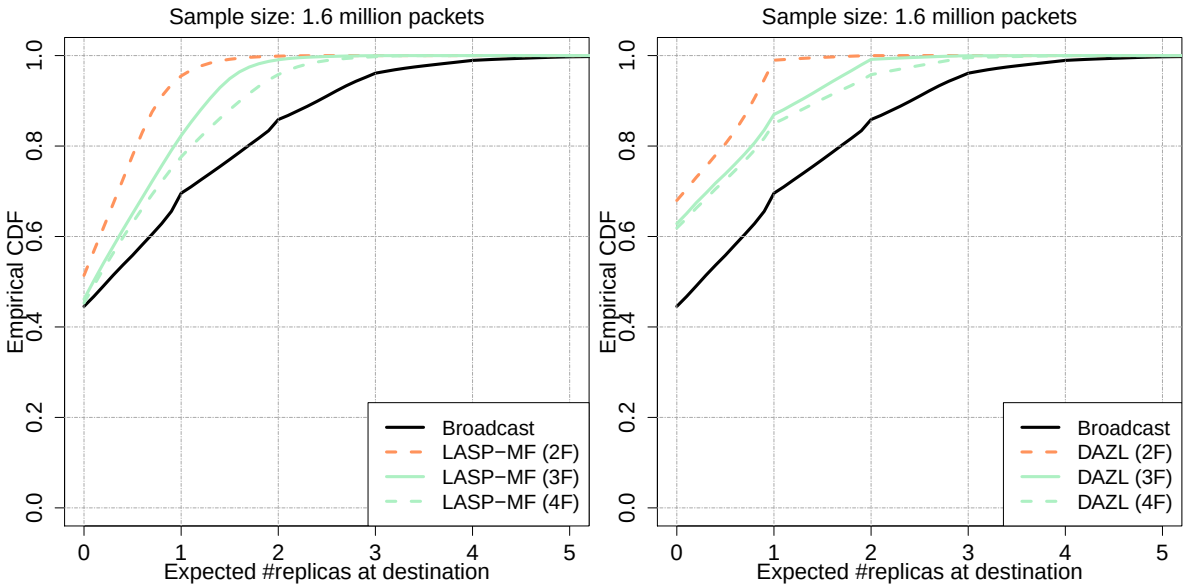

(a) LASP-MF

(b) DAZL

Figure 5.9: LASP-MF expected number of replicas observed at the destination trace-based results.

for roughly 15% of packets. Within the DAZL protocol family, increasing the number of concurrent forwarders resulted in an increase in replication, which is to be expected due to the possibility of hidden terminals within the forwarder set.

We now turn our attention to Figure 5.9a, which shows the replication generated by the LASP-MF protocols. All LASP-MF variants produced significantly less replication than the broadcast protocol. Considering the values at the last quartile (i.e. ECDF = 0.75), the 1.4 replicas observed by the broadcast protocol compare with roughly 0.45 for the 2-forwarder LASP-MF protocol (68% less) and 0.9 for the 4-forwarder variant (36% less). When compared with DAZL, LASP-MF generated more replication, which is consistent with its higher end-to-end PDR results. For example, 4-forwarder DAZL created 1 or more replicas for 15% of the packets, while 4-forwarder LASP-MF did so for roughly 20% of them.

As expected and much like with the DAZL protocols, increasing the number of potential forwarders also increased the level of replication in the LASP-MF protocol family, with the difference between the 2 and 3-forwarder variants being larger than the difference between the 3 and 4-forwarder variants.

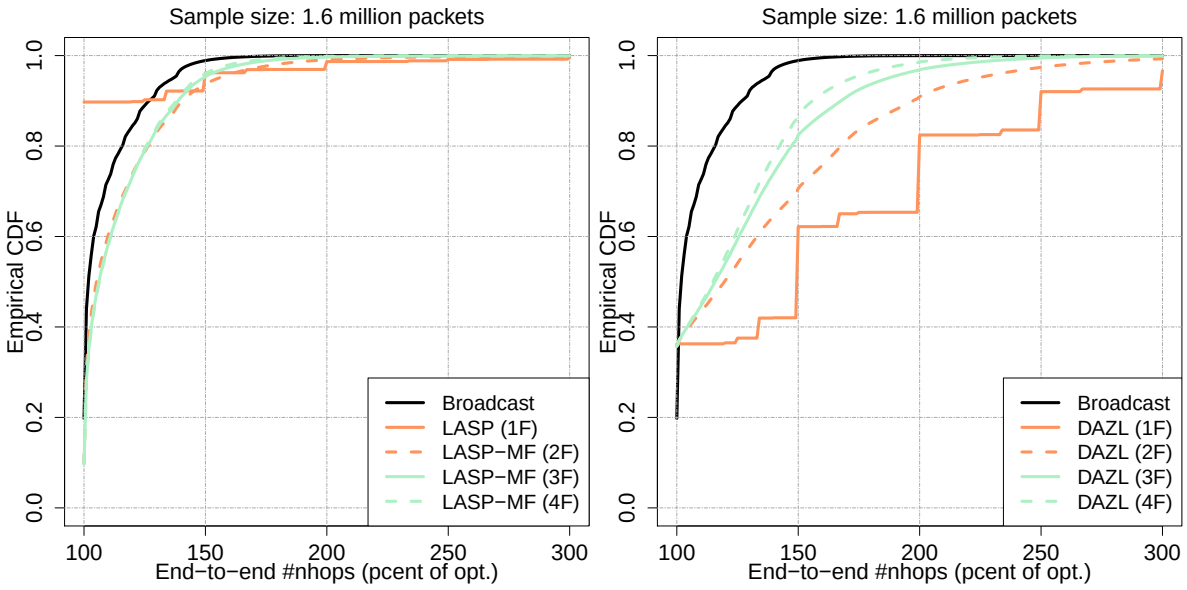

(a) LASP-MF

(b) DAZL

Figure 5.10: LASP-MF expected end-to-end hop count trace-based results.

Hop Count

Finally, we examine the end-to-end hop count results, depicted in Figure 5.10. Hop count can be seen as a proxy for latency. The plots show the ECDF of the ratio between the hop count obtained by each protocol and the degree of separation between source and destination nodes in the network graph, which represents the shortest possible path between them. Therefore the x-axis begins at 100% and the higher the curve, the better the performance.

The rightmost plot—Figure 5.10b, shows DAZL's hop count results. Here, the limitations of the greedy, distance-to-destination-based metric employed by this protocol become apparent. The 1-forwarder variant found the longest paths by far, showing that distance alone is not an ideal heuristic for vehicular multi-hop communication, as previously discussed in Section 4.2. Increasing the number of forwarders in DAZL allows it to compensate for this shortcoming, and leads to significantly shorter paths, but still noticeably longer than the other protocols, as we shall see next.

Figure 5.10a shows the results for the LASP and LASP-MF protocols. Overall, LASP and LASP-MF found significantly shorter paths than DAZL. When we compare 1-forwarder DAZL with LASP at the upper quartile (i.e. ECDF = 0.75) for example, we note that LASP halves the hop count relative to DAZL, from 200 to 100% of the optimal.

LASP is able to match the optimal hop count for 90% of the packets. LASP-MF can only do

the same for less than 40% of them, regardless of the number of potential forwarders. The delta then slowly decreases up to the 90^{th} percentile, where both ECDFs converge. This difference can be explained by two main factors. First, when LASP encounters the destination within its look-ahead, it forwards the packet in its direction without trying longer paths. LASP-MF, on the other hand, explores multiple paths, so it is able to find longer, higher PDR paths, which increase the expected hop count. Second, as mentioned before, most source-destination pairs in this data set are separated by only 2 hops (Figure 4.12b), meaning that even one additional hop represents a large relative increase of 50%.

It is interesting to note that there were no significant differences between the results of the different LASP-MF variants. This signifies that the additional paths found by the 3- and 4-forwarder LASP-MF variants are not significantly longer than the ones found by the 2-forwarder variant, likely a consequence of the small diameter of the network used in the analysis.

Discussion

In summary, we can identify three main takeaways from these results. First, we saw that adding multiple forwarder support to LASP significantly improved the end-to-end packet delivery ratio, at the cost of some replication and additional transmissions. Second, we found a saturation point in the performance benefit achieved by these additional forwarders around the 3-forwarder mark. Lastly, we saw the benefit provided by the spatial connectivity metric that LASP and LASP-MF employ over the greedy metric used in DAZL, in terms of both PDR and hop count.

These results indicate that the basic concepts behind the LASP-MF design, spatial connectivity and node diversity, are indeed able to provide noticeable benefits in the context of vehicular network routing. The parameterization of the maximum number of forwarders and forwarding zone size influence the tradeoff between PDR and transmission count/replication. Adapting these parameters to different network environments is a potential avenue for further research.

5.4 Experimental Evaluation

In this section we use the HarborNet testbed presented in Section 2.4 to experimentally evaluate LASP-MF and LASP against the benchmark protocol GPSR.

5.4.1 Setup

We leveraged the Click framework [KMC+00] to create a prototype routing and forwarding agent (henceforth referred to as router) that is able to execute LASP, LASP-MF and GPSR in parallel.

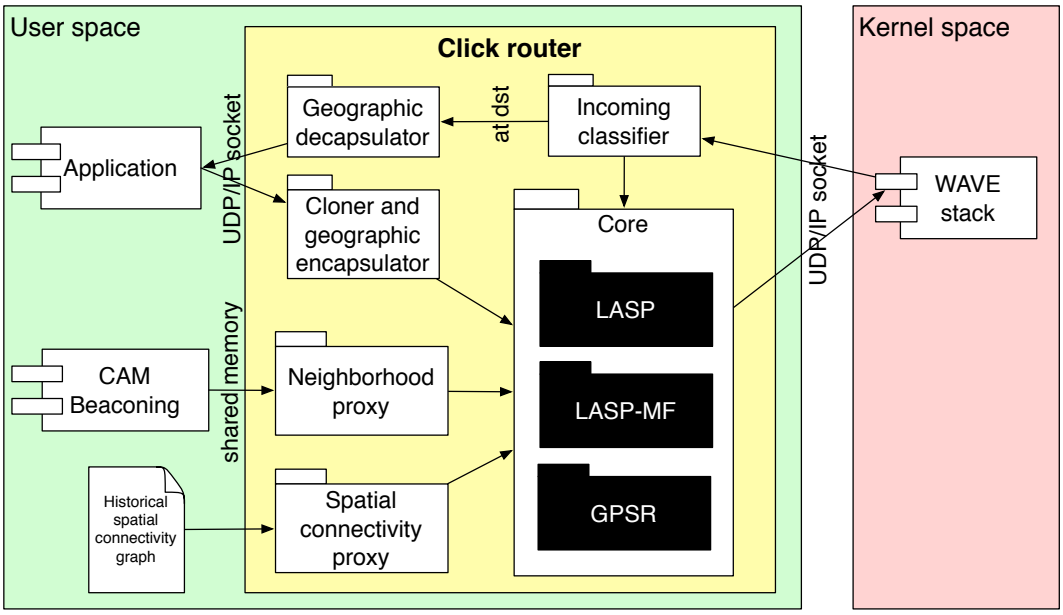

Figure 5.11: Router prototype architecture.

This is important because it allowed us to compare these three protocols while holding all other variables, such as vehicle mobility, network topology and line of sight obstructions, constant.

Figure 5.11 depicts the prototype's architecture. Applications that generate and/or consume traffic interface with the router through a UDP socket. Packets entering the router from an application are cloned so there are a total of three copies, one for each of the protocols under evaluation. Then, each copy is extended with the geographic header used by the corresponding protocol. This header is added in-between the UDP header and the packet data, in order to make geographic routing transparent to the existing WAVE protocol stack.

Each protocol then makes its own forwarding decision, taking the location of the packet's destination into account. In order to make this decision the protocols have access to two inputs. First there is the neighborhood information generated by an external CAM beaconing application and accessed via shared memory. This input is used by all three protocols. Second, there is a file that stores the historical spatial connectivity information that is used by LASP and LASP-MF. This is accessed through a proxy with caching functionality for improved performance.

Once a forwarding decision has been made, the headers are updated and the packet is sent to the kernel through an UDP/IP socket to be processed by the WAVE protocol stack. Eventually the packet is transmitted over the air interface using 802.11p at the 3 Mbps base data rate.

Packets arriving to the router from the kernel are inspected by a classifier to decide whether they should be delivered to a local application, or routed through to another node. In the former

case, the geographic header is stripped and the message is delivered to the application. In the latter, the packet is handed to the corresponding protocol for evaluation.

In our prototype we wanted, for fairness, all protocols to have the same number of available retransmissions. Furthermore, we needed to be able to count the number of transmissions performed by each protocol, so we could compare them using that metric.

This created a problem. GPSR and LASP use a single forwarder per hop so they can be implemented using unicast packets, which feature retransmissions at the 802.11p MAC layer. LASP-MF uses multiple forwarders per packet, so it needs to use broadcast packets, which do not feature MAC layer retransmissions. Therefore, if we used unicast packets for GPSR and LASP, LASP-MF would be handicapped and we would not be able to count the number of retransmissions performed at the MAC layer for GPSR and LASP. Using unicast packets in conjunction with promiscuous mode for LASP-MF with was also not a option because: i) the custom wireless driver installed on the testbed did not support promiscuous mode and, ii) we would still not be able to count the MAC-layer retransmissions.

Our solution was to use broadcast packets for all protocols and implement our own retransmission scheme as part of the router. In our router, after a packet is transmitted, a timer was created. If the timer ran out before an acknowledgment from the intended next hop was heard, the packet was retransmitted. This cycle repeats until such an acknowledgment was received or the limit number of retransmissions was reached. The retransmission timing, limits and other protocol parameters used during the experiments are summarized in Table 5.2.

Parameter	**Applicability**	**Value**
Max. transmissions per hop	All protocols	5
Retransmission delay (ms)	All protocols	100
Backtracking delay (ms)	LASP, LASP-MF	400
Spatial cell size (m)	LASP, LASP-MF	50×50
Real-time neighborhood size (hops)	LASP, LASP-MF	1
Max. forwarders per hop	LASP-MF	5
Nodes per forwarding slot	LASP-MF	1
Forwarding slot length (ms)	LASP-MF	40
Minimum PDR between forwarding zone cells	LASP-MF	0.7

Table 5.2: Configuration parameters used in LASP-MF's experimental evaluation.

The geographic header contents for each protocol are depicted in Figure 5.12. All include source, previous hop and destination location information, as well as the id of the chosen next hop node.

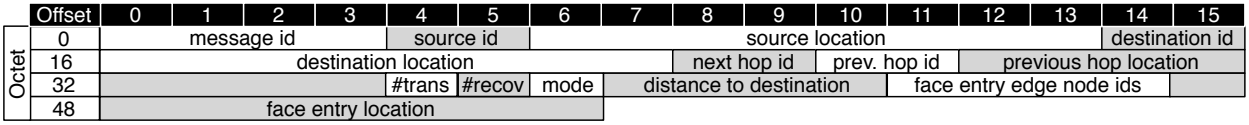

(a) GPSR header (55 bytes)

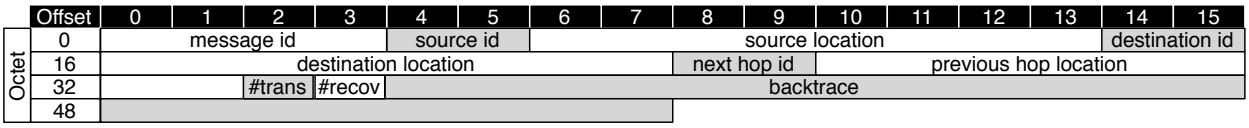

(b) LASP header (56 bytes)

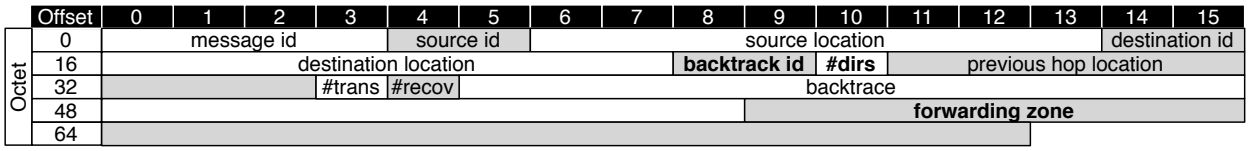

(c) LASP-MF header (77 bytes)

Figure 5.12: LASP-MF, LASP and GPSR geographic header formats.

Also, they all include counters for the number of transmissions and the number of times that the recovery procedure (perimeter mode for GPSR, backtracking for LASP and LASP-MF) has been activated. These fields are not used by the protocols themselves, they are used to collect information for our performance evaluation. Additionally, GPSR includes data relevant to its perimeter recovery mode, while LASP includes a backtrace of previous hops for its backtracking feature. LASP-MF's header differs from LASP's in the following fields:

backtrack id The LASP header has a *next hop id* field that is used to specify the id of the intended next hop forwarder. By contrast, in LASP-MF forwarding decisions are made on the receiver side. Therefore, *next hop id* is replaced by a *backtrack id* field. This field is always set to zero except when regular multi-forwarder routing fails and the packet has to backtrack to a previous node to explore a different path. In that case, *backtrack id* is set to the id of the node to which the packet is backtracking to.

#dirs This is an addition relative to the LASP header which specifies the number of times the packet has alternated between the forward direction (i.e. exploring novel nodes) and backtracking to previously visited nodes. This is used by the duplicate detection mechanism to prevent redundant transmissions. The source sets it to one and it is incremented every time the direction changes.

forwarding zone This is also a new addition relative to the LASP header. It specifies the geographic area inside which nodes can cooperate in forwarding the packet. The forwarding

zone is defined as a list of spatial cells. To save space, each cell is represented as pair of (x, y) offsets that are relative to the previous hop's location, which is included in the packet. Each cell then uses 2 bytes. The header supports a maximum of 10 cells, for a total of 20 bytes. If the forwarding zone is set to zero, then forwarding is unrestricted (i.e. any receiver can forward, regardless of its location).

The CAM beaconing application that generated the neighborhood information used by all protocols was also created by us. It broadcast CAMs as WSMP packets at a rate of 10 per second. The CAMs included the sender's id and location but not its neighborhood. Therefore, the protocols had only 1-hop real-time neighborhood information available to them. During our work we discovered that, even with such a small neighborhood, due to the network's dynamic nature it is was not easy to maintain an accurate representation of the neighbors, (i.e. they kept appearing and disappearing). In order to avoid the selection of transient neighbors we established the following two conditions that nodes needed to obey in order to be included in the neighborhood. In order for b to be a's neighbor:

1. The first CAM received by node a from node b must had been received at least 1000 ms ago;
2. Node a must had received at least one CAM from node b in the last 300 ms.

Each entry in the neighborhood stores the neighbor's id and location, as well as an estimate of the PDR between the current node and the neighbor in question. The latter is computed as the number of CAMs received from the neighbor during the last 5 seconds divided by the number of CAMs sent during that same time frame. The number 5 was chosen through data analysis. We took the connectivity data set we used for the trace-based evaluation in the previous subsection, and experimented to see which PDR window best predicted the PDR observed in the following second. We tested windows between between 1 and 10 seconds, and 5 seconds resulted in the best prediction (i.e. smallest mean square error).

The traffic pattern was as follows. Each node generated a new 100-byte payload packet every second and addressed it to another node, chosen uniformly at random. When the chosen destination was an RSU, its location was known *a priori* (i.e. hard-coded into the router). When it was an OBU, the location was obtained via cellular link from a management server that was collecting location and connectivity data as per Section 4.2.1. This obviated the need for a fully-developed location service, which was outside the scope of this thesis.

The cellular link was also used to upload a log describing the packets that were sent and received by each node to our server. The connectivity data obtained from CAMs was also uploaded, as per Section 4.2.1. Using this data we evaluated the results in terms of the following end-to-end

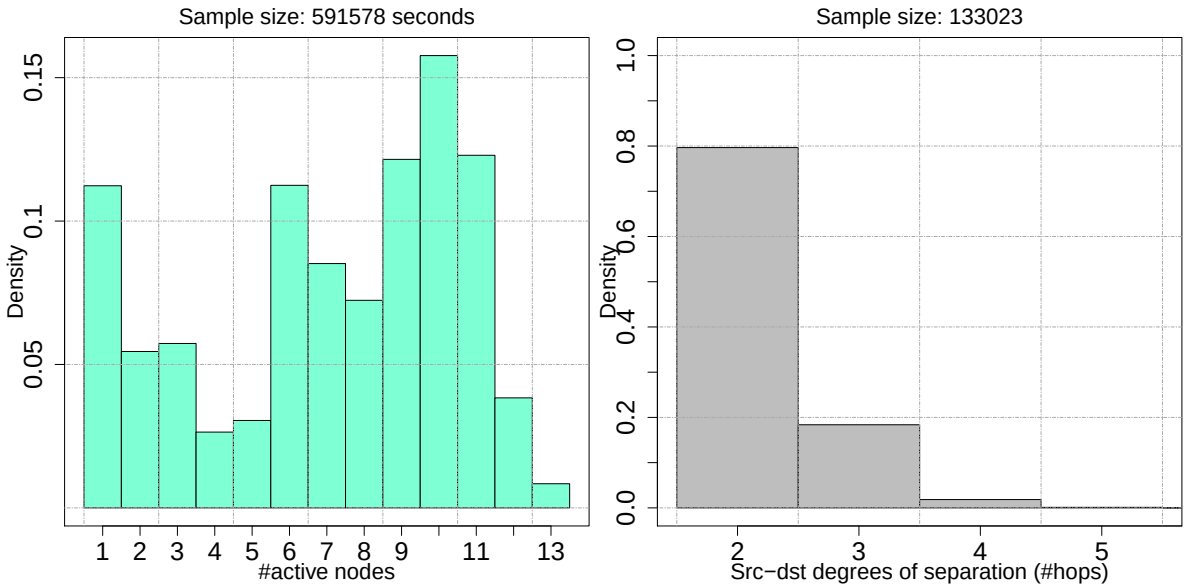

(a) Number of active nodes

(b) Hops of separation between source and destination

Figure 5.13: Network conditions during LASP-MF's experimental evaluation.

performance metrics: PDR, replication, transmission count, hop count and latency. PDR measures communication reliability. Replication, transmission count and hop count provide a measure of the load placed on the network by the different protocols. Latency measures the protocol's efficiency concerning time.

The experiments were performed between May 28$^{\text{th}}$ and June 8$^{\text{th}}$, 2015. Figure 5.13a presents the distribution of the number of simultaneously active nodes during the experiments as a histogram. As previously discussed in Section 4.4, not all 30 HarborNet nodes are normally active at the same time. The number of active nodes fluctuates with the amount of ships and containers that need moving on any given day and the availability of GPS and cellular connectivity. The mean number of nodes active during the experiments was 7.1, with a standard deviation of 3.46. The mode was 10 and the maximum, 13. Compared with the traces used in the trace-based analysis (Figure 4.12a), there were significantly fewer nodes available during the experiments. Namely, on average, 55% fewer nodes. This was outside of our control, and caused by a combination of changes in Harbor activity and hardware failures.

Figure 5.13b presents a histogram of the number of hops separating source and destination for the packets sent during the experiments, according to the collected beaconing data. Roughly 80% of the nodes were separated by only 2 hops and 18% by 3 hops. This distribution is similar to the one in the trace-based analysis (Figure 4.12b), but with an even larger prevalence of node pairs

separated by just 2 hops (80 versus 70%).

5.4.2 Results

Packet Delivery Ratio

We now look at the performance metrics of the different protocols. For each metric we use GPSR as a reference point and discuss LASP and LASP-MF's performance relative to it. We start by focusing on end-to-end PDR. In an experimental setting, it is difficult to compute absolute PDRs because the ground truth of whether a packet is deliverable or not is generally unknown. We tackled this issue in two different ways. First, we considered the PDR of packets that are known to be deliverable because at least one of the protocols did in fact deliver it. Second, we used time-indexed CAM reception data (as per Sec. 4.2.1) to estimate the probability of delivery, which was then compared with the actual results.

Figure 5.14a shows the per-protocol results for the packets that at least one of them delivered. The benchmark GPSR protocol delivered 72% of the packets. LASP delivered 15% more (83%) and LASP 30% more (94%). Two points can be made here. First, GPSR's greedy distance-based strategy proved to be noticeably more prone to failure than LASP and LASP-MF's spatial connectivity-based approach. Second, since LASP obtained roughly half of LASP-MF's improvement while not making use of node diversity, it can be said that node diversity and the spatial connectivity heuristic both contribute to LASP-MF's performance in roughly equal amounts.

We now consider the comparison between the PDR obtained by the actual protocols and the PDR estimated from CAM data. The estimation was performed as previously described in Section 4.4. Each node broadcast 10 CAMs per second. The percentage of those CAMs that a given node pair was able to exchange successfully was defined to be the PDR of an erasure channel between them. All links were then grouped into a graph structure and the Floyd-Warshall algorithm used to find the PDR-maximizing paths between each source-destination pair. This represents an optimal protocol with that uses a single forwarder per hop.

Figure 5.14b presents the results. GPSR obtained the lowest performance, delivering less than 80% of the packets with an estimated PDR of 100%. Relative to GPSR, LASP provided a consistent improvement of roughly 15% over the entire estimated PDR range.

LASP-MF outperformed LASP throughout the whole estimated PDR range, but the magnitude of the improvement varied according to the estimated end-to-end PDR. LASP-MF did not provide a very significant advantage over LASP for packets with very high estimated PDRs. For example, for packets with 100% estimated PDR the improvement was 6% (93% for LASP-MF versus 88% for LASP). This makes sense because when link quality is good, the gains to be had by exploiting

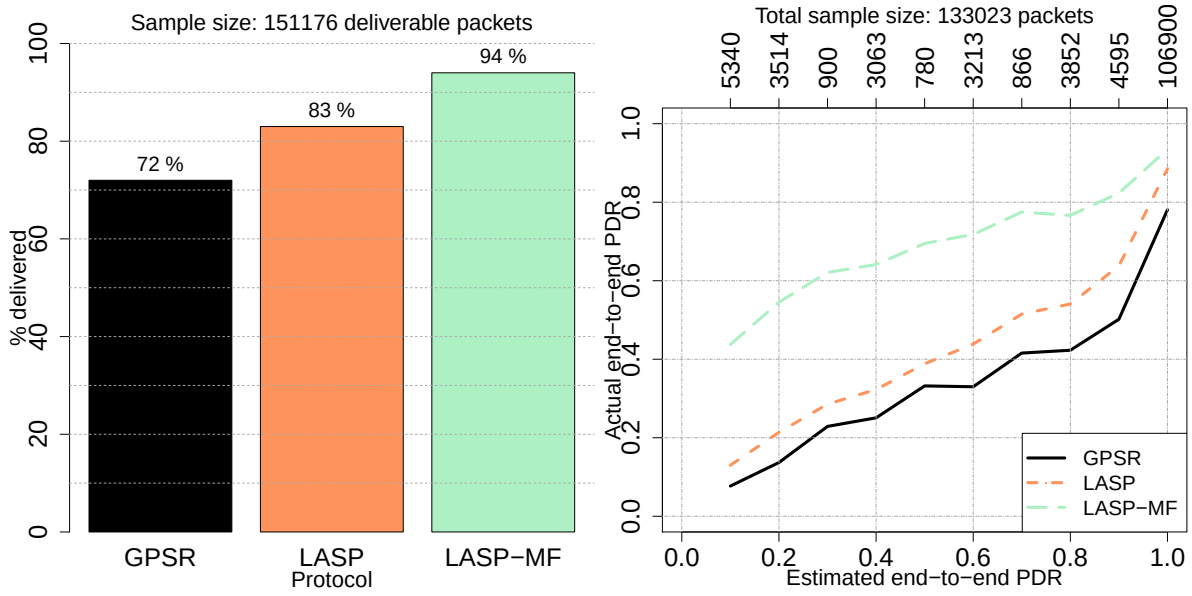

(a) PDR of deliverable packets

(b) PDR relative to estimated 1-forwarder optimal

Figure 5.14: LASP-MF experimental packet delivery ratio results.

node diversity are small (i.e. there are few losses to recover from).

On the other hand, for packets with lower estimated PDRs, LASP-MF was able to improve upon LASP's performance very significantly. For example, for the subset of packets with an estimated end-to-end PDR of 40%, LASP-MF doubled LASP's performance (64% for LASP-MF versus 32% for LASP). These results are justified by the fact that, when links are poor, there are more losses that can be recovered by exploiting node diversity. Note also that LASP-MF was able to surpass the estimated optimal end-to-end PDR for low estimated PDR values. This is a consequence of the fact that the estimation uses a single forwarder per hop, while LASP-MF can use multiple forwarders to increase PDR.

Figure 5.15 shows what percentage of packets that were delivered by all protocols needed to use a recovery procedure to find the destination: perimeter mode using the right-hand rule for GPSR and backtracking for LASP and LASP-MF. 16% of GPSR packets used its recovery procedure, while only 11% of the LASP packets did so, a relative reduction of 31%. Because recovery is used when the heuristic fails, this illustrates how spatial connectivity is able to model network conditions better than distance alone. LASP-MF, on the other hand, used recovery as often as GPSR. Since LASP-MF uses the same heuristic LASP does but introduces additional delay at the forwarding level for inter-forwarder coordination, it is possible for the timeout used by the previous hop to detect a loss and trigger recovery to have been too aggressive.

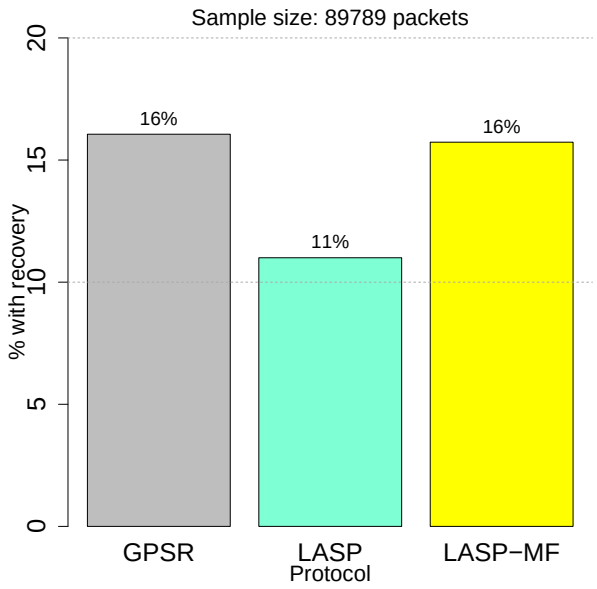

Figure 5.15: LASP-MF experimental recovery mechanism usage results.

Hop Count

We now turn our attention to the length of the paths found by the different protocols. In the interest of fairness, we compare the lengths of the paths for the subset of packets that were successfully delivered to the destination by all three protocols. Figure 5.16a depicts the Empirical Cumulative Distribution Function (ECDF) for this subset of paths. GPSR obtained the shortest paths of all, which is consistent with its greedy distance-based relay selection strategy. In fact, its ECDF closely mimics the source-destination hop separation histogram of Figure 5.13b. LASP found the longest paths, with roughly double the number of 3 hop or longer paths relative to GPSR (20% of the ECDF above 3 for LASP versus less than 10% for GPSR). LASP-MF fell in between the other two. This means that leveraging multiple forwarders allowed LASP-MF to opportunistically explore shorter paths that the spatial connectivity heuristic would not pick by itself.

Transmission count

Figure 5.16b presents the ECDF for the total transmission count of the different protocols. GPSR and LASP behaved very similarly in terms of transmission count, despite the longer paths used by LASP. This leads us to conclude that the spatial connectivity-based metric chooses better connected neighbors, reducing the need for retransmissions. LASP-MF generated noticeably more transmissions than the other two protocols. GPSR and LASP cross the ECDF's 80^{th} percentile at around 3 transmissions, while LASP-MF does so around the 12 transmission mark. This leads us

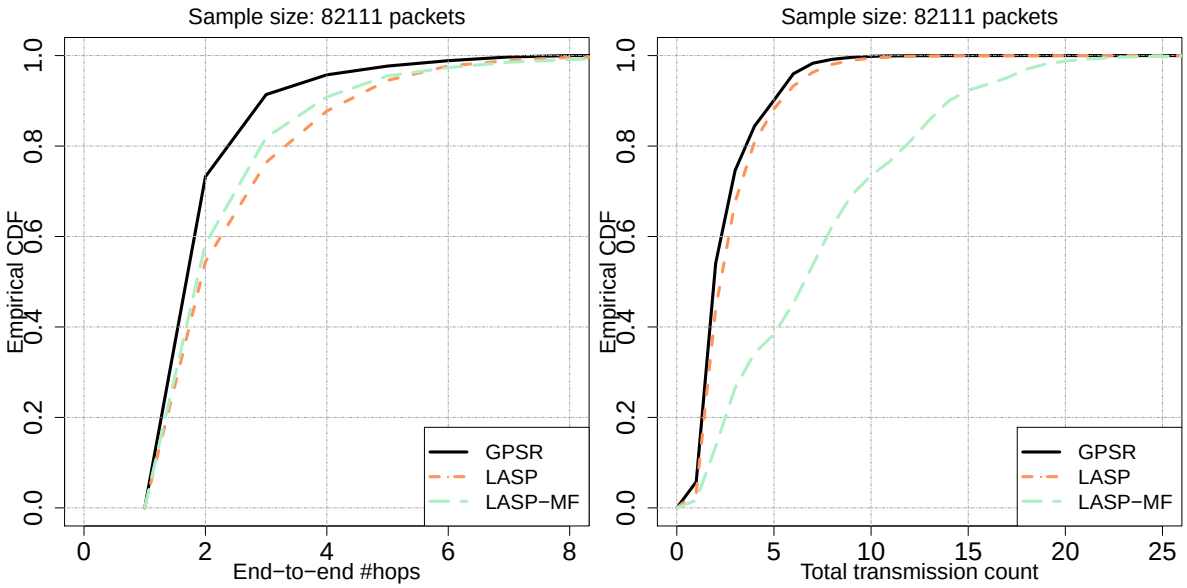

(a) Hop count

(b) Total transmission count

Figure 5.16: LASP-MF experimental results: transmission and hop count.

to believe that further tuning of the waiting time before forwarding is necessary. It was likely too short to allow for proper redundant forwarding cancellation.

Number of replicas

Figure 5.17a depicts the ECDF of the amount of replica packets observed at the destination. GPSR is not shown because, as it does not detect reception failures of the chosen relay, it can not create replication. LASP, on the other hand, can create duplicates if the chosen next hop receives and forwards a packet but the sender fails to overhear it and therefore activates the recovery procedure. However, according to our results, this is a very rare occurrence: only roughly 5% of packets generated a replica, and none generated more than a single replica. LASP-MF, due to its multi-forwarder nature, is more prone to replication due to hidden terminals and insufficient temporal separation between forwarders. Results show that LASP-MF produced one or more replicas for 30% of packets. This could be reduced by tuning the timing parameters and enforcing a stricter minimum PDR between forwarding zone cells to prevent hidden nodes.

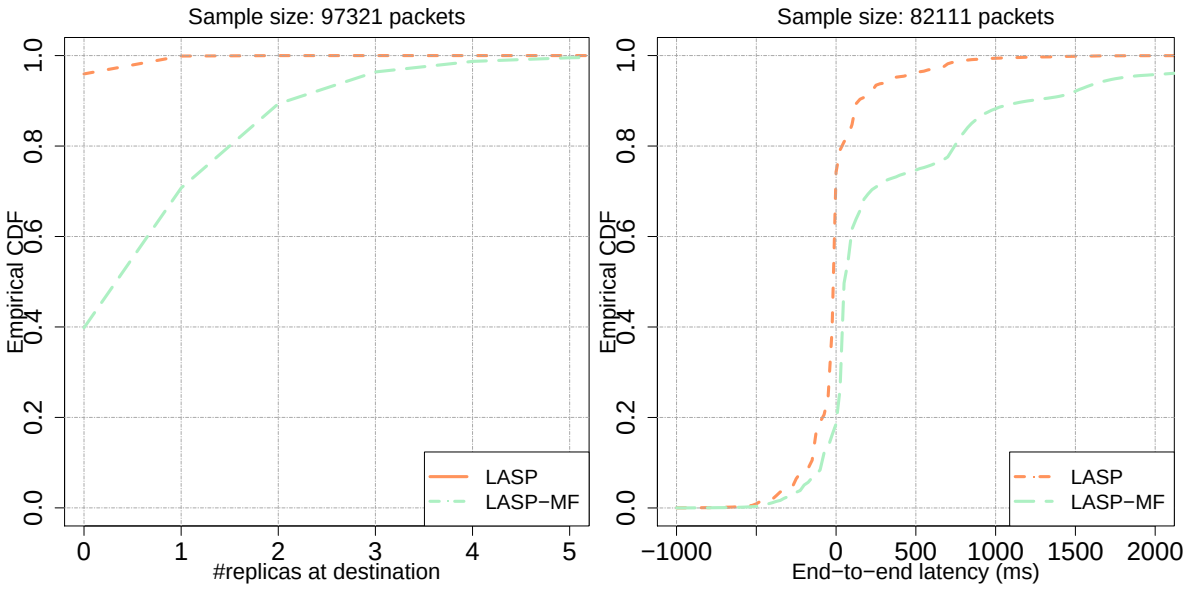

(a) Replicas

(b) Delay

Figure 5.17: LASP-MF experimental results: number of replicas and end-to-end latency.

Latency

Finally we focus on latency. Given that end-to-end acknowledgments were not implemented, we could not use Round Trip Time (RTT) to measure latency. We therefore use a unidirectional latency measurement taken at the destination. Furthermore, because of imperfect clock synchronization between nodes, use use relative measurements, not absolute measurements.

We defined the time at which a packet was delivered by GPSR to be zero, and measured LASP's and LASP-MF's delays relative to that baseline. Figure 5.17b presents the ECDF of this relative delay for each of the 3 protocols. LASP's ECDF crosses zero at around the 70^{th} percentile, meaning most LASP packets arrived earlier than the corresponding GPSR packets. This is an indication that the spatial connectivity metric chooses better connected nodes, which need fewer retransmissions. LASP-MF, on the other hand, crosses zero at around the 30^{th} percentile and features a long tail beyond the 80^{th} percentile. This is likely caused by the delay introduced by the forwarder coordination and recovery mechanisms.

Discussion

In summary, these results show that leveraging spatial connectivity and node diversity can significantly improve multi-hop communication reliability. Spatial connectivity, represented by LASP,

improved end-to-end PDR by around 15% relative to GPSR, with little to no trade-off in the other measured performance metrics. Combining node diversity with spatial connectivity in the LASP-MF protocol resulted in a 30% improvement in PDR relative to GPSR at a cost in terms of congestion and latency. Node diversity yielded the largest gains when connectivity was poor, i.e. low estimated PDR.

Comparing the improvement in end-to-end PDR provided by LASP relative to GPSR between the experiments and the trace-based analysis of Section 4.4, we can see the results were consistent. The results of the trace-based analysis were presented as expected values and not actually delivered packets, so a direct comparison is not possible. However, if we divide the expected end-to-end PDR achieved by LASP by the one achieved by GPSR for the packets that both could deliver with 10% or higher probability[1], we obtain an improvement of 13.3%. This is agreement with the 15% improvement observed in the experiments.

When we compare LASP and LASP-MF using the same procedure, the results are more disparate. The trace-based analysis shows an improvement of 59% while the experiments showed an improvement of 13%. We can identify two main factors contributing to this discrepancy. First, the number of active nodes was significantly larger during the time period in which the trace-based analysis was performed (Figure 4.12a versus Figure 5.13a). The mean number of active nodes during the trace-based analysis was 80% higher than the number of nodes active during the experiments (12.8 vs 7.1). Larger networks with more nodes and links have more opportunities to exploit node diversity. By definition, if there is a single path connecting source and destination, there is no diversity gain to be exploited. Second, in the trace-based analysis, there was no enforcement of a minimum PDR between spatial cells in the forwarding zone selection process, meaning the chosen forwarding zones were larger, which benefits reliability at the cost of additional congestion.

LASP and LASP-MF's performance in a practical context is subject to external factors such as OBU market penetration rate, node density and vehicle speed. We now consider the effect of these aspects on our protocols.

OBU market penetration rate refers to the percentage of vehicles equipped with wireless vehicular communication devices. According to the U.S. Department of Transportation, the average age of light vehicles in the United States in the year 2014 was 11.4 years [oT15]. This means that, even if OBUS installation becomes mandatory for new vehicles, there will still be a long period of time where partial deployment will be an unavoidable reality.

Partial deployment reduces the number of vehicles available for relaying packets, which can potentially cause a problem to our protocols. Because we focus on real-time communication, if source and destination are not part of one and the same connected component, the packet will be

[1]If we included packets with very low expected PDRs the gains would be unrealistically inflated.

lost. In a partial deployment situation this limitation is exacerbated.

To understand the effect of partial OBU deployment in vehicular network connectivity we refer to a study by Ferreira *et al.* [FCaFT09] that analyzes this issue by leveraging aerial photography of the city of Porto, Portugal. They started by using the photographs to mark the position of each vehicle in the city and, assuming a simple communication model (250 m range in line of sight, 140 m in non-line of sight conditions), defining a network topology. Then, they simulated different market penetration rates by eliminating a portion of the vehicles uniformly at random. The connectivity for each level of market penetration was estimated by counting the number of vehicles that were part of the connected component of a source vehicle located in the city center. The results showed that for this particular scenario, a penetration rate of around 33% is necessary to achieve percolation and allow the source to connect with roughly 80% of the networked vehicles.

Delivering packets between nodes that are not part of the same connected component is outside the scope of this thesis and is discussed in Section 6.2 as a potential avenue for future work.

Node density refers to the number of vehicles available for relaying packets, which varies according to spatial and temporal traffic patterns. This creates two contrasting problems for multi-hop communication: scarcity of relays in empty areas and an overwhelming number of relays leading to network congestion and ultimately saturation in crowded areas.

The usage of historical spatial connectivity helps LASP and LASP-MF mitigate these issues. A scarcity of vehicles in a given area will be reflected in the historical spatial connectivity map by a low estimated delivery probability, since this probability takes into account not only the quality of communication between vehicles but also the likelihood of there being vehicles in that area to communicate in the first place. Furthermore, if a given spatial area is prone to network congestion leading to significant packet loss, this will also be reflected in the historical map as a low delivery probability. Furthermore, through its coordination and prioritization mechanism, LASP-MF is able to control congestion even when it has to traverse very node-dense regions.

In order to capture temporal patterns, such as rush hour traffic, the historical spatial connectivity information can be divided into different maps which would then be indexed by time of day or day of the week. This strategy creates a trade-off between storage space and information accuracy.

Vehicle speed affects how dynamic the network topology and links are. At higher speeds, links will tend not to last as long and be more unstable due to quicker rate of change in inter-vehicle distance and obstacle profiles. Because LASP-MF is a geographic protocol that builds route hop-by-hop and leverages node diversity to recover from packet losses, it is well suited to cope with such a dynamic environment. We expect that the more dynamic the environment is, the larger the benefit provided by LASP-MF will be. This phenomenon could be observed in our experimental results: LASP-MF provided the largest increase in end-to-end PDR when connectivity between

source and destination was poor (Figure 5.14b).

5.5 Summary

LASP uses spatial connectivity to find well-connected paths. But, by choosing a single node to relay the packet in each hop, it is susceptible to the instability that characterizes wireless vehicular links. Conversely, in DAZL, the forwarding decision is made on the receiver-side, allowing for cooperation amongst multiple potential forwarders. However, it is only able to forward in a straight line towards the destination.

In this chapter we presented a multi-forwarder version of LASP, designated LASP-MF, that combines LASP's spatial connectivity approach to routing with a DAZL-like two-step zone-based forwarding process. In LASP-MF, sender nodes choose not a specific next hop relay, but a geographic forwarding zone. Nodes inside this zone then use a distributed coordination scheme to prioritize the most promising forwarding zone node in actually relaying the packet. The ranking metric candidate forwarders use is not distance to destination like in DAZl, but rather LASP's spatial connectivity-based probability of delivery estimator.

Once more leveraging the HarborNet testbed, we evaluated LASP-MF through a combination of experiments and a mathematical analysis fed by real-world connectivity traces. Compared with LASP, LASP-MF was able to increase PDR upwards of 50% in the trace-based analysis and 13% in the experimental evaluation.

LASP-MF therefore exemplifies how the two basic concepts behind this thesis, spatial connectivity and node diversity, complement each other in vehicular multi-hop communication.

Chapter 6

Conclusions

In this chapter we summarize the significance of the work presented in this thesis and, reflecting upon the lessons learned during this process, propose potential avenues for future work in this area.

6.1 Contributions

The contributions of this work can be summarized as follows:

Quantification of the potential of node diversity in vehicular multi-hop In order to validate the use of node diversity in forwarding for vehicular networks, we performed on-the-road experiments that allowed us to quantify the potential reliability improvements to be had by allowing multiple nodes to cooperate in forwarding packets. The results showed significant gains over traditional single-forwarder strategies, thus corroborating our initial intuition and justifying the pursuit of an opportunistic forwarding solution.

Design, implementation and evaluation of DAZL We presented the DAZL (Density-Aware Zone-base Limited) forwarding protocol. DAZL exploits node diversity by proposing to do forwarding based on geographical forwarding zones, rather than the traditional node-based approach. The challenge is how the different candidate forwarders inside a forwarding zone can cooperate without introducing excessive control overhead and packet replication. To this effect, DAZL employs a distributed coordination mechanism with distance-based prioritization rules so that only the best-positioned forwarders actually forward packets. DAZL was evaluated using both experiments and simulations, providing in both instances a significant performance boost over a benchmark neighbor-based single-forwarder protocol.

Spatial connectivity and its usefulness for vehicular multi-hop We introduced the concept

of spatial connectivity and collected data from two real-world vehicular testbeds to test its usefulness as an heuristic for vehicular multi-hop. The results showed the presence of spatial autocorrelation in vehicular packet delivery ratio data and that this relationship between spatial location and connectivity was long lasting. The use of spatial connectivity was thus warranted.

As a byproduct of this study, a large data set comprising information regarding vehicles' locations and communications was created. Besides our own, this data set has already proved itself useful in many other research efforts. For example, it has been utilized to analyze vehicle mobility patterns; the economics of handing off data from the cellular network to the vehicular network and; the performance of vehicular data collecting protocols.

Design, implementation and evaluation of LASP We put forward the Look-Ahead Spatial routing Protocol (LASP). LASP combines real-time connectivity information for the local neighborhood with global historical spatial connectivity information (look-ahead) to estimate the end-to-end probability of delivery and choose, at each hop, the most promising next hop forwarder. We evaluated LASP through a trace-based analysis of data collected from the HarborNet testbed and experiments performed on the same testbed using a prototype LASP implementation. Results showed an improvement in end-to-end PDR over the reference protocol GPSR of around 15%, significant considering the network's small diameter.

Design, implementation and evaluation of LASP-MF Finally, we combined both DAZL's and LASP's key features into a single protocol: LASP Multi-Forwarder, or LASP-MF. LASP-MF uses zone-based forwarding like DAZL does, but instead of forwarding in a straight line towards the destination, leverages spatial connectivity to select a forwarding zone that maximizes the probability of delivery to the destination. Moreover, spatial connectivity is used again inside the forwarding zone to prioritize forwarders. Thus, the benefits of using both spatial connectivity and node diversity are realized. Again we took advantage of the HarborNet testbed to perform both a traced-based analysis and actual experiments. Results showed an increase in end-to-end PDR relative to the benchmark protocol GPSR of 30% for LASP-MF, with a trade-off in terms of network load.

6.2 Future Work

We now present future work ideas stemming from the knowledge acquired during the development of the work presented in this thesis:

Larger-scale testing As vehicular network technology matures and comes closer to commercial-

ization and widespread use, proper testing and evaluation under realistic conditions becomes more and more important. In our work we made a serious effort to experimentally validate all of our ideas and protocols. Using the HarborNet testbed, we were able to perform experiments with up to 30 nodes. However, because the testbed is confined to a relatively small area of 1 Km^2, source and destination were most often separated by no more than 2 or 3 hops. It is our belief that larger-diameter networks will tend to amplify performance differences between protocols and make for a better evaluation.

Also, HarborNet's connectivity patterns represent a very particular environment, where vehicles tend to cluster around ships and obstructions are mostly created by metal containers. Different testbeds with different connectivity patterns would allow for a more complete evaluation. For example, a testbed deployed in a freeway environment would provide a significant contrast to the more city-like environment of the harbor.

PortoVANET, in the city of Porto, has recently passed the 400 node mark and is a good candidate for such tests. However, given the large deployment area and the fact that only a portion of these vehicles are circulating at any given time, this testbed can only support multi-hop tests for delay-tolerant protocols. If a delay-tolerant component is added to LASP, it could be deployed and tested in PortoVANET. Given that PortoVANET nodes use the same communication boxes and software as the HarborNet nodes, most of the codebase could be reused.

In the United States, the Department of Transportation is backing the creation of several large scale testbeds [oT]. From these, the Southeast Michigan testbed is the largest and thus most interesting from a multi-hop communication perspective, with around 3000 DSRC-equipped vehicles.

Spatial connectivity representation In the implementation of our LASP and LASP-MF protocols we used a simple square grid representation to index spatial data. The 50×50 m cell size used was chosen in order to have nodes in the same cell experience similar connectivity conditions, according to the spatial autocorrelation analysis we performed. However, this fine-grained spatial division limits the size of the area for which nodes can realistically store and maintain historical spatial connectivity information.

Moreover, we note that information concerning faraway locations tends to be of less importance than information concerning closer locations. There are two main reasons for this. First, most envisioned vehicular applications tend to exhibit a high degrees of locality regarding their communications [LCG08]. Second, if needed, packets destined to faraway locations will be able to make corrections further down the path, when more accurate information becomes available.

It makes therefore sense to adapt our spatial connectivity representation to this reality and consequently increase our protocols' scalability. For instance, multiple layers of information with different granularities could be combined, with finer grids being used for close-by locations and coarser ones for faraway locales. Also note that in open areas communication ranges are larger and more predictable due to the lack of obstacles. Therefore we can think of a representation that uses cells of different sizes for different areas, depending on the local propagation characteristics. Or even using road maps to approximate connectivity for faraway locations and spatial connectivity for closer ones.

Geocast and multicast In this thesis we focused on unicast communication. However, multicast and specially geocast, are also important in the context vehicular networks. Our unicast LASP and LASP-MF protocols could be used as building blocks in the design of protocols for these other types of communication.

Since our protocols use geographic addressing, they can be used in a geocast context to reach the Zone of Relevance (ZOR) by simply setting the packet's destination to be inside the ZOR. Then, a broadcast procedure would be required to disseminate the packet inside it [WTP+07]. Multicast could be implemented by grouping the destination nodes into subsets according to their locations, and then use LASP or LASP-MF to reach those locations.

Transport service Our work has focused on the creation of a network layer multi-hop communication service that attempts to maximize packet delivery ratio. However, this is not sufficient for applications, for multiple reasons. First, reliability is not ensured, for instance when the allotted number of retransmissions is insufficient to recover from channel losses. Second, since different packets may follow different paths, they can reach the destination out of order. Furthermore our protocols do not provide end-to-end flow and congestion control.

These issues are traditionally addressed at the transport layer. TCP, as used on the internet, is the reference transport protocol, providing all of the aforementioned features: reliability, ordering, flow and congestion control. However, TCP was designed with wired networks in mind, where network topology is stable and error rates are low. When applied to wireless ad-hoc networks, and specially vehicular ad-hoc networks, which suffer from high channel error rates and a highly dynamic topology and links, TCP is not a good solution.

First, let us consider reliability. TCP is designed to deliver packets between a source and destination that are connected through some real-time path. However, in vehicular networks, there may not exist a path between source and destination at the time of transmission: i.e. source and destination may not be part of the same connected component.

This necessitates the creation of different reliability mechanisms. For instance, in vehicular networks, node mobility can be exploited to deliver packets between temporarily disconnect

nodes, as long as packets are not delay sensitive [CLGH10, LM07]. Multihoming could also be used for the same purpose. It has been shown that open WiFi hotspots can be used opportunistically by passing vehicles to access the internet [BMV+08, OK04]. It has also been shown that WiFi can be used for offloading data from the cellular network [BMV10, HDD11]. We envision a vehicular network transport protocol that can use both WiFi and cellular links as complements to DSRC communication: WiFi in urban environments and cellular links in rural areas where there are no other vehicles around to relay packets.

TCP's congestion control algorithms are also not suited to vehicular network use. In order to gauge network capacity, TCP begins connections by sending packets at a slow rate, which is then gradually increased as acknowledgements from the destination are received. This strategy is known as *slow start* and is well suited to the long-lived links and paths of wired networks. However, as we have seen in Chapter 2, vehicular links are short lived so this slow start approach will not be able to fully utilize the available capacity while the link exists.

Another problem with TCP's congestion control it assumes packet losses are caused by congestion. This is a good approximation in wired networks, where channels have very small error rates. However, as we have also seen in Chapter 2, this is not the case in vehicular networks, where channel losses can be severe. The transport protocol therefore needs to distinguish between congestion losses and channel losses.

As a consequence of these and other issues, TCP has been shown to perform poorly when used the vehicular context [DCD11]. There exist several transport protocol proposals in the literature which distinguish between congestion and channel losses (e.g. [LS01, SAHS05, BJW05, VBT11]). We believe there is further work to be done in terms of refinement and integration of these new congestion control strategies with delay-tolerant and multihoming reliability mechanisms, in order to create a complete transport solution for vehicular networks.

Location service In this thesis we used geographical addressing, which implies that the source must be able to determine the destination's location before sending the packet. The actual design and implementation of this location service was outside of the thesis scope. However, given how important this location service is to the functioning of a unicast geographical multi-hop protocol, it is a natural avenue for further research.

The literature on location services for mobile ad-hoc networks is extensive. Most disseminate location information throughout the network [CBW02, GS06], much like traditional routing protocols do with topology information. And much like in routing, this creates convergence and scalability problems in the highly dynamic vehicular context. Other protocols [LJDC+00, SBLB10] try to address these concerns by dividing space into a grid, and avoiding inter-cell location requests as much as possible, but their performance in practical scenarios still requires

further evaluation.

For maximum scalability, we envision the possibility of a cloud-based multihomed location service where internet-connected RSUs would register the location of the nodes passing through them in a central server. Nodes could then use DSRC, WiFi or cellular links, depending on their availability, to query the service for the location of any given node.

Glossary

CAM a Cooperative Awareness Message (CAM) is a short message broadcast by every node 10 times per second indicating its position, velocity vector and other relevant information.

DSRC Dedicated Short Range Communications (DSRC) are a set of communication channels in the 5.9 GHz band reserved for vehicular use.

edge a connection between a pair of vertices in LASP's routing graphs; each edge is annotated with the probability of packet delivery between its vertices.

forwarding zone the geographic area inside which multiple nodes can cooperate in forwarding a packet; in DAZL a forwarding zone is defined by a pair of distances to the destination which specify an annulus centered at the destination; in LASP a forwarding zone is defined by a set of one or more spatial cells.

HarborNet A vehicular testbed composed of 25 OBU-equipped trucks and 5 RSUs deployed in the Leixões Harbor, in Porto, Portugal.

IEEE 802.11p is an amendment to the physical and media access control IEEE 802.11 standard to support vehicular communication in the DSRC channels.

link the wireless connection between two neighbors; each link has an associated PDR measured by dividing the number of CAM receptions by the number of CAM transmissions.

neighbor a node u is a neighbor of node v if v can communicate directly with u and vice-versa.

node a communication device that is part of the vehicular network; can represent an OBU installed in a vehicle or an infrastructure RSU.

OBU an On-Board Unit (OBU) is a vehicular communication device installed in a vehicle.

PDR Packet Delivery Ratio (PDR) is the ratio of received to sent messages.

PortoVANET A vehicular testbed composed of around 400 public transportation vehicles (buses and taxis) deployed in the city of Porto, Portugal.

relay see forwarder.

RSU a Road-Side Unit (RSU) is an infrastructure vehicular communication device installed on the side of a road.

spatial cell the smallest unit of space considered by LASP; in the current implementation each cell covers a 50×50 m area.

vertex the fundamental unit of which the routing graphs used by LASP are made; in the historical graph, each vertex represents a spatial cell; in the real-time graph, both spatial cells and network nodes can be vertices.

WAVE Wireless Access in Vehicular Road-Side Unit (RSU) is an American family of standards that specify the architecture and basic services and applications that are to support vehicular communication.

Bibliography

[ACN+14] C. Ameixieira, A. Cardote, F. Neves, R. Meireles, S. Sargento, L. Coelho, J. Afonso, B. Areias, E. Mota, R. Costa, R. Matos, and J. Barros. HarborNet: a Real-World Testbed for Vehicular Networks. *Communications Magazine, IEEE*, 52(9):108–114, Sep 2014.

[AHW09] M. Abolhasan, B. Hagelstein, and J. C P Wang. Real-world Performance of Current Proactive Multi-hop Mesh Protocols. In *Communications, 2009. APCC 2009. 15th Asia-Pacific Conference on*, pages 44–47, Oct 2009.

[AMM+11] C. Ameixieira, J. Matos, R. Moreira, A. Cardote, A. Oliveira, and S. Sargento. An IEEE 802.11p/WAVE Implementation with Synchronous Channel Switching for Seamless Dual-channel Access (Poster). In *Proc. of the 2011 Vehicular Networking Conference (VNC)*. IEEE, 2011.

[B+12] C. Brandstaetter et al. (2012) Annual Statistical Report, Deliverable D3.9 of the EC FP7 project DaCoTA. Technical report, European Road Safety Observatory, 2012.

[BGLB02] Ljubica Blažević, Silvia Giordano, and Jean-Yves Le Boudec. Self Organized Terminode Routing. *Cluster Computing*, 5(2):205–218, April 2002.

[BJW05] Marc Bechler, Sven Jaap, and Lars Wolf. An Optimized TCP for Internet Access of Vehicular Ad Hoc Networks. In *NETWORKING 2005. Networking Technologies, Services, and Protocols; Performance of Computer and Communication Networks; Mobile and Wireless Communications Systems*, volume 3462 of *Lecture Notes in Computer Science*, pages 869–880. Springer Berlin Heidelberg, 2005.

[BK09] Fan Bai and Bhaskar Krishnamachari. Spatio-temporal variations of vehicle traffic in VANETs: facts and implications. In *VANET '09: Proceedings of the sixth ACM International Workshop on VehiculAr InterNETworking*, 2009.

[BKS+06] Fan Bai, Hariharan Krishnan, Varsha Sadekar, Gavin Holl, and Tamer Elbatt. Towards Characterizing and Classifying Communication-based Automotive Applications

from a Wireless Networking Perspective. In *Proceedings of IEEE Workshop on Automotive Networking and Applications (AutoNet)*, 2006.

[BM05] S. Biswas and R. Morris. ExOR: Opportunistic Multi-Hop Routing for Wireless Networks. *Computer Communication Review*, 35(4), 2005.

[BMB+11] Mate Boban, Rui Meireles, João Barros, Ozan Tonguz, and Peter Steenkiste. Exploiting the Height of Vehicles in Vehicular Communication. In *Vehicular Networking Conference (VNC), 2011 IEEE*, 2011.

[BMB+14] M. Boban, R. Meireles, J. Barros, P. Steenkiste, and O. Tonguz. TVR - Tall Vehicle Relaying in Vehicular Networks. *IEEE Transactions on Mobile Computing*, 13(5):1118–1131, May 2014.

[BMV+08] Aruna Balasubramanian, Ratul Mahajan, Arun Venkataramani, Brian Neil Levine, and John Zahorjan. Interactive WiFi Connectivity for Moving Vehicles. *SIGCOMM Comput. Commun. Rev.*, 38(4):427–438, August 2008.

[BMV10] Aruna Balasubramanian, Ratul Mahajan, and Arun Venkataramani. Augmenting Mobile 3G Using WiFi. In *Proceedings of the 8th International Conference on Mobile Systems, Applications, and Services*, MobiSys '10, pages 209–222, New York, NY, USA, 2010. ACM.

[BRAHH04] R. Baroody, A. Rashid, N. Al-Holou, and S. Hariri. Next Generation Vehicle Network (NGVN): Internet access utilizing dynamic discovery protocols. In *Pervasive Services, 2004. ICPS 2004. Proceedings. The IEEE/ACS International Conference on*, pages 81 – 88, Jul 2004.

[Bri01] Linda Briesemeister. *Group Membership and Communication in Highly Mobile Ad Hoc Networks*. PhD thesis, Technischen Universität Berlin, 2001.

[BSK10] Fan Bai, Daniel D. Stancil, and Hariharan Krishnan. Toward Understanding Characteristics of Dedicated Short Range Communications DSRC from a Perspective of Vehicular Network Engineers. In *Proc. of the 16th Conference on Mobile Computing and Networking (MobiCom)*. ACM, 2010.

[Bur12] U.S. Census Bureau. Statistical Abstract of the United States - Transportation, 2012.

[Cab] Luís Cabrita. Ship-To-Shore and Rail Mounted Stacking Cranes at the Leixões Harbor. Panoramio, `http://www.panoramio.com/photo/64416319`. accessed on December 8, 2014.

[CABM05] D.S.J.D. Couto, D. Aguayo, J. Bicket, and R. Morris. A High-Throughput Path Metric for Multi-Hop Wireless Routing. *Wireless Networks*, 11(4):419–434, 2005.

[CBW02] T. Camp, J. Boleng, and L. Wilcox. Location Information Services in Mobile Ad Hoc Networks. In *Communications, 2002. ICC 2002. IEEE International Conference on*, volume 5, 2002.

[CHC+08] Lin Cheng, B.E. Henty, R. Cooper, D. Stancil, and Fan Bai. A Measurement Study of Time-Scaled 802.11a Waveforms Over the Mobile-to-Mobile Vehicular Channel at 5.9 GHz. *Communications Magazine, IEEE*, 46(5):84 –91, May 2008.

[Chr11] J Chroboczek. RFC 6126 - The Babel Routing Protocol, 2011.

[CJ03] T. Clausen and P. Jacquet. RFC 3626 - Optimized Link State Routing Protocol (OLSR), 2003.

[CJKK07] S. Chachulski, M. Jennings, S. Katti, and D. Katabi. Trading Structure for Randomness in Wireless Opportunistic Routing. In *Proceedings of the 2007 conference on Applications, technologies, architectures, and protocols for computer communications*. ACM, 2007.

[CLGH10] Pei-Chun Cheng, KevinC. Lee, Mario Gerla, and Jrme Hrri. GeoDTN+Nav: Geographic DTN Routing with Navigator Prediction for Urban Vehicular Environments. *Mobile Networks and Applications*, 15(1):61–82, 2010.

[Cre93] Noel A. C. Cressie. *Statistics for Spatial Data*. Wiley, 1993.

[DCD11] Kusum Dalal, Prachi Chaudhary, and Pawan Dahiya. Performance Evaluation of TCP and UDP Protocols in VANET Scenarios using NCTUns-6.0 Simulation Tool. *International Journal of Computer Applications*, 36(6), 2011.

[DRGM06] Floriano De Rango, Mario Gerla, and Salvatore Marano. A scalable routing scheme with group motion support in large and dense wireless ad hoc networks. *Computers and Electrical Engineering*, 32(1-3):224–240, January 2006.

[EGH+06] Tamer ElBatt, Siddhartha K. Goel, Gavin Holland, Hariharan Krishnan, and Jayendra Parikh. Cooperative Collision Warning Using Dedicated Short Range Wireless Communications. In *Proceedings of the 3rd International Workshop on Vehicular Ad hoc NETworks*, VANET '06, pages 1–9, New York, NY, USA, 2006. ACM.

[ETS05] ETSI. EN 12253:2004 Dedicated Short-Range Communication Physical layer using microwave at 5.8 GHz, Oct 2005.

[ETS09] ETSI. TS 102 638: Intelligent Transport Systems (ITS); Vehicular Communications; Basic Set of Applications; Definitions, 2009.

[ETS11] ETSI. TS 102 637-2: Intelligent Transport Systems (ITS); Vehicular Communications; Basic Set of Applications; Part 2: Specification of Co-operative Awareness Basic Service, 2011.

[FBZ+08] Andreas Festag, Roberto Baldessari, Wenhui Zhang, Long Le, Amardeo Sarma, and Masatoshi Fukukawa. CAR-2-X Communication for Safety and Infotainment in Europe. *NEC Technical Journal*, 3(1), 2008.

[FCaFT09] M. Ferreira, H. Conceição, R. Fernandes, and O.K. Tonguz. Urban Connectivity Analysis of VANETs through Stereoscopic Aerial Photography. In *Vehicular Technology Conference Fall (VTC 2009-Fall), 2009 IEEE 70th*, 2009.

[FGEG11] Raphael Frank, Eugenio Giordano, Thomas Engel, and Mario Gerla. Performance Bound for Routing in Urban Scenarios. In *Proc. of the 7th Asian Internet Engineering Conference (AINTEC)*. ACM, 2011.

[FH08] Marco Fiore and Jérôme Härri. The Networking Shape of Vehicular Mobility. In *Proceedings of the 9th ACM International Symposium on Mobile Ad Hoc Networking and Computing*, MobiHoc '08, pages 261–272, New York, NY, USA, 2008. ACM.

[FWK+03] H. Füßler, J. Widmer, M. Käsemann, M. Mauve, and H. Hartenstein. Contention-based forwarding for mobile ad hoc networks. *Ad Hoc Networks*, 1(4), 2003.

[GS06] Venkata C. Giruka and Mukesh Singhal. Two scalable location service protocols for wireless ad hoc networks. *Pervasive and Mobile Computing*, 2(3), 2006.

[HDD11] Xiaoxiao Hou, P. Deshpande, and S.R. Das. Moving Bits from 3G to Metro-Scale WiFi for Vehicular Network Access: An Integrated Transport Layer Solution. In *Network Protocols (ICNP), 2011 19th IEEE International Conference on*, pages 353–362, Oct 2011.

[HHH08] Yao H. Ho, Ai H. Ho, and Kien A. Hua. Routing protocols for inter-vehicular networks: A comparative study in high-mobility and large obstacles environments. *Computer Communications*, 31(12):2767 – 2780, 2008.

[IEE10] IEEE. 1609.3 Standard for Wireless Accesses in Vehicular Environments (WAVE) - Networking Services, Dec 2010.

[JBW05] Sven Jaap, Marc Bechler, and Lars Wolf. Evaluation of Routing Protocols for Vehicular Ad Hoc Networks in City Traffic Scenarios. In *Proc. of the 11th EUNICE Open European Summer School on Networked Applications*, 2005.

[JMB01] David B. Johnson, David A. Maltz, and Josh Broch. *DSR: The Dynamic Source Routing Protocol for Multi-Hop Wireless Ad Hoc Networks in Ad Hoc Networking*, chapter 5, pages 139–172. Addison-Wesley, 2001.

[JNA08] David Johnson, Ntsibane Ntlatlapa, and Corinna Aichele. A simple pragmatic approach to mesh routing using BATMAN. In *2nd Int. Symposium on Wireless Communications and Information Technology in Developing Countries (WCTID)*. IFIP, 2008.

[JS08] M. Jerbi and S.M. Senouci. Characterizing Multi-Hop Communication in Vehicular Networks. In *Proc. of the 2008 Wireless Communications and Networking Conference (WCNC)*, pages 3309–3313. IEEE, March 2008.

[JSMGD07] M. Jerbi, S.-M. Senouci, R. Meraihi, and Y. Ghamri-Doudane. An Improved Vehicular Ad Hoc Routing Protocol for City Environments. *Proc. of the 2007 Int. Conference on Communications (ICC)*, June 2007.

[KA10] S.M. Kamruzzaman and M.S. Alam. Dynamic TDMA Slot Reservation Protocol for Cognitive Radio Ad Hoc Networks. In *Computer and Information Technology (ICCIT), 2010 13th International Conference on*, 2010.

[Ken11] J.B. Kenney. Dedicated Short-Range Communications (DSRC) Standards in the United States. *Proceedings of the IEEE*, 99(7):1162–1182, Jul 2011.

[KK00] Brad Karp and H. T. Kung. GPSR: Greedy Perimeter Stateless Routing for Wireless Networks. In *Proc. of the 6th Conference on Mobile Computing and Networking (MobiCom)*. ACM, August 2000.

[KMC+00] Eddie Kohler, Robert Morris, Benjie Chen, John Jannotti, and M. Frans Kaashoek. The Click Modular Router. *ACM Transactions on Computer Systems*, 18(3):263–297, August 2000.

[LCG08] Uichin Lee, Ryan Cheung, and Mario Gerla. Emerging Vehicular Applications. In *Handbook on Vehicular Networks*. Taylor & Francis Group, 2008.

[LCGZ05] J. LeBrun, Chen-Nee Chuah, D. Ghosal, and M. Zhang. Knowledge-Based Opportunistic Forwarding in Vehicular Wireless Ad Hoc Networks. In *2005 Spring Vehicular Technology Conference (VTC)*, 2005.

[LHT+03] Christian Lochert, Hannes Hartenstein, Jing Tian, Holger Fuessler, Dagmar Hermann, and Martin Mauve. A Routing Strategy for Vehicular Ad Hoc Networks in City Environments. In *Proc. of the 2003 Intelligent Vehicles Symposium (IV)*. IEEE, 2003.

[LJDC+00] J. Li, J. Jannotti, D.S.J. De Couto, D.R. Karger, and R. Morris. A Scalable Location Service for Geographic Ad Hoc Routing. In *Proc. of the 16th Conference on Mobile Computing and Networking (MobiCom)*. ACM, 2000.

[LM07] I. Leontiadis and C. Mascolo. GeOpps: Geographical Opportunistic Routing for Vehicular Networks. In *World of Wireless, Mobile and Multimedia Networks, 2007. WoWMoM 2007. IEEE International Symposium on a*, pages 1–6, Jun 2007.

[LMFH05] Christian Lochert, Martin Mauve, Holger Füßler, and Hannes Hartenstein. Geographic Routing in City Scenarios. *ACM SIGMOBILE Mobile Computing and Communications Review*, 9(1), 2005.

[LPD10] N. Loulloudes, G. Pallis, and M. D. Dikaiakos. The Dynamics of Vehicular Networks in Urban Environments. *ArXiv e-prints*, July 2010.

[LS00] X. Lin and I. Stojmenovic. GPS Based Distributed Routing Algorithms for Wireless Networks. published on CiteSeer, 2000.

[LS01] J. Liu and S. Singh. ATCP: TCP for Mobile Ad Hoc Networks. *Selected Areas in Communications, IEEE Journal on*, 19(7):1300–1315, Jul 2001.

[LSC09] Mei-Hsuan Lu, Peter Steenkiste, and Tsuhan Chen. Design, Implementation and Evaluation of an Efficient Opportunistic Retransmission Protocol. In *Proceedings of the 15th Annual international Conference on Mobile Computing and Networking*, MobiCom '09. ACM, 2009.

[LWW07] Wei Li, Ji-Bo Wei, and Shan Wang. An Evolutionary-Dynamic TDMA Slot Assignment Protocol for Ad Hoc Networks. In *Wireless Communications and Networking Conference, 2007.WCNC 2007. IEEE*, 2007.

[Mai04] C. Maihofer. A Survey of Geocast Routing Protocols. *Communications Surveys Tutorials, IEEE*, 6(2):32 –42, 2004.

[MBK05] Allen Miu, Hari Balakrishnan, and Can Emre Koksal. Improving Loss Resilience with Multi- Rradio Diversity in Wireless Networks. In *Proceedings of the 11th annual international conference on Mobile computing and networking*, MobiCom '05. ACM, 2005.

[MBS+10] R. Meireles, M. Boban, P. Steenkiste, O. Tonguz, and J. Barros. Experimental Study on the Impact of Vehicular Obstructions in VANETs. In *Proc. of the 2010 Vehicular Networking Conference (VNC)*. IEEE, 2010.

[MFB09] R. Meireles, M. Ferreira, and J. Barros. Vehicular Connectivity Models: From Single-Hop Links to Large-Scale Behavior. In *Vehicular Technology Conference Fall (VTC 2009-Fall), 2009 IEEE 70th*, pages 1–5, Sep 2009.

[MJJ+08] Cui Miao, Yin JunXun, Nie JianYao, Zhang JinJuan, and Cao YingLie. An Evolutionary Dynamic Slots Assignment Algorithm Based on P-TDMA for Mobile Ad Hoc Networks. In *Communication Systems, 2008. ICCS 2008. 11th IEEE International Conference on*, 2008.

[MLP08] Yiannos Mylonas, Marios Lestas, and Andreas Pitsillides. Speed Adaptive Probabilistic Flooding in Cooperative Emergency Warning. In *Proceedings of the 4th Annual International Conference on Wireless Internet*, WICON '08. ICST, 2008.

[MMKH11] Thomas Mangel, Matthias Michl, Oliver Klemp, and Hannes Hartenstein. Real-World Measurements of Non-Line-Of-Sight Reception Quality for 5.9GHz IEEE 802.11p at Intersections. In *Proc. of the 3rd Int. conference on Communication Technologies for Vehicles*, Nets4Cars/Nets4Trains'11. Springer-Verlag, 2011.

[MNW04] Gurmeet Singh Manku, Moni Naor, and Udi Wieder. Know thy Neighbor's Neighbor: the Power of Lookahead in Randomized P2P Networks. In *Proc. of the 36th annual Symposium on Theory Of Computing (STOC)*, pages 54–63. ACM, 2004.

[MW04] AF. Molisch and M.Z. Win. MIMO Systems with Antenna Selection. *Microwave Magazine, IEEE*, 5(1):46–56, Mar 2004.

[NCMS11] Filipe Neves, André Cardote, Ricardo Moreira, and Susana Sargento. Real-world Evaluation of IEEE 802.11p for Vehicular Networks. In *Proc. of the 8th Int. Workshop on VehiculAr InterNETworking (VANET)*, pages 89–90. ACM, 2011.

[ns3] The ns-3 network simulator. `http://www.nsnam.org`.

[NTCS99] Sze-Yao Ni, Yu-Chee Tseng, Yuh-Shyan Chen, and Jang-Ping Sheu. The Broadcast Storm Problem in a Mobile Ad Hoc Network. In *Proceedings of the 5th annual ACM/IEEE international conference on Mobile computing and networking*, MobiCom '99. ACM, 1999.

[OBB09] J. S. Otto, F. E. Bustamante, and R. A. Berry. Down the Block and Around the Corner – The Impact of Radio Propagation on Inter-vehicle Wireless Communication.

In *Proc. of the Int. Conference on Distributed Computing Systems (ICDCS)*. IEEE, 2009.

[OK04] J. Ott and D. Kutscher. Drive-thru Internet: IEEE 802.11b for "Automobile" Users. In *INFOCOM 2004. Twenty-third Annual Joint Conference of the IEEE Computer and Communications Societies*, volume 1, pages –373, Mar 2004.

[oT] U.S. Department of Transportation. Connected Vehicle Test Bed. `http://www.its.dot.gov/testbed.htm`. accessed on November 26, 2014.

[oT15] U.S. Department of Transportation. National Transportation Statistics 2015, 2015.

[PB94] Charles E. Perkins and Pravin Bhagwat. Highly Dynamic Destination-Sequenced Distance-Vector Routing (DSDV) for Mobile Computers. *SIGCOMM Comput. Commun. Rev.*, 24(4):234–244, October 1994.

[Per99] Charles E. Perkins. Ad-hoc On-Demand Distance Vector Routing. In *Proc. of the 2nd Workshop on Mobile Computing Systems and Applications (WMCSA)*. IEEE, 1999.

[SAHS05] K. Sundaresan, V. Anantharaman, Hung-Yun Hsieh, and R. Sivakumar. ATP: A Reliable Transport Protocol for Ad Hoc Networks. *Mobile Computing, IEEE Transactions on*, 4(6):588–603, Nov 2005.

[SBLB10] H. Saleet, O. Basir, R. Langar, and R. Boutaba. Region-Based Location-Service-Management Protocol for VANETs. *Vehicular Technology, IEEE Transactions on*, 59(2):917–931, February 2010.

[SLL+04] Boon-Chong Seet, Genping Liu, Bu-Sung Lee, Chuan-Heng Foh, Kai-Juan Wong, and Keok-Kee Lee. A-STAR: A Mobile Ad Hoc Routing Strategy for Metropolis Vehicular Communications. In *NETWORKING 2004.*, volume 3042 of *Lecture Notes in Computer Science*. Springer Berlin / Heidelberg, 2004.

[Soc10] IEEE Computer Society. IEEE Standard 802.11p, June 2010.

[STE+09] Jose Santa, Manabu Tsukada, Thierry Ernst, Olivier Mehani, and Antonio F. Gomez-Skarmeta. Assessment of VANET Multi-Hop Routing over an Experimental Platform. *Int. Journal of Internet Protocol Technology*, 4(3):158–172, September 2009.

[TB10] Ozan K. Tonguz and Mate Boban. Multiplayer games over Vehicular Ad Hoc Networks: A new application. *Ad Hoc Networks*, 8(5):531–543, July 2010.

[THR03] Jing Tian, Lu Han, and K. Rothermel. Spatially Aware Packet Routing for Mobile Ad Hoc Inter-vehicle Radio Networks. In *Proc. of the 2003 Conference on Intelligent Transportation Systems (ITS)*, volume 2. IEEE, 2003.

[VBT11] W. Viriyasitavat, Fan Bai, and O.K. Tonguz. Toward end-to-end control in VANETs. In *Vehicular Networking Conference (VNC), 2011 IEEE*, pages 78–85, Nov 2011.

[vKKH09] Martijn Eenennaam van, Wouter Klein Wolterink, Georgios Karagiannis, and Geert Heijenk. Exploring the Solution Space of Beaconing in VANETs. In *Proceedings 2009 IEEE Vehicular Networking Conference (VNC)*. IEEE Communications Society, Oct 2009.

[VTB09] Wantanee Viriyasitavat, Ozan K. Tonguz, and Fan Bai. Network Connectivity of VANETs in Urban Areas. In *Proceedings of the 6th Annual IEEE Communications Society Conference on Sensor, Mesh and Ad Hoc Communications and Networks*, SECON'09, pages 646–654, Piscataway, NJ, USA, 2009. IEEE Press.

[WTP+07] N. Wisitpongphan, O.K. Tonguz, J.S. Parikh, P. Mudalige, F. Bai, and V. Sadekar. Broadcast Storm Mitigation Techniques in Vehicular Ad Hoc Networks. *Wireless Communications, IEEE*, 14(6), 2007.

[YLL+10] Qing Yang, Alvin Lim, Shuang Li, Jian Fang, and Prathima Agrawal. ACAR: Adaptive Connectivity Aware Routing for Vehicular Ad Hoc Networks in City Scenarios. *Mobile Networks and Applications*, 15, 2010.